Host monitoring of quorum sensing during *Pseudomonas aeruginosa* infection

Authors: Pedro Moura-Alves[1,2*], Andreas Puyskens[1], Anne Stinn[1,3,4,5], Marion Klemm[1], Ute Guhlich-Bornhof[1], Anca Dorhoi[1,6,7], Jens Furkert[8], Annika Kreuchwig[8], Jonas Protze[8], Laura Lozza[1,9] , Gang Pei[1], Philippe Saikali[1], Carolina Perdomo[1], Hans J. Mollenkopf[10], Robert Hurwitz[11], Frank Kirschhoefer[12], Gerald Brenner-Weiss[11], January Weiner 3[rd1], Hartmut Oschkinat[8], Michael Kolbe[3,4,5] , Gerd Krause[8], Stefan H.E. Kaufmann[1,13*]

Affiliations:

[1]Max Planck Institute for Infection Biology, Department of Immunology, Charitéplatz 1, 10117 Berlin, Germany.

[2]Nuffield Department of Clinical Medicine, Ludwig Institute for Cancer Research, University of Oxford, Oxford, UK.

[3]Max Planck Institute for Infection Biology, Structural Systems Biology, Charitéplatz 1, 10117 Berlin, Germany.

[4]Department of Structural Infection Biology, Centre for Structural Systems Biology (CSSB), Helmholtz-Centre for Infection Research (HZI), Notkestraße 85, 22607 Hamburg, Germany.

[5]Faculty of Mathematics, Informatics and Natural Sciences, University of Hamburg, Rothenbaumchaussee 19, 20148 Hamburg, Germany.

[6]Institute of Immunology, Friedrich-Loeffler Institut, Greifswald - Insel Riems, Germany.

[7]Faculty of Mathematics and Natural Sciences, University of Greifswald, Greifswald, Germany.

[8]Leibniz-Forschungsinstitut für Molekulare Pharmakologie (FMP), Robert-Rössle-Strasse 10, 13125 Berlin, Germany.

[9]Epiontis GmbH - Precision for Medicine, Barbara-McClintock- Str. 6, 12489 Berlin, Germany.

[10]Microarray Core Facility, Max Planck Institute for Infection Biology, Department of Immunology, Charitéplatz 1, 10117 Berlin, Germany.

[11]Protein Purification Core Facility, Max Planck Institute for Infection Biology, Charitéplatz 1, 10117 Berlin, Germany.

[12]Institute of Functional Interfaces, Karlsruhe Institute of Technology, Karlsruhe, Germany.

[13]Hagler Institute for Advanced Study at Texas A&M University, College Station, TX 7843.

*Correspondence to: pedro.mouraalves@ludwig.ox.ac.uk ; kaufmann@mpiib-berlin.mpg.de

Abstract: *Pseudomonas aeruginosa* (*P.aeruginosa*) rapidly adapts to altered conditions by *quorum sensing* (QS), a communication system used to collectively modify its behaviour, via production, release and detection of signalling molecules. QS molecules can also be sensed by hosts, however respective receptors and signalling pathways are poorly understood. We describe a unique pattern of regulation in the host by the Aryl hydrocarbon Receptor (AhR), critically dependent on qualitative and quantitative sensing of *P.aeruginosa quorum*. QS molecules bind to the AhR and distinctly modulate its activity. This is mirrored upon infection with *P.aeruginosa* collected from diverse growth stages and with QS-mutants. We propose that by spying on bacterial *quorum*, the AhR is a major sensor of infection dynamics, capable of orchestrating host defence according to the *status quo* of infection.

One Sentence Summary: By sensing bacterial communication the Aryl hydrocarbon Receptor modulates host defence according to the level of threat.

Main Text:

Pseudomonas aeruginosa (*P.aeruginosa*) is a resourceful and ubiquitous gram-negative bacterium that causes infectious diseases in a broad spectrum of organisms, including plants, animals and humans(*1*). Its prevalence in burn victims, Cystic Fibrosis (CF) patients and immunocompromised individuals, such as AIDS patients, is commonly associated with a poor, often fatal outcome(*2*). *P.aeruginosa* is also a major cause of nosocomial infections, such as bacterial pneumonia, urinary tract infection and surgical-wound contamination(*1*). Because of its profound antibiotic resistance, therapy of *P.aeruginosa* is extremely difficult(*1*). Moreover, this pathogen possesses a wide range of mechanisms to adapt to different and sometimes harsh environments, further aggravating its eradication, even by antibiotic treatment(*1*). One such important and unifying mechanism is the capacity of *P.aeruginosa* to perform *quorum sensing* (QS)(*1, 3, 4*). QS is a cell-to-cell signalling mechanism employed by different bacteria to coordinate their activities in response to changes in community density, via chemical communication using different diffusible molecules, so called autoinducers (AI), and their receptors (Fig.1A)(*3, 4*). In *P.aeruginosa*, QS regulates production of a vast set of virulence factors, such as extracellular proteases and phenazines, and is crucial for colonization and infection, regulating diverse mechanisms such as biofilm formation and antimicrobial resistance(*1, 3-5*). Differences in *P.aeruginosa* virulence and transition from acute to chronic infection have been linked to changes in autoinducer levels, as well as in the expression of QS

regulated genes(*1, 3, 6-8*). Consequently, QS constitutes an obvious target in the current search for novel treatment options for *P.aeruginosa* infections(*3, 4, 9*). Noteworthy, changes in expression of AI, and QS regulated genes, may not only impact on bacterial community dynamics, but also on the host response during infection. It has been previously reported that different QS regulated molecules, such as homoserine lactones (HSL), quinolones and phenazines, can interact with host cells, influencing a broad range of responses, including immunomodulation(*9*). Thus far, the host receptors and signalling pathways, as well as the mechanisms involved in monitoring infection dynamics are incompletely understood.

Recently, we have demonstrated that the Aryl Hydrocarbon Receptor (AhR), a highly conserved ligand dependent transcription factor, directly recognizes *P.aeruginosa* phenazines, and thereby plays an important role in infection control(*10*). AhR binds to phenazines, mediates their degradation and regulates the expression of several host genes including detoxifying enzymes, chemokines and cytokines. Accordingly, resistance of AhR deficient ($AhR^{-/-}$) mice to *P.aeruginosa* is diminished(*10*). Taking into consideration the vast set of ligands that the AhR is able to detect and the numerous biological roles it can exert, we hypothesized that AhR monitors the course of bacterial infection and disease by sensing different bacterial QS molecules expressed at various stages of infection (Fig.1A), and thereby orchestrates the most appropriate immune response against different stages of infection.

Results

AhR senses bacterial QS molecules *in vitro*

Using luciferase AhR reporter cells(*10*), we infected THP-1 macrophages (THP-1 AhR reporter) and A549 alveolar type II pneumocytes (A549 AhR reporter) with *P.aeruginosa* laboratory wild type (WT) UCBPP-PA14 (PA14 WT) and GFP labelled (PA14 WT-GFP) strains collected from distinct stages of bacterial growth (early log: OD600<0.3; mid log: 0.5<OD600<0.8; late log: OD600>1). AhR was more profoundly activated by bacteria from later growth phases (Fig.1B and Fig.S1A), while multiplicity of infection (MOI, Fig.S1B) and percentage of infected cells remained comparable over the different growth stages (Fig.S1C,D).Similar results were obtained with filtered bacterial supernatants from PA14-WT strains (Fig.1C and Fig.S1E), pointing to different AhR signalling by distinct *P.aeruginosa* molecules. A comparable phenotype was observed using supernatants from PAO1, a different commonly used *P.aeruginosa* laboratory strain (Fig.S1F). Amongst the obvious candidates are

the *P.aeruginosa* phenazines, previously identified as AhR ligands (*10*). Consistently, increasing concentrations of the *P.aeruginosa* phenazine pyocyanin (Pyo) were detected in PA14 supernatants along bacterial growth (Fig.S1G, H), correlating with the observed AhR activation (Fig.1B,C and Fig.S1A,E).

Phenazines are part of the QS regulated molecules expressed by *P.aeruginosa*, with Pyo providing a terminal signal of QS(*3, 4, 11, 12*). *P.aeruginosa* QS is regulated by four tightly controlled pathways, namely Las, Rhl, Pqs and Iqs (Fig.1A)(*3, 4, 12*). These pathways are tightly interconnected and their cognate autoinducer molecules are capable of activating a distinct downstream transcriptional pathway (Fig.1A). In brief, N-3-oxo-dodecanoyl-homoserine lactone (3-o-C12-L-HSL) and N-butanoyl-homoserine lactone (C4-L-HSL) are produced in a sequential manner via Las and Rhl systems, and activate the receptors LasR and RhlR, respectively(*3, 4, 12*). A third pathway, Pqs, leads to the synthesis of the *Pseudomonas* quinolone signalling molecule (2-heptyl-3-hydroxy-4-quinolone, PQS), and its precursor 4-hydroxy-2-heptylquinoline (HHQ), which signal via the PqsR(*3, 4, 12*). Recently, the Iqs pathway has been discovered, however the mechanism of 2-(2-hydroxyphenyl)-thiazole-4-carbaldehyde (IQS) production and its receptor are less understood(*1, 3*). Using high-performance liquid chromatography (HPLC), we confirmed a sequential autoinducer abundance in the supernatants of PA14 (Fig.1D). Considering the unique expression profiles of the QS molecules 3-o-C12-L-HSL, C4-L-HSL, HHQ and PQS, we determined their ability to modulate canonical AhR signalling. Stimulation of THP-1 and A549 AhR reporter cells with the different *P.aeruginosa* QS molecules resulted in differential modulation of AhR signalling (Fig.1E). The 3-o-C12-L-HSL and HHQ potently inhibited AhR activation by the known *Pseudomonas* AhR ligand 1-hydroxyphenazine (1-HP)(*10*), in a dose dependent manner (Fig.1F,G). Several QS molecules have been reported to induce apoptosis in host cells, depending on the concentration, cell type and exposure time(*13, 14*). No major differences in cell viability were detected for the majority of the conditions tested here, as measured by lactate dehydrogenase (LDH) release (Fig.S2A). An exception occurred after 24h stimulation of THP-1 cells with high concentrations of 3-o-C12-L-HSL (Fig.S2A). These results are in agreement with previous studies showing that epithelial cells, such as A549, are more resistant to 3-o-C12-L-HSL induced apoptosis than macrophages(*13, 14*). All experiments with THP-1 cells in the presence of 3-o-C12-L-HSL were performed at earlier time points, when no differences in cell viability were detected. Yet, we decided to further exclude a possible relationship between

apoptosis related effects and AhR modulation in this cell type. As shown in Fig.S2B-E, no relationship was observed and we decided to focus on A549 cells in following experiments.

Previous studies unveiled that concentrations of QS molecules in *P.aeruginosa*, such as 3-o-C12-L-HSL, can vary profoundly. These include the growth status, type of cultures (planktonic cultures (1-5 μM) or biofilms (up to 600 μM)) and sample type (sputum or murine infection samples)(*15-18*). Notably, high concentrations of these molecules have been detected in biofilms of CF patients' lungs, and thus in close contact with the epithelium(*18*). Consequently, we decided to use 50 μM of the different QS molecules in subsequent studies.

A hallmark of AhR activity is the transcriptional induction of detoxifying enzymes, such as *CYP1A1* and *CYP1B1*, and of the AhR repressor (*AhRR*)(*19*). As previously reported(*10*), stimulation of A549 cells with 1-HP induces mRNA expression of these genes (Fig.1H and Fig.S3A). Intriguingly, 3-o-C12-L-HSL and HHQ inhibited 1-HP induced gene expression (Fig.2F and Fig.S3A). Due to its involvement in tryptophan metabolism, alterations in CYP1A1 expression and activity can influence AhR activation(*20, 21*). We took advantage of an established model using mouse liver cells (Hepa-1c1c7), which due to the expression of copious levels of CYP1A1 is best suited to detect its expression and enzymatic activity(*22*). Similar to other cell types, AhR activation in hepatocytes was induced by 1-HP, as measured by increased luciferase activity in an AhR reporter cell line and increased CYP1A1 enzymatic activity, measured by the EROD assay (Fig.1I and Fig.S3B, C). Intriguingly, 3-o-C12-L-HSL, HHQ and PQS, inhibited 1-HP induced AhR activation and CYP1A1 enzymatic activity in these cells, whereas C4-L-HSL did not (Fig.1J and Fig. S3B, C). In sum, QS molecules, including HSLs, quinolones and phenazines, modulated AhR activity in both a stimulatory and an inhibitory direction.

QS molecules are not only expressed by *P.aeruginosa*; several other gram-negative bacteria also produce HSLs, with subtle modifications, mostly in the carbon side chain(*3, 4*) (Table S1). Since the crystal structure of the AhR has not yet been solved, it is challenging to predict ligands that bind to AhR. Taking advantage of the AhR modulatory properties of a vast number of HSLs and their tested analogues (Fig.S4A-C), we optimized an existing *in silico* model(*10*) to interrogate whether and how these QS molecules from *P.aeruginosa* can be accommodated in the AhR binding pocket (Fig.2A). The ligands were divided by impact on agonistic or competitive behaviour and sorted with increasing MM-GBSA binding energies (ΔG^{Bind}), revealing 3-o-C12-L-HSL as the strongest binder and C4-L-HSL as the weakest binder in this study (Fig.S4D). In this model, all residues previously found to interact with

TCDD by mutagenesis experiments(*23, 24*), are predicted to be involved in forming the binding pocket. The key residues, Thr289, His291, Phe295, Ser365 and Gln383, form hydrogen bonds with most of the ligands investigated here (Fig.S4D, E). Furthermore, and in agreement with data retrieved from ligand-selective modulation of AhR ligand binding, AhR complexes with bound competitors showed additional hydrophobic interactions with Phe287, Leu308 and Leu315 (Fig.S4D,E)(*25*). 1-HP is predicted to contact Phe324 via interactions of the aromatic rings (Fig.S4E). This residue is known to mediate agonist/antagonist switching upon mutation (Phe324Ala/Leu) and converts agonists such as 3MC or BNF into antagonists(*25*). Predictions were validated by ligand-binding studies (*10*), confirming the binding of 3-o-C12-L-HSL and HHQ, with dissociation constant (K_d) values of 4.67 μM or 3.77 μM, respectively (Fig.2B and Fig.S4F). In addition, we developed a complementary method to detect AhR binding of different ligands, including the bona fide AhR ligand 2,3,7,8-tetrachlorodibenzodioxin (TCDD)(*26*), using purified AhR and ARNT proteins in a Microscale thermophoresis (MST) assay (Fig.S4G). This approach also demonstrated AhR binding to QS molecules, including 3-o-C12-L-HSL, PQS and 1-HP, but not to C4-L-HSL (Fig.2C). Of note, HHQ binding could not be analysed by MST due to its intrinsic fluorescence properties, which interfere with the assay. Altogether, various QS molecules, other than phenazines, bind to AhR and modulate its activity, endorsing this pathway as potential target for sensing bacterial infection dynamics in the host.

AhR QS ligand interactions were further defined using an A549 AhR CRISPR KO cell line (Fig.3A and Fig.S5A). Induction of AhR dependent genes was detected upon 1-HP stimulation of CRISPR Scramble control, and absent in the AhR-KO cells (Fig.S5B). In contrast, and as previously shown in WT A549 cells, 3-o-C12-L-HSL and HHQ caused AhR inhibition (Fig.S5B,C). Major functions of AhR include xenobiotic metabolism, toxin degradation and excretion(*26*). Previously, we demonstrated that AhR mediates the degradation of bacterial molecules, such as *P.aeruginosa* phenazines and *Mycobacterium tuberculosis* naphthoquinone phthiocol(*10*). Using an established *P.aeruginosa* 3-o-C12-L-HSL luminescence reporter strain (PA14-R3)(*27*) to detect 3-o-C12-L-HSL levels (Fig.S5D), we evaluated its degradation profile upon exposure to AhR proficient and deficient cells (Fig.S5E). Bioluminescence emitted by the bacterial reporter cells decreased in a time dependent manner, indicating reduced abundance of 3-o-C12-L-HSL (Fig.3B). In contrast, no differences were detected between Scramble control and AhR-KO cells (Fig.3B). These results were confirmed by HPLC (Fig.3C). A similar approach was used to determine the metabolism

of HHQ (Fig.S5E), using the PAO1 *pqsA* CTX-lux::*pqsA* reporter strain (Fig.S5F)(*28*) and by HPLC. Surprisingly, no degradation of HHQ was observed by any of the methods when exposing cells to 50 μM of HHQ (Fig.S5G,H). However, exposing cells to a lower concentration of HHQ (0.5 μM), diminished levels of HHQ were detected at late time points, although no differences between AhR proficient and AhR deficient cells were observed (Fig.3D). Altogether, under the conditions tested, our results argue against an involvement of AhR in the degradation of *P.aeruginosa* 3-o-C12-L-HSL or HHQ. In addition to its role in xenobiotic metabolism, AhR participates in the regulation of different immune mediators(*10, 19, 26, 29*). Accordingly, we evaluated whether upon exposure to different QS molecules, AhR regulates cytokine and chemokine expression. Different bacterial ligands induced different gene expression patterns (Fig.3E, F). It has been previously reported that infection with *P.aeruginosa*, or exposure to 3-o-C12-L-HSL, leads to *IL-6* and *IL-8* expression(*30, 31*). Consistently, amongst the genes induced by 3-o-C12-L-HSL, *IL-6* and *IL-8* were highly induced in the AhR-KO cells, as compared to Scramble control. Elevated induction of IL-8 was also observed upon exposure of AhR-KO cells to HHQ, whilst 1-HP stimulation led to reduced induction. A similar profile was observed for *CXCL1*, *CXCL2* and *CXCL3* (Fig.3E, F). These results emphasize differential AhR modulation of host responses, where sensing the different levels of QS molecules expressed along the infection process can differentially regulate the composition of multiple cytokines and chemokines. Thus, sensing of QS molecules by AhR shapes immunity to infection.

AhR senses bacterial QS molecules *in vivo*

As aforementioned, the AhR is conserved between different species (including human, mouse and zebrafish) and few amino acid positions differ in the ligand binding site of AhR proteins (Fig.S6A). However, subtle amino acid differences have been reported to impact binding to specific ligands(*26*). For example, the human V381, corresponding to A in mouse and zebrafish, is implicated in species related differences regarding the binding affinity to TCDD(*26, 32*). The mouse AhR has higher binding affinity to TCDD, as compared to the human AhR(*26, 32*). Consistently, using our *in silico* modeling, higher TCDD binding affinities of mouse and zebrafish AhR were detected, when compared to the human AhR (Fig.

S6B). A similar approach was chosen for the *P.aeruginosa* QS molecules, and MM-GBSA ΔG^{Bind} values were calculated starting from the same ligand pose as obtained for the human AhR (Fig.S6C). Strikingly, no species specific differences were predicted to occur, further pointing to a conserved mechanism of sensing of *P.aeruginosa* infection.

The zebrafish (*Danio rerio*) has become a powerful model in developmental biology and genetics, and more recently, in toxicology and immunology(*33-36*). The AhR pathway is conserved in zebrafish and has been shown to be also involved in xenobiotic metabolism(*36*). Due to genome-wide duplication events, teleosts express various co-orthologues of mammalian genes, though not all are functional. Zebrafish express three AhR isoforms (*ahr1a*, *ahr1b* and *ahr2*), and the AhR2 is the primary isoform for recognition of toxic ligands, such as TCDD (*36*). Upon ligand activation, AhR2 drives the expression of hallmark genes, such as *cyp1a, ahhra and ahrrb(36)*.

It has been previously reported that static immersion of zebrafish larvae in a bacterial suspension, including *P.aeruginosa*, increases *cyp1a* expression(*37, 38*). Similar results were obtained from microarray analysis of 2 days post fertilization (dpf) larvae infected with PA14-WT for 5h or 24h (Fig.S7A and Table S2, S3). Moreover, in addition to *cyp1a*, increased expression of additional AhR related genes was observed, such as *ahrra* and *cyp1c1(36)*. Therefore, we evaluated whether we could recapitulate our *in vitro* findings using this *in vivo* model organism. Here, 5h exposure of 2dpf larvae to PA14 WT collected from different phases of bacterial growth with distinct expression patterns of QS molecules (e.g. 3-o-C12-L-HSL and Pyo, Fig.4A), resulted in distinct AhR activation, as measured by *cyp1a* mRNA expression (Fig.4B). To mimic the course of infection, bacteria were collected from different growth phases, washed and further resuspended in E3 medium to a final OD similar to the point of collection (i.e. Early log-OD600=0.2; Mid log-OD600=0.7; Late log-OD600=1). Exposure of larvae to these bacterial suspensions led to increasing *cyp1a* expression along the growth phase (Fig.4B). Still, this could be the result of higher expression of QS molecules and/or increasing bacterial density. To exclude the latter option, we exposed zebrafish larvae to bacterial supernatants after filtration and dilution in E3 medium (1:25 ratio), or to similar bacterial numbers collected from the different growth stages. Exposure of 2dpf larvae to filtered supernatants or to infection by immersion resulted in elevated *cyp1a* expression towards late stages of bacterial growth (Fig.4C, D). These results are in agreement with our *in vitro* findings (Fig.1B, C and Fig.S1A,E) confirming that *P.aeruginosa* molecules expressed during diverse growth phases modulate AhR differentially.

Next, we verified in the zebrafish model our *in vitro* findings that *P.aeruginosa* expresses QS molecules, which either activate or inhibit the canonical AhR pathway. We have previously demonstrated that *P.aeruginosa* phenazines (e.g. 1-HP) activate the AhR pathway in human and mouse(*10*). Here, exposure of zebrafish larvae 2 dpf to TCDD induced the expression of AhR dependent genes*(36)* (Fig.S7B). AhR dependency was confirmed by reduced gene expression in the presence of the AhR inhibitor CH223191(*39*)(Fig.S7B, C). Similarly, we observed AhR modulation upon exposure to the *P.aeruginosa* phenazine 1-HP, at the transcriptional level (Fig.4E), and Cyp1a protein expression in response to 1-HP (Fig.4F). To determine whether increased Cyp1a expression translates into enhanced enzymatic activity, we measured its activity *in vivo* in a semi-high throughput assay (Fig.S7D, E). An increment in fluorescence, as readout of increased Cyp1a enzymatic activity was detected upon exposure to 1-HP or TCDD, and inhibited by CH223191 (Fig.4G and Fig.S7E, F). AhR was the major sensor of *P.aeruginosa* phenazines *in vivo* because microarray analysis of larvae exposed to 1-HP, in the presence or absence of the AhR inhibitor revealed that AhR dependent genes(*36*) were amongst the top10 1-HP induced genes, and their induction was reverted by the CH223191 inhibitor (Fig.4H,I, Fig.S7G and Table S4). Not all of the differentially 1-HP induced genes had been previously shown to be transcriptionally regulated by AhR in the zebrafish. Therefore, we performed an *in silico* analysis to identify xenobiotic responsive elements (XRE) in their promotor regions(*40*). We identified putative XREs in the promoter regions of all evaluated genes (Fig.S7H).

Given that our *in vitro* studies demonstrated that *P.aeruginosa* also expresses QS molecules that inhibit the AhR pathway, we exposed larvae *in vivo* to 3-o-C12-L-HSL or HHQ, in the presence or absence of 1-HP. Simultaneous exposure to 3-o-C12-L-HSL or HHQ together with 1-HP, reduced induction of AhR related genes by 1-HP (Fig.5A and Fig.S8A-D). Moreover, Cyp1a enzymatic activity was diminished when zebrafish larvae were co-exposed to 3-o-C12-L-HSL, HHQ and PQS, together with 1-HP, whereas C4-L-HSL did not affect 1-HP induced activation (Fig.5B and Fig.S8B). Remarkably, 3-o-C12-L-HSL and HHQ even inhibited AhR activation by TCDD (Fig.5A, B and Fig.S8A,B). Microarray analysis further confirmed that 3-o-C12-L-HSL inhibited AhR activation by 1-HP (Table S5). None of the ligands induced toxicity in zebrafish larvae, under the conditions tested (Fig.S8E). Overall, our results demonstrate that zebrafish AhR recognizes diverse *P.aeruginosa* QS molecules.

Taking advantage of *P.aeruginosa* mutants producing dissimilar levels of distinct QS molecules, we tested whether AhR is differentially modulated *in vivo* in response to bacteria

297 expressing different QS molecules. We used the mutant PA14 Δ*rsaL* and PA14 09480
298 *P.aeruginosa* strains, which overproduce 3-o-C12-L-HSL(*27, 41*) or phenazines(*10*),
299 respectively. No differences in bacterial growth or in the sequential expression of QS molecules
300 were observed amongst these strains (Fig.S9A, B), whereas the levels of 3-o-C12-L-HSL and
301 phenazines differed as previously documented (Fig.S9C). Consistent with earlier studies(*41*),
302 Pyo levels were also elevated in the PA14 Δ*rsaL*, when compared to PA14-WT (Fig.S9C).
303 Therefore, we focused on bacteria collected from one distinct growth phase (mid log phase),
304 with consistent differences in the levels of 3-o-C12-L-HSL and Pyo (Fig.5C). Static immersion
305 of larvae to similar bacterial numbers ($1x10^9$ CFU/mL, Fig.S10A), led to distinct Cyp1a
306 expression and activity (Fig.5D,E), apparently related to the proportions of the AhR activators
307 and inhibitors (Fig.5C and Fig.S10B). Higher expression of phenazines (PA14 09480)
308 increased, whereas higher expressions of 3-o-C12-L-HSL (PA14 Δ*rsaL*) decreased Cyp1a
309 activity as compared to PA14 WT (Fig.5E). We conclude that AhR recognition of these
310 molecules, whose expressions are tightly regulated in *P.aeruginosa*, allows for quantitative
311 sensing of the course of infection.

312 Recognition of phenazines by AhR is important for clearance of *P.aeruginosa(10)*.
313 Infection of WT and *AhR*$^{-/-}$ mice with a Pyo overexpressing strain (PA14 09480)(*10*) (Fig.S9C,
314 S11A) confirmed the importance of the AhR in bacterial clearance in responses to these
315 molecules (Fig.6A). Intriguingly, infection with bacteria from earlier stages of growth, not
316 expressing phenazines (Fig.S11A), had detrimental consequences mediated by the AhR
317 (Fig.6A). These results further illustrate that distinct *P.aeruginosa* molecules expressed at
318 different growth stages modulate AhR signalling differentially. In order to evaluate the impact
319 of AhR sensing of QS molecules expressed at early stages, focusing on the AhR inhibitor 3-o-
320 C12-L-HSL identified here, we infected mice with the *P.aeruginosa* strain (PA14 Δ*rsaL*). We
321 focused on bacteria from mid log growth phase, to exclude differences in lung CFUs between
322 the 2 mouse strains (WT and *AhR*$^{-/-}$) after 8h of infection (Fig.S11B, C). Differential expression
323 of various cytokines and chemokines depended not only on the mouse strain, but also on the
324 *P.aeruginosa* strain (Fig.6B, C and Fig.S11D). These *in vivo* results are consistent with our *in*
325 *vitro* experiments (Fig.3E, F), where AhR differentially regulated expression of distinct
326 cytokines and chemokines, depending on the presence of distinct QS molecules. Previously we
327 reported a critical role of AhR in the recruitment of neutrophils to the lungs of *P.aeruginosa*
328 infected mice(*10*). Likewise, lower numbers of neutrophils were detected in the lungs of *AhR*$^{-}$
329 $^{/-}$ mice upon infection with PA14 WT (Fig.6D). Strikingly, these differences were lost when

infecting mice with PA14 Δ*rsaL*, where we observed comparable numbers of neutrophils in the lungs of WT and *AhR*$^{-/-}$ mice (Fig.6D).

In sum, these results reveal differential modulation of AhR during the course of infection, depending on the relative abundances of distinct QS molecules. Taken together, our data determines that the AhR not only detects *P.aeruginosa* QS molecules in a qualitative way, but rather quantifies their relative levels. This quantitative assessment endows the host with the capacity to sense bacterial community densities, and consequently infection dynamics. Thus, our findings emphasize a crucial role of AhR as master regulator of host defence responses, capable of tuning immunity according to the stage of infection and disease and hence to their threat to the host.

Discussion

Recently we revealed that by binding bacterial pigmented virulence factors, such as *P.aeruginosa* phenazines, AhR regulates host resistance to infection(*10*). Here, we demonstrate that, in addition to phenazines, AhR recognizes QS molecules comprising different chemical entities including homoserine lactones and quinolones. In contrast to phenazines, the QS cognates, 3-o-C12-L-HSL and HHQ, inhibit the canonical AhR signalling by competing and antagonizing effects of known AhR activators, such as *P.aeruginosa* 1-HP(*10*), or the *bona fide* AhR ligand, TCDD(*19, 42*). Strikingly, AhR sensing of QS molecules is not restricted to a particular cell type or a specific *in vitro* model: First, mammalian macrophages, hepatocytes and epithelial cells responded in a similar fashion, and in all cases subtle alterations in the ratios of bacterial ligands influenced the outcome of AhR activation and its downstream responses, such as cytokine and chemokine expression. Second, these results are reciprocated *in vivo* using zebrafish, where exposure of larvae to different concentrations of *P.aeruginosa* QS molecules modulated AhR activation and elicited downstream responses. Moreover, exposure of zebrafish larvae to different *P.aeruginosa* mutants producing distinct QS molecules at different abundances at a given point of infection, resulted in a unique AhR activation profile. Complementing these findings, an experimental mouse infection model with *P.aeruginosa* strains expressing variable levels of QS molecules, revealed that the AhR regulates bacterial elimination upon sensing bacterial *quorum*. In sum, the AhR resembles a “processing-hub”, integrating the information linked to the abundance of different QS molecules, both activators

and inhibitors, thereby mobilizing the most appropriate host defence mechanisms at a given stage of infection.

QS is employed by certain bacteria to coordinate their gene expression in response to changes in their population density, or their stage of infection(*1, 3, 4*). Accordingly, direct correlation between different QS molecules, and severity of infection has been observed(*7, 43*). In *P.aeruginosa*, QS is crucial for coordinated colonization of a new environment, regulating different virulence and adaptation mechanisms(*1, 3, 4, 12*). Differences in *P.aeruginosa* virulence and transition from acute to chronic infection have been linked to altered expression of QS molecules and their regulated genes(*1, 6, 8, 43*). For instance, the expression of phenazines plays a critical role in biofilm formation and development(*7, 43, 44*), and *P. aeruginosa* QS mutants producing thinner and less developed biofilms, are more sensitive to antibiotics and eradication(*1, 5, 45*). Furthermore, high concentrations of *P. aeruginosa* phenazines are detected in the sputum of CF patients, who are severely affected by this pathogen(*2, 7, 43*). Therefore, depending on its metabolic state, mirrored by a distinct composition of QS molecules, the bacteria may pose different threats to the host, who needs to adapt its response accordingly. Interestingly, inter- and intra- *P.aeruginosa* species differences in virulence and expression of secreted molecules have been reported to occur, not restricted to clinical isolates but also among laboratory strains (e.g. between PAO1 sublines or between PA14 and PAO1). For example, expression levels of Pyo, rhamnolipids, PQS, exopolysaccharides and elastase have been reported to differ between PA14 and PAO1 or among diverse PAO1 sublines(*46-49*). It is tempting to speculate that due to its capacity to detect different levels of *P.aeruginosa* QS molecules, including Pyo or PQS, the AhR is also well suited to detect strain-related differences during the course of infection, and consequently regulate host responses accordingly. Though, further studies are needed to evaluate this hypothesis.

Interactions of *P.aeruginosa* QS molecules with different host receptors and signalling pathways have been reported(*9*). For example, 3-o-C12-L-HSL has been found to be sensed by the Ras GTPase-activating-like protein IQGAP1 or the Peroxisome proliferator-activated receptors (PPAR β/δ/γ)(*9, 50, 51*). Additionally, *P.aeruginosa* HSLs (e.g. 3-o-C12-L-HSL) and quinolones (HHQ and PQS) modulate different host signalling pathways, involving NF-kB or PPAR(*9, 51-53*). Curiously, interactions between the AhR and the indicated signalling pathways (e.g. NF-kB and PPAR) have been described(*19*), but their interplay and elicited responses upon *P.aeruginosa* infection remain unknown, and should be the focus of future

394 studies. Nevertheless, the unique capacity of the AhR to bind and recognize three distinct types
395 of QS molecules (HSLs, quinolones and phenazines), as well as its capacity to monitor and
396 integrate their relative expression levels, endorses this receptor as a unique and major host
397 sensor of bacterial *quorum* and infection dynamics. It is tempting to speculate that host AhR
398 and bacterial QS systems can actively spy on each other by recognizing similar molecules, even
399 beyond the QS molecules described here. Recently *Ismail et al*(*54*) described that host epithelia
400 can produce QS-like molecules, including an AI-2 mimic, enabling it to interfere bacterial QS
401 circuits. Bacteria derived AI-2 does not modulate the AhR pathway in epithelial cells
402 (unpublished data). However, due to its capacity to sense *P.aeruginosa* QS molecules and to
403 its vast ligand binding properties, we cannot exclude the possibility that the host AhR senses
404 and modulates the expression of different host molecules (such as host QS-like molecules and
405 others), which may be involved in this host-bacteria interkingdom crosstalk during infection
406 (grey arrows in Fig.1A).

407 Given that the AhR acts as host sensor which monitors different QS molecules and their
408 expression profiles along the course of infection and disease, the host can tune immune defence
409 according to the stage and density of the bacterial community and the threat of infection. This
410 mechanism would be particularly apt for nosocomial pathogens, which can be tolerated by the
411 immunocompetent host at low density but become harmful once a threshold of tolerability has
412 been exceeded. In this way, cost of energy for defence would be focused on the harmful trait
413 only, with the harmless trait being ignored. Because *P. aeruginosa* is an opportunistic
414 pathogen, defence mobilization is avoided at low bacterial densities, which can be tolerated,
415 and it kicks in only with increasing population densities, which can harm the host. We propose
416 that by spying on inter-bacterial communication, AhR is capable of sensing the *status quo* of
417 the *P.aeruginosa* community during infection, allowing the host to mobilize the most
418 appropriate defence mechanism according to the severity of threat.

419

420 **References and Notes:**

421 1. M. F. Moradali, S. Ghods, B. H. Rehm, Pseudomonas aeruginosa Lifestyle: A
422 Paradigm for Adaptation, Survival, and Persistence. *Front Cell Infect Microbiol* **7**, 39
423 (2017).
424 2. J. C. Davies, Pseudomonas aeruginosa in cystic fibrosis: pathogenesis and persistence.
425 *Paediatr Respir Rev* **3**, 128-134 (2002).
426 3. K. Papenfort, B. L. Bassler, Quorum sensing signal-response systems in Gram-
427 negative bacteria. *Nat Rev Microbiol* **14**, 576-588 (2016).
428 4. C. M. Waters, B. L. Bassler, Quorum sensing: cell-to-cell communication in bacteria.
429 *Annu Rev Cell Dev Biol* **21**, 319-346 (2005).

5. P. C. Shih, C. T. Huang, Effects of quorum-sensing deficiency on Pseudomonas aeruginosa biofilm formation and antibiotic resistance. *J Antimicrob Chemother* **49**, 309-314 (2002).
6. C. Winstanley, J. L. Fothergill, The role of quorum sensing in chronic cystic fibrosis Pseudomonas aeruginosa infections. *FEMS Microbiol Lett* **290**, 1-9 (2009).
7. B. Rada, T. L. Leto, Pyocyanin effects on respiratory epithelium: relevance in Pseudomonas aeruginosa airway infections. *Trends Microbiol* **21**, 73-81 (2013).
8. H. L. Barr *et al.*, Pseudomonas aeruginosa quorum sensing molecules correlate with clinical status in cystic fibrosis. *Eur Respir J* **46**, 1046-1054 (2015).
9. Y. C. Liu, K. G. Chan, C. Y. Chang, Modulation of Host Biology by Pseudomonas aeruginosa Quorum Sensing Signal Molecules: Messengers or Traitors. *Front Microbiol* **6**, 1226 (2015).
10. P. Moura-Alves *et al.*, AhR sensing of bacterial pigments regulates antibacterial defence. *Nature* **512**, 387-392 (2014).
11. L. E. Dietrich, A. Price-Whelan, A. Petersen, M. Whiteley, D. K. Newman, The phenazine pyocyanin is a terminal signalling factor in the quorum sensing network of Pseudomonas aeruginosa. *Mol Microbiol* **61**, 1308-1321 (2006).
12. P. N. Jimenez *et al.*, The multiple signaling systems regulating virulence in Pseudomonas aeruginosa. *Microbiol Mol Biol Rev* **76**, 46-65 (2012).
13. A. Crabbe *et al.*, Alveolar epithelium protects macrophages from quorum sensing-induced cytotoxicity in a three-dimensional co-culture model. *Cell Microbiol* **13**, 469-481 (2011).
14. K. Tateda *et al.*, The Pseudomonas aeruginosa autoinducer N-3-oxododecanoyl homoserine lactone accelerates apoptosis in macrophages and neutrophils. *Infect Immun* **71**, 5785-5793 (2003).
15. J. P. Pearson *et al.*, Structure of the autoinducer required for expression of Pseudomonas aeruginosa virulence genes. *Proc Natl Acad Sci U S A* **91**, 197-201 (1994).
16. T. S. Charlton *et al.*, A novel and sensitive method for the quantification of N-3-oxoacyl homoserine lactones using gas chromatography-mass spectrometry: application to a model bacterial biofilm. *Environ Microbiol* **2**, 530-541 (2000).
17. D. L. Erickson *et al.*, Pseudomonas aeruginosa quorum-sensing systems may control virulence factor expression in the lungs of patients with cystic fibrosis. *Infect Immun* **70**, 1783-1790 (2002).
18. P. K. Singh *et al.*, Quorum-sensing signals indicate that cystic fibrosis lungs are infected with bacterial biofilms. *Nature* **407**, 762-764 (2000).
19. B. Stockinger, P. Di Meglio, M. Gialitakis, J. H. Duarte, The aryl hydrocarbon receptor: multitasking in the immune system. *Annu Rev Immunol* **32**, 403-432 (2014).
20. C. Schiering *et al.*, Feedback control of AHR signalling regulates intestinal immunity. *Nature* **542**, 242-245 (2017).
21. E. Wincent *et al.*, Inhibition of cytochrome P4501-dependent clearance of the endogenous agonist FICZ as a mechanism for activation of the aryl hydrocarbon receptor. *Proc Natl Acad Sci U S A* **109**, 4479-4484 (2012).
22. C. J. Sinal, J. R. Bend, Aryl hydrocarbon receptor-dependent induction of cyp1a1 by bilirubin in mouse hepatoma hepa 1c1c7 cells. *Mol Pharmacol* **52**, 590-599 (1997).
23. A. Pandini, M. S. Denison, Y. Song, A. A. Soshilov, L. Bonati, Structural and functional characterization of the aryl hydrocarbon receptor ligand binding domain by homology modeling and mutational analysis. *Biochemistry* **46**, 696-708 (2007).

24. A. Pandini *et al.*, Detection of the TCDD binding-fingerprint within the Ah receptor ligand binding domain by structurally driven mutagenesis and functional analysis. *Biochemistry* **48**, 5972-5983 (2009).
25. A. A. Soshilov, M. S. Denison, Ligand promiscuity of aryl hydrocarbon receptor agonists and antagonists revealed by site-directed mutagenesis. *Mol Cell Biol* **34**, 1707-1719 (2014).
26. R. Pohjanvirta, *The AH Receptor in Biology and Toxicology*. (Wiley, 2011).
27. F. Massai *et al.*, A multitask biosensor for micro-volumetric detection of N-3-oxo-dodecanoyl-homoserine lactone quorum sensing signal. *Biosens Bioelectron* **26**, 3444-3449 (2011).
28. M. Fletcher, M. Camara, D. A. Barrett, P. Williams, Biosensors for qualitative and semiquantitative analysis of quorum sensing signal molecules. *Methods Mol Biol* **1149**, 245-254 (2014).
29. C. Esser, A. Rannug, The aryl hydrocarbon receptor in barrier organ physiology, immunology, and toxicology. *Pharmacol Rev* **67**, 259-279 (2015).
30. M. L. Mayer, J. A. Sheridan, C. J. Blohmke, S. E. Turvey, R. E. Hancock, The Pseudomonas aeruginosa autoinducer 3O-C12 homoserine lactone provokes hyperinflammatory responses from cystic fibrosis airway epithelial cells. *PLoS One* **6**, e16246 (2011).
31. R. S. Smith *et al.*, IL-8 production in human lung fibroblasts and epithelial cells activated by the Pseudomonas autoinducer N-3-oxododecanoyl homoserine lactone is transcriptionally regulated by NF-kappa B and activator protein-2. *J Immunol* **167**, 366-374 (2001).
32. P. Ramadoss, G. H. Perdew, Use of 2-azido-3-[125I]iodo-7,8-dibromodibenzo-p-dioxin as a probe to determine the relative ligand affinity of human versus mouse aryl hydrocarbon receptor in cultured cells. *Mol Pharmacol* **66**, 129-136 (2004).
33. A. Planchart *et al.*, Advancing toxicology research using in vivo high throughput toxicology with small fish models. *ALTEX* **33**, 435-452 (2016).
34. S. A. Renshaw, N. S. Trede, A model 450 million years in the making: zebrafish and vertebrate immunity. *Dis Model Mech* **5**, 38-47 (2012).
35. A. H. Meijer, H. P. Spaink, Host-pathogen interactions made transparent with the zebrafish model. *Curr Drug Targets* **12**, 1000-1017 (2011).
36. T. C. King-Heiden *et al.*, Reproductive and developmental toxicity of dioxin in fish. *Mol Cell Endocrinol* **354**, 121-138 (2012).
37. J. J. van Soest *et al.*, Comparison of static immersion and intravenous injection systems for exposure of zebrafish embryos to the natural pathogen Edwardsiella tarda. *BMC Immunol* **12**, 58 (2011).
38. F. Diaz-Pascual, J. Ortiz-Severin, M. A. Varas, M. L. Allende, F. P. Chavez, In vivo Host-Pathogen Interaction as Revealed by Global Proteomic Profiling of Zebrafish Larvae. *Front Cell Infect Microbiol* **7**, 334 (2017).
39. B. Zhao, D. E. Degroot, A. Hayashi, G. He, M. S. Denison, CH223191 is a ligand-selective antagonist of the Ah (Dioxin) receptor. *Toxicol Sci* **117**, 393-403 (2010).
40. M. E. Jonsson, A. Kubota, A. R. Timme-Laragy, B. Woodin, J. J. Stegeman, Ahr2-dependence of PCB126 effects on the swim bladder in relation to expression of CYP1 and cox-2 genes in developing zebrafish. *Toxicol Appl Pharmacol* **265**, 166-174 (2012).
41. M. T. Cabeen, Stationary phase-specific virulence factor overproduction by a lasR mutant of Pseudomonas aeruginosa. *PLoS One* **9**, e88743 (2014).
42. P. K. Mandal, Dioxin: a review of its environmental effects and its aryl hydrocarbon receptor biology. *J Comp Physiol B* **175**, 221-230 (2005).

43. R. C. Hunter *et al.*, Phenazine content in the cystic fibrosis respiratory tract negatively correlates with lung function and microbial complexity. *Am J Respir Cell Mol Biol* **47**, 738-745 (2012).
44. I. Ramos, L. E. Dietrich, A. Price-Whelan, D. K. Newman, Phenazines affect biofilm formation by Pseudomonas aeruginosa in similar ways at various scales. *Res Microbiol* **161**, 187-191 (2010).
45. L. K. Nelson, G. H. D'Amours, K. M. Sproule-Willoughby, D. W. Morck, H. Ceri, Pseudomonas aeruginosa las and rhl quorum-sensing systems are important for infection and inflammation in a rat prostatitis model. *Microbiology* **155**, 2612-2619 (2009).
46. J. Klockgether *et al.*, Genome diversity of Pseudomonas aeruginosa PAO1 laboratory strains. *J Bacteriol* **192**, 1113-1121 (2010).
47. L. Wiehlmann *et al.*, Population structure of Pseudomonas aeruginosa. *Proc Natl Acad Sci U S A* **104**, 8101-8106 (2007).
48. C. E. Chandler *et al.*, Genomic and Phenotypic Diversity among Ten Laboratory Isolates of Pseudomonas aeruginosa PAO1. *J Bacteriol* **201**, (2019).
49. S. Chugani *et al.*, Strain-dependent diversity in the Pseudomonas aeruginosa quorum-sensing regulon. *Proc Natl Acad Sci U S A* **109**, E2823-2831 (2012).
50. T. Karlsson, M. V. Turkina, O. Yakymenko, K. E. Magnusson, E. Vikstrom, The Pseudomonas aeruginosa N-acylhomoserine lactone quorum sensing molecules target IQGAP1 and modulate epithelial cell migration. *PLoS Pathog* **8**, e1002953 (2012).
51. A. Jahoor *et al.*, Peroxisome proliferator-activated receptors mediate host cell proinflammatory responses to Pseudomonas aeruginosa autoinducer. *J Bacteriol* **190**, 4408-4415 (2008).
52. V. V. Kravchenko *et al.*, Modulation of gene expression via disruption of NF-kappaB signaling by a bacterial small molecule. *Science* **321**, 259-263 (2008).
53. K. Kim *et al.*, HHQ and PQS, two Pseudomonas aeruginosa quorum-sensing molecules, down-regulate the innate immune responses through the nuclear factor-kappaB pathway. *Immunology* **129**, 578-588 (2010).
54. A. S. Ismail, J. S. Valastyan, B. L. Bassler, A Host-Produced Autoinducer-2 Mimic Activates Bacterial Quorum Sensing. *Cell Host Microbe* **19**, 470-480 (2016).
55. M. W. Pfaffl, A new mathematical model for relative quantification in real-time RT-PCR. *Nucleic Acids Res* **29**, e45 (2001).
56. L. Lozza *et al.*, Crosstalk between human DC subsets promotes antibacterial activity and CD8+ T-cell stimulation in response to bacille Calmette-Guerin. *Eur J Immunol* **44**, 80-92 (2014).
57. A. Mohammadi-Bardbori, Assay for quantitative determination of CYP1A1 enzyme activity using 7-Ethoxyresorufin as standard substrate (EROD assay). (2014).
58. M. E. Ritchie *et al.*, limma powers differential expression analyses for RNA-sequencing and microarray studies. *Nucleic Acids Res* **43**, e47 (2015).
59. J. Weiner 3rd, Domaszewska, T., tmod: an R package for general and multivariate enrichment analysis. *PeerJ Preprints* **4:e2420v1**, (2016).
60. J. Zyla, M. Marczyk, J. Weiner, J. Polanska, Ranking metrics in gene set enrichment analysis: do they matter? *BMC Bioinformatics* **18**, 256 (2017).
61. N. Eswar *et al.*, Comparative protein structure modeling using Modeller. *Curr Protoc Bioinformatics* **Chapter 5**, Unit-5 6 (2006).
62. M. Y. Shen, A. Sali, Statistical potential for assessment and prediction of protein structures. *Protein Sci* **15**, 2507-2524 (2006).
63. T. A. Halgren *et al.*, Glide: a new approach for rapid, accurate docking and scoring. 2. Enrichment factors in database screening. *J Med Chem* **47**, 1750-1759 (2004).

64. N. Huang *et al.*, Crystal structure of the heterodimeric CLOCK:BMAL1 transcriptional activator complex. *Science* **337**, 189-194 (2012).
65. C. Nüsslein-Volhard, Dahm, R., *Zebrafish*. C. Nüsslein-Volhard, Dahm, R., Ed., (Oxford University Press, 2002), pp. 303.
66. D. C. Nacci, L; Kuhn,A; Champlin, D; Munns, W; Specker, J; Cooper, K, Nondestructive indicator of ethoxyresorufin-O-deethylase activity in embryonic fish. *ENVIRONMENTAL TOXICOLOGY AND CHEMISTRY* **17**, 2481-2486 (1998).
67. V. Link, A. Shevchenko, C. P. Heisenberg, Proteomics of early zebrafish embryos. *BMC Dev Biol* **6**, 1 (2006).
68. S. Subramoni, V. Venturi, LuxR-family 'solos': bachelor sensors/regulators of signalling molecules. *Microbiology* **155**, 1377-1385 (2009).
69. A. Neumann, D. Patzelt, I. Wagner-Dobler, S. Schulz, Identification of new N-acylhomoserine lactone signalling compounds of Dinoroseobacter shibae DFL-12(T) by overexpression of luxI genes. *Chembiochem* **14**, 2355-2361 (2013).
70. M. Elasri *et al.*, Acyl-homoserine lactone production is more common among plant-associated Pseudomonas spp. than among soilborne Pseudomonas spp. *Appl Environ Microbiol* **67**, 1198-1209 (2001).
71. R. L. Ulrich *et al.*, Role of quorum sensing in the pathogenicity of Burkholderia pseudomallei. *J Med Microbiol* **53**, 1053-1064 (2004).
72. R. L. Ulrich, D. Deshazer, H. B. Hines, J. A. Jeddeloh, Quorum sensing: a transcriptional regulatory system involved in the pathogenicity of Burkholderia mallei. *Infect Immun* **72**, 6589-6596 (2004).
73. G. Brader, S. Sjoblom, H. Hyytiainen, K. Sims-Huopaniemi, E. T. Palva, Altering substrate chain length specificity of an acylhomoserine lactone synthase in bacterial communication. *J Biol Chem* **280**, 10403-10409 (2005).
74. A. M. Pomini, G. P. Manfio, W. L. Araujo, A. J. Marsaioli, Acyl-homoserine lactones from Erwinia psidii R. IBSBF 435T, a guava phytopathogen (Psidium guajava L.). *J Agric Food Chem* **53**, 6262-6265 (2005).
75. O. Geisenberger *et al.*, Production of N-acyl-L-homoserine lactones by P. aeruginosa isolates from chronic lung infections associated with cystic fibrosis. *FEMS Microbiol Lett* **184**, 273-278 (2000).
76. G. D. Geske, J. C. O'Neill, D. M. Miller, M. E. Mattmann, H. E. Blackwell, Modulation of bacterial quorum sensing with synthetic ligands: systematic evaluation of N-acylated homoserine lactones in multiple species and new insights into their mechanisms of action. *J Am Chem Soc* **129**, 13613-13625 (2007).
77. G. D. Geske, R. J. Wezeman, A. P. Siegel, H. E. Blackwell, Small molecule inhibitors of bacterial quorum sensing and biofilm formation. *J Am Chem Soc* **127**, 12762-12763 (2005).
78. V. Nagar, V. Sinha, J. R. Bandekar, Diverse Profiles of N-acyl Homoserine L-Lactones, Biofilm, Virulence Genes and Integrons in Food-Borne Aeromonas Isolates. *J Food Sci* **80**, M1861-1870 (2015).
79. A. L. Schaefer *et al.*, A new class of homoserine lactone quorum-sensing signals. *Nature* **454**, 595-599 (2008).
80. K. Riedel *et al.*, N-acylhomoserine-lactone-mediated communication between Pseudomonas aeruginosa and Burkholderia cepacia in mixed biofilms. *Microbiology* **147**, 3249-3262 (2001).
81. P. Williams, Quorum sensing, communication and cross-kingdom signalling in the bacterial world. *Microbiology* **153**, 3923-3938 (2007).
82. J. P. Kirwan *et al.*, Quorum-sensing signal synthesis by the Yersinia pestis acyl-homoserine lactone synthase YspI. *J Bacteriol* **188**, 784-788 (2006).

628 83. C. A. Ortori *et al.*, Comprehensive profiling of N-acylhomoserine lactones produced
629 by Yersinia pseudotuberculosis using liquid chromatography coupled to hybrid
630 quadrupole-linear ion trap mass spectrometry. *Anal Bioanal Chem* **387**, 497-511
631 (2007).
632 84. A. Rajput, K. Kaur, M. Kumar, SigMol: repertoire of quorum sensing signaling
633 molecules in prokaryotes. *Nucleic Acids Res* **44**, D634-639 (2016).
634 85. M. W. Tan, S. Mahajan-Miklos, F. M. Ausubel, Killing of Caenorhabditis elegans by
635 Pseudomonas aeruginosa used to model mammalian bacterial pathogenesis. *Proc Natl*
636 *Acad Sci U S A* **96**, 715-720 (1999).
637 86. E. K. Shiner *et al.*, Pseudomonas aeruginosa autoinducer modulates host cell
638 responses through calcium signalling. *Cell Microbiol* **8**, 1601-1610 (2006).

639

640 **Acknowledgments:** The authors gratefully acknowledge those who have provided tools and
641 materials for this work. Brigitta Stockinger (The Francis Crick Institute, London, UK) for the
642 *AhR*$^{-/-}$ mice. Clemens Grabher (Karlsruhe Institute of Technology, Karlsruhe, Germany) and
643 Daniela Panakova (Max Delbruck Center, Berlin, Germany) for the zebrafish AB WT strain.
644 Livia Leoni (University Roma Tre, Rome, Italy) for *P.aeruginosa* strains PA14 Δ*rsaL* and
645 PA14-R3; Burkhard Tuemmler (Medizinsche Hochschule Hannover, Germany) for PA14 WT
646 and PA14 09480; Fred Ausubel (Harvard Medical School/Massachusetts General Hospital,
647 Boston, USA) for PA14-GFP; Paul Williams (University of Nottingham, Nottingham, UK) for
648 PAO1 WT, PAO1 *pqsA* CTX-lux::*pqsA*. We acknowledge Uwe Klemm for mouse breedings
649 and Norman Fielko, Jens Otto, Andrey Fadeev (Max Planck Institute for Infection Biology,
650 Berlin, Germany) and Mariana Simões (Max Delbruck Center, Berlin, Germany) for zebrafish
651 breedings. Anne Diehl (Leibniz-Institut for Molekulare Pharmakologie, Berlin, Germany) for
652 technical help to prepare mouse liver lysates. A special thanks to Annemarie Meijer and
653 Vincenzo Torraca (University of Leiden, Leiden, The Netherlands) for the support in setting
654 up a zebrafish facility, zebrafish handling and experimental design; **Funding:** This work was
655 generously supported by the Max Planck Society; AS and MKB work was funded by the
656 European Research Council under the Horizon 2020 programme of the European Commission,
657 grant number 311371; FK and GBW acknowledge support from the Helmholtz BioInterfaces
658 in Technology and Medicine (BIFTM) program of KIT; **Author contributions:** PM-A and
659 SHEK conceived and designed the study and wrote the manuscript. PM-A designed and
660 performed experiments and data analysis. AP, GP, UG and MK provided technical help for in
661 vitro and in vivo experiments. AD, PS and CP performed mouse infection experiments. LL
662 performed and analysed Fluidigm experiments. MKB, AS and JF performed binding studies.
663 RH, FK and GBW performed and analysed HPLC experiments. AK, JP, GK and HO performed
664 virtual docking studies. HJM and JW performed and analysed microarray experiments. All

665 authors commented on the paper; **Competing interests:** Authors declare no competing
666 interests; **Data and materials availability:** All data is available in the main text or the
667 supplementary materials. Data are deposited in GEO under accession number GSE121101.

668 **Supplementary Materials:**

669 Materials and Methods

670 Figs. S1 to S11

671 Tables S1 to S11

672 References (55-86)

673

674 **Fig. 1. AhR modulation by *P. aeruginosa*. (A)** Scheme of AhR sensing of *P.aeruginosa* QS
675 molecules during infection. *P.aeruginosa* signalling cascade during different bacterial growth
676 stages. QS molecules depicted in black and proteins in coloured circles, with different colours
677 corresponding to each QS molecule. Black arrow with asterisk depicts known interaction
678 between *P.aeruginosa* phenazines and host AhR. **(B, C)** Luciferase activity of AhR reporter
679 THP-1 (monocytic) and A549 (pneumocytic) cells upon 24h **(B)** infection with *P.aeruginosa*
680 PA14-wild type (WT) strain grown in lysogeny broth (LB) medium, at a multiplicity of
681 infection (MOI) 50 (n=3 independent experiments) or **(C)** stimulation with *P.aeruginosa*
682 filtered supernatants (1:25 diluted), collected from different bacterial growth phases (n=4
683 independent experiments). **(D)** Expression of QS molecules in supernatants of PA14 WT,
684 detected by high-performance liquid chromatography (HPLC). Data from 1 representative
685 experiment out of 2 independent experiments. **(E-G)** Luciferase activity of AhR reporter THP-
686 1 and A549 cells upon 4h stimulation with different concentrations of *P.aeruginosa*
687 homoserine lactones (3-o-C12-L-HSL or C4-L-HSL) and quinolones (HHQ or PQS) in **(E)**
688 absence (THP-1 (n=6) or A549 (n=4) independent experiments) or **(F,G)** presence of
689 *P.aeruginosa* 1-hydroxyphenazine (1-HP; pooled data from: F- THP-1 (n=3) or A549 (n=4)
690 independent experiments; G- THP-1 (n=3), A549 top (n=9), A549 bottom (n=3) independent
691 experiments). **(H)** *CYP1A1* gene expression upon 24h stimulation of A549 cells with QS
692 molecules. Data from 1 representative experiment out of at least 3 independent experiments
693 (n=3 biological replicates). **(I, J)** CYP1A1 enzymatic activity after 24h stimulation of Hepa-
694 1c1c7 cells with **(I)** 1-HP (50 μM), in **(J)** presence or absence of other QS molecules. Data are
695 pooled from: I (n=7) or J (n=4) independent experiments. Pyo: pyocyanin, 1-HP: 1-

hydroxyphenazine, PCA: phenazine-1 carboxylic acid, PCN: phenazine carboxamide, 3-o-C12-L-HSL: N-(3-oxodecanoyl)-L-homoserine lactone, C4-L-HSL: N-butyril-L-homoserine lactone, HHQ: 4-hydroxy-2-heptylquinoline, PQS: 2-heptyl-3,4- dihydroxyquinoline, IQS: 2-(2 -hydroxylphenyl)-thiazole-4-carbaldehyde. **(B-C,E-G,I)** Means +/- S.E.M. are depicted **(H)** Means +/- S.D. are depicted. **(B,C,E,F,H, J)** One-way ANOVA. **(I)** Two-tailed Student's t-test. * $p<0.05$, ** $P<0.01$, *** $p<0.001$, **** $p<0.0001$.

Fig. 2- Binding of *P.aeruginosa* QS molecules to AhR. **(A)** *In silico* docking of *P.aeruginosa* QS molecules into the AhR ligand binding pocket. **(B,C)** Binding of QS molecules to AhR measured by **(B)** displacement of radioactive[^{3}H] labelled 2,3,7,8-tetrachlorodibenzodioxin (TCDD, [^{3}H]TCDD) from AhR in WT mouse liver cytosol and **(C)** Microscale thermophoresis assay. **(B)** (Kd values: 3-o-C12-L-HSL=4.67 µM HHQ=3.77 µM; 1-HP=4.48 µM). **(C)** (Kd values: 3-o-C12-L-HSL= 2.69 µM; PQS= 130 µM ; 1-HP= 1.18 µM). **(B)** Data are pooled from: 3-o-C12-L-HSL (n=3), C-4-L-HSL (n=2), HHQ (n=4), PQS (n=2) or 1-HP (n=3) independent experiments **(C)** Data are pooled from: 3-o-C12-L-HSL (n=4), C4-L-HSL (n=3), PQS (n=4) or 1-HP (n=4) independent experiments.

Fig. 3- AhR dependent responses. **(A)** Western blot detection of AhR protein expression in A549 CRISPR Scramble control and CRISPR AhR-KO cells. **(B-D)** Degradation of **(B,C)** 3-o-C12-L-HSL or **(D)** HHQ, measured in the supernatants of stimulated A549 CRISPR cells, compared to control without cells. 3-o-C12-L-HSL expression levels detected by **(B)** bacterial PA14-R3 bioluminescence reporter assay (n=3 independent experiments) or **(C)** HPLC (n=3 independent experiments), and **(D)** expression of HHQ detected by HPLC (n=4 independent experiments). **(E,F)** Gene expression analysis of different cytokines and chemokines in A549 CRISPR cells upon 24h stimulation with *P. aeruginosa* QS molecules. Data are pooled from: 3-o-C12-L-HSL (n=6), HHQ (n=5) or 1-HP (n=7) independent experiments. **(B-D,F)** Data depicted as means +/- S.E.M. **(B)** Two-way ANOVA. **(F)** Two-tailed Student's t-test. n.s.- not significant, *$p<0.05$, **$p<0.01$, ***$p<0.001$ and **** $p<0.0001$.

Fig. 4-AhR activation by *P.aeruginosa* QS molecules in zebrafish larvae. **(A)** Expression of 3-o-C12-L-HSL and Pyo in supernatants of *P.aeruginosa* (PA14) WT strain, collected at different growth phases in LB medium. 3-o-C12-L-HSL determined by PA14-R3 bioluminescence reporter assay and Pyo concentrations evaluated by spectrophotometry (n=9 independent experiments). **(B-D)** *cyp1a* expression in 2dpf zebrafish larvae **(B,D)** infected by immersion with PA14WT strain or **(C)** exposed to bacterial supernatants for 5h (n=7 independent experiments). **(B,D)** Infection with **(B)** different bacterial loads collected from various phases of PA14 WT growth, according to the defined final OD600 in E3 (adjusted to Early log-OD600=0.2; Mid log-OD600=0.7; Late log-OD600=1; n= 3 independent experiments) or **(D)** $1x10^9$ colony forming units (CFU)/mL infection with PA14WT collected from various phases of bacterial growth (n=7 independent experiments). **(E)** Gene expression analysis of *cyp1a*, *ahrra* and *ahrrb* transcripts from zebrafish larvae (2 days post-fertilization, dpf) treated (red) or untreated (blue) for 2h with 5 µM of the AhR inhibitor CH223191, followed by further 4h exposure with 1-HP (5 µM) or DMSO vehicle control. One representative experiment out of at least 3 independent experiments. Triplicates of 12 larvae depicted at each data point. **(F)** Cyp1a protein expression detected by Western Blot analysis in 2dpf zebrafish larvae treated for 24h with DMSO, 1-HP (5 µM), in the presence or absence of CH223191 (5 µM). **(G)** Cyp1a enzymatic activity expressed as total intensity of resorufin (EROD assay) detected per 2dpf larvae treated (red) or not (blue) for 2h with CH223191 (5 µM) followed by further 4h exposure with 1-HP (5 µM) or DMSO vehicle control (each dot represents one larvae). One representative experiment out of at least 3 independent experiments. **(H,I)** Microarray analysis of 2dpf larvae pre-exposed to DMSO or CH223191 (5µM) for 2h, followed by 4h exposure to 1-HP (5µM) or DMSO, in the presence or absence of CH223191 (5µM). Pooled data from 5 independent experiments. **(H)** Venn diagram depicting the differentially expressed genes and **(I)** AhR gene enrichment curve. **(A-D)** Means +/- S.E.M. are depicted. **(E)**. Means +/- S.D. are shown. **(G)** Medians are depicted. **(B-E,G)** One-way ANOVA. * $p<0.05$, ** $P<0.01$, *** $p<0.001$, **** $p<0.0001$.

Fig. 5- AhR modulation by *P.aeruginosa* QS molecules in zebrafish larvae. **(A,B)** Cyp1a **(A)** gene expression and **(B)** enzymatic activity upon 4h exposure of 2dpf larvae to diverse *P.aeruginosa* QS molecules or TCDD. One representative experiment out of at least 3 independent experiments; (A) triplicates of 12 larvae depicted at each data point; (B) each dot

represents one larvae. **(C)** Expression of 3-o-C12-L-HSL and Pyo in supernatants of *P.aeruginosa* (PA14) WT strain, collected at different growth phases in LB medium. **(C)** Expression of 3-o-C12-L-HSL and Pyo in the supernatants of different PA14 strains collected at Mid log growth phase. 3-o-C12-L-HSL determined by PA14-R3 bioluminescence reporter assay and Pyo concentrations evaluated by spectrophotometry (n=6 independent experiments). **(D,E)** Infection of 2dpf zebrafish larvae by immersion for 5h with $1x10^9$ CFU/mL of different *P.aeruginosa* strains collected at Mid log growth phase. One representative experiment out of at least 3 independent experiments; (D) triplicates of 12 larvae depicted at each data point; (E) each dot represents one larvae. **(D)** *cyp1a* gene expression and **(E)** Cyp1a enzymatic activity. **(A,D)** Means +/- S.D. are shown. **(B,E)** Medians are depicted **(C)** Means +/-S.E.M. are depicted. **(A,B,D,E)** One-way ANOVA. * $p<0.05$, ** $P<0.01$, *** $p<0.001$, **** $p<0.0001$.

Fig. 6- AhR mediated responses upon *P.aeruginosa* infection in mice. **(A)** Bacterial clearance in the lungs of WT and AhR-knockout ($AhR^{-/-}$) mice after 8h of infection with *P.aeruginosa* PA14 09480 ($2x10^6$ colony forming units (CFU) administered per mouse). Bacterial growth phases: early log-OD600<0.3; mid log- 0.5<OD600<0.8 and late log-OD600>1. Each dot represents 1 mouse (n=2 independent experiments). **(B-D)** Infection of WT and $AhR^{-/-}$ mice for 8h with PA14 WT or PA14 Δ*rsaL* strains (pooled data from 2 independent experiments). **(B)** Gene expression analysis of different cytokines and chemokines in the lungs of infected mice, compared to the respective non-infected mouse strain (WT: n=8 and $AhR^{-/-}$: n=6 mice) **(C)** Cytokine and chemokine protein levels in lung homogenates after infection. Each dot represents 1 mouse (n=2 independent experiments) **(D)** Neutrophil numbers in the lungs of infected and non-infected mice. Each dot represents 1 mouse (n=2 independent experiments). **(A,C,D)** Medians are depicted. **(B)** Means +/- S.E.M. are depicted. **(A, D)** Mann-Whitney U-test. **(B)** Two-tailed Student's t-test. **(C)** Two-way ANOVA). * $p<0.05$, ** $P<0.01$, *** $p<0.001$, **** $p<0.0001$.

Science
AAAS

Supplementary Materials for

Host monitoring of quorum sensing during *Pseudomonas aeruginosa* infection

Pedro Moura-Alves[1,2*], Andreas Puyskens[1], Anne Stinn[1,3,4,5], Marion Klemm[1], Ute Guhlich-Bornhof[1], Anca Dorhoi[1,6,7], Jens Furkert[8], Annika Kreuchwig[8], Jonas Protze[8], Laura Lozza[1,9] , Gang Pei[1], Philippe Saikali[1], Carolina Perdomo[1], Hans J. Mollenkopf[10], Robert Hurwitz[11], Frank Kirschhoefer[12], Gerald Brenner-Weiss[11], January Weiner 3[rd1], Hartmut Oschkinat[8], Michael Kolbe[3,4,5] , Gerd Krause[8], Stefan H.E. Kaufmann[1,13*]

[1]Max Planck Institute for Infection Biology, Department of Immunology, Charitéplatz 1, 10117 Berlin, Germany.[2]Nuffield Department of Clinical Medicine, Ludwig Institute for Cancer Research, University of Oxford, Oxford, UK.[3]Max Planck Institute for Infection Biology, Structural Systems Biology, Charitéplatz 1, 10117 Berlin, Germany.[4]Department of Structural Infection Biology, Centre for Structural Systems Biology (CSSB), Helmholtz-Centre for Infection Research (HZI), Notkestraße 85, 22607 Hamburg, Germany. [5]Faculty of Mathematics, Informatics and Natural Sciences, University of Hamburg, Rothenbaumchaussee 19, 20148 Hamburg, Germany.[6]Institute of Immunology, Friedrich-Loeffler Institut, Greifswald - Insel Riems, Germany.[7]Faculty of Mathematics and Natural Sciences, University of Greifswald, Greifswald, Germany.[8]Leibniz-Forschungsinstitut für Molekulare Pharmakologie (FMP), Robert-Rössle-Strasse 10, 13125 Berlin, Germany.[9]Epiontis GmbH - Precision for Medicine, Barbara-McClintock- Str. 6, 12489 Berlin, Germany.[10]Microarray Core Facility, Max Planck Institute for Infection Biology, Department of Immunology, Charitéplatz 1, 10117 Berlin, Germany.[11]Protein Purification Core Facility, Max Planck Institute for Infection Biology, Charitéplatz 1, 10117 Berlin, Germany.[12]Institute of Functional Interfaces, Karlsruhe Institute of Technology, Karlsruhe, Germany. [13]Hagler Institute for Advanced Study at Texas A&M University, College Station, TX 7843.

*Correspondence to: pedro.mouraalves@ludwig.ox.ac.uk; kaufmann@mpiib-berlin.mpg.de

This PDF file includes:

Materials and Methods
Figs. S1 to S11
Tables S1 to S11
References 55-86

Materials and Methods

Cells

THP-1 (human monocytes, ATCC TIB-202) and THP-1 AhR reporter(*10*) cells were grown in RPMI 1640 (GIBCO), supplemented with 10% (v/v) heat-inactivated fetal calf serum (FCS; GIBCO), 1% (v/v) penicillin–streptomycin (GIBCO), 1% (v/v) sodium pyruvate (GIBCO), 1% (v/v) L-glutamine (GIBCO), 1% (v/v) non-essential amino acids (GIBCO), 1% (v/v) HEPES buffer (GIBCO) and 0.05 M 2-mercaptoethanol (GIBCO). HEK293T (human embryonic kidney epithelial cells, ATCC CRL-11268), A549 cells (human type II pneumocytes, ATCC CRL-11268), A549 AhR reporter(*10*) and Hepa-1c1c7 (mouse hepatocytes, ATCC CRL-2026) were grown in DMEM (GIBCO), supplemented with 10% (v/v) Fetal Calf Serum (FCS), 1% (v/v) penicillin–streptomycin, 1% (v/v) sodium pyruvate, 1% (v/v) L-glutamine and 1% (v/v) HEPES buffer. All AhR reporter cell lines were kept with additional 5 mg/mL of Puromycin (Calbiochem). For CYP1A1 enzymatic activity measurements, Hepa-1c1c7 cells were kept in DMEM medium without Phenol Red (GIBCO). Cells were kept at 37ºC in 5% CO_2. THP-1 cells were differentiated into macrophages with 200 nM of phorbol 12-myristate 13-acetate (PMA, Calbiochem). Upon differentiation with PMA, cells were washed and kept in medium for 4d before further experiments.

Lentiviral production

Lentiviruses were produced according to the described TRC lentiviral proceedings (https://www.broadinstitute.org/genome_bio/trc/publicProtocols.html). Briefly, HEK293T cells were seeded at a density of 2×10^5 cells/ml in DMEM without antibiotics in 96 well plates. After 24h incubation, cells were transfected with lentiviral packaging mix (Sigma-Aldrich) and 100 ng of the respective CRISPR lentiviral vector (listed in Table S6) containing pLV-U6g-EPCG vector (Sigma Aldrich), using Fugene 6 (Roche, Berlin, Germany) in Optimem medium (Gibco). After 18h of incubation, medium was replaced with high serum growth medium (30% FCS (v/v)). Viruses were harvested at 48h and 72h post-transfection. The lentiviral construct for the generation of AhR reporter cell lines was obtained from SABiosciences (http://www.sabiosciences.com/reporter_assay_product/HTML/CLS-9045L.html).

Lentiviral infection for CRISPR generation and AhR Reporter cells

Lentiviral infection was performed as described previously(*10*) and according to the protocols available at RNAi Consortium website (https://portals.broadinstitute.org/gpp/public/). A similar protocol was used to generate the A549 CRISPR Scramble and A549 CRISPR AhR-KO or to produce the Hepa-1c1c7 AhR reporter cell line. In brief, cells were seeded at a density of $2.2x10^4$ cells per well in a 96 well plate (NUNC). The following day, supernatants were removed and lentiviruses were added to the cells in medium containing 8 µg/ml of polybrene (Sigma-Aldrich). Plates were spun down for 90 min at 2200 rpm at 37ºC. Transduced cells were further selected using Puromycin (Calbiochem; 5 mg/ml) 2d after infection. For CRISPR cell lines, based on their GFP expression, cells were single cell sorted (FACSAria II, BD Biosciences) into 96 well plates and further expanded. After expansion, DNA was extracted and sequenced to verify the KO efficiency. Further validation was performed by Western blot (WB) detection.

Bacterial ligands, analogues, chemicals and AhR controls

All ligands used in this study were obtained from either academic or commercial sources, as depicted in Table S7. TCDD was provided in toluene, and solvent was exchanged to DMSO and further stored at 4°C. All other ligands were solubilized in DMSO, and kept at RT, 4°C or 20°C, as mentioned in Table S7.

Luciferase assay

AhR reporter cell lines were challenged for the specified time and concentration of ligands, bacteria or bacterial culture supernatants. Afterwards, cells were harvested in reporter lysis buffer (Promega) and lysates were used to determine luciferase activity using Luciferase Assay System (Promega) according to manufacturer's instructions. Luciferase activity was normalized to the amount of protein determined by Bradford reaction (Pierce Coomassie Plus, Pierce). Results are shown as fold induction determined upon normalization to the luciferase values of the respective control.

Gene expression analysis by quantitative real time PCR and fluidigm

Total RNA was extracted using RNeasy Plus Mini kit (Qiagen) and RNA quality and concentration determined by spectrophotometry (Nanodrop 2000c, Thermo Fisher Scientific). Complementary

DNA (cDNA) synthesis was carried out using iScript cDNA synthesis kit (Biorad) according to manufacturer's instructions. Quantitative RT-PCR (qRT-PCR) was performed using Power SYBR green Roche LightCycler® 480 Instrument II. The average threshold cycle of triplicate reactions was used for all subsequent calculations using the △△Ct method(*55*). Gene expression was normalized to the glyceraldehyde-3-phosphate dehydrogenase (GAPDH) or β-actin of the respective samples, for human and zebrafish, respectively. qRT-PCR data were generated from independent experiments, with 3 biological replicates per experiment. Primer and probe sequences are listed in Table S8.

Fluidigm gene expression was performed with the 96.96 Dynamic Array Integrated Fluidic Circuits from Fluidigm, as previously described(*56*). Preamplification of genes by reverse transcription and cDNA synthesis (18 cycles) was performed with Cells Direct one-Step qPCR kit (Life Technologies, Inc.). Gene expression was evaluated using TaqMan gene expression assay mix (Applied Biosystems) normalized to GAPDH. TaqMan probes are listed in Table S8. Data represent fold changes (2−ΔΔCT) in transcripts relative to the appropriate internal control (DMSO). qRT-PCR data were generated from technical replicates from at least 5 independent experiments.

Ethoxyresorufin-O-deethylase (EROD) activity in hepatocytes

The EROD assay was used to detect the CYP1A1 enzymatic activity in Hepa-1c1c7 cells by measuring the conversion of ethoxyresorufin to resorufin(*57*). Briefly after stimulation of the cells with the diverse ligands, 4 µM resorufin ethyl ether (EROD, Sigma-Aldrich) and 10 µM dicoumarol (Sigma-Aldrich) were added to cell culture for 1h, followed by measuring the relative fluorescence of resorufin using a TECAN Infinite M200 pro plate reader (TECAN). The activity was corrected to the amount of protein, measured by Bradford reaction (Pierce Coomassie Plus, Pierce), and normalized to the respective control as mentioned in each figure legend.

Lactate dehydrogenase (LDH) assay

LDH was determined using the Cytotoxicity Detection Kit Plus (Roche) according to the manufacturer's instruction. Percentage (%) of cytotoxicity was calculated as:

$$\text{Cytotoxicity}(\%) = \frac{\text{experimental value} - \text{low control}}{\text{high control} - \text{low control}} \times 100$$

Percentage of infection and Caspases 3/7 positive cell determination

Caspase activity was determined using the Cell Event Caspase 3/7 Green detection reagent (Thermo Fisher Scientific) according to manufacturer's protocol. In brief, after different stimulations, cell nucleus was labelled using NucRed Live 647 Ready probes (Thermo Fisher Scientific). Cells were then labelled with the Caspase 3/7 Green detection reagent for 30 min and images were acquired in an Array Scan TM XTI Live High Content Platform (Thermo Fisher Scientific). After acquisition, nuclear labelling was used to identify cells and green fluorescence spots were used to determine caspase 3/7 positive cells.

A similar approach was used to determine the percentage of infected cells. In short, nuclear staining was used to identify the cell and green fluorescence spots of bacteria (PA14-GFP) to assign infected cells.

Western blot

Cell lysates were prepared using RIPA buffer (Cell Signaling technology) containing Complete protease inhibitor cocktail (Roche). Lysates were boiled at 95°C for 10 min in presence of Sample Buffer (Biorad), loaded in Mini-protean TGX precast Polyacrylamide gels (Biorad) and further transferred into nitrocellulose membranes (Biorad). Protein expression was detected upon incubation with specific antibodies for each protein (Table S9), and visualized using SuperSignal West Pico Plus (Thermo Fisher Scientific) on a ChemiDoc Imaging System (Biorad).

Pyo determination by spectrophotometry

Pyo concentration was determined by spectrophotometry as previously described(*10, 41, 43*). Briefly, optical density at 690 nm (OD 690 nm) was measured and the relative Pyo concentrations were determined by comparison with a Pyo standard curve. Concentrations of secreted Pyo from different bacteria were measured after filtration of supernatants using 0.22 μm Spin-X centrifuge tube filters (Corning). Concentrations of Pyo in the water from Zebrafish larvae infection studies were determined directly in the water collected at the indicated time points after infection with different strains and growth conditions of *P.aeruginosa*.

QS molecules determination by HPLC

P.aeruginosa culture supernatants (2 mL) were extracted two times with Ethylacetate/0.5% (v/v) acetic acid. The organic phases (containing phenazines, quinolones and homoserine lactones) were evaporated, extracts dissolved in methanol (100 µL) and centrifuged for 5 min at 10000 g to remove insoluble material. Under these conditions, Pyo was extracted into the aqueous phase, which was lyophilized and further dissolved in 2 mL chloroform/methanol (2:1) and 1 mL water. The Pyo containing chloroform phase was acidified with 10 µL of 1N HCl and extracted with 1 mL of methanol/water (1:1). The aqueous upper phase was dried by rotary evaporation and dissolved in 200 µL methanol and 4 µl of these extracts were loaded onto a Waters Acquity UPLC-column (2.1 x100 mm HSS C18, 1.8 µm). Compounds were eluted with a linear gradient from 20% acetonitrile to 100% acetonitrile containing 10 mM ammonium acetate, pH5.5 at 45°C at a flow rate of 0.5 ml/min within 6 min. Phenazines were detected and identified by UV/Vis (Waters PDA Detector) and ESI-MS (Waters QDa detector). The QDa detector was operated in an electrospray positive ion mode by applying a voltage of 0.8 kV. The cone voltage was set at 15 V. The probe temperature was set at 600 °C. A full mass spectrum between m/z 100 and 1000 was acquired at a sampling rate of 2.0 points/sec: 1-HP: Molecular weight: 196.2, m/z found for [M+H]+: 197.1; PCA: Molecular weight: 224.4, m/z found for [M+H]+: 225.2; PCN: Molecular weight: 223.2, m/z found for [M+H]+: 224.1; Pyo: Molecular weight: 210.2, m/z found for [M+H]+: 211.3. Quantification of phenazines was performed by integration of the UV-absorbance peaks at 370nm and 330nm. A five point calibration from 1 to 200 pmol of the standard compounds was prepared for the quantification.

LC-MS/MS analysis for target quantification

Mass spectrometric (MS) analysis was performed using an API 4000TM quadrupole mass spectrometer (Applied Biosystems / MDS Sciex Toronto, Canada), equipped with an electro spray ionization (ESI) source. MS spectra were generated by infusion experiments using a syringe pump (Harvard Apparatus Inc. South Natick, MA, USA). Single MS experiments (Q1-scan) and MS/MS experiments (product ion scan, PIS) were used to retrieve structural information. Nitrogen 5.0 was used as curtain gas, nebulizer gas and collision gas. The standard compounds of 3-o-C12-HSL, C4-HSL and HHQ were diluted in a solvent mixture of acetonitrile/0.1% acetic acid (50:50, v/v) and infused with a flow rate of 0.80 ml/h. MS experiments were carried out in the positive

ionization mode using an ion spray voltage (IS) of 4800 V, a declustering potential (DP) of 30 V and an entrance potential (EP) of 10 V. MS/MS experiments were generated using the compound optimization mode in the software Analyst V 1.6. For all targets, three mass transitions (one quantifier and two qualifiers) were selected (Table 1).

Table 1–LC-MS/MS analysis of 3-o-C12-L-HSL, C4-L-HSL and HHQ.

Target compound	Mw [g/mol]	m/z Quantifier	m/z Qualifier 1	m/z Qualifier 2
3-o-C12-L-HSL	297.39	298.2/102.2	298.2/197.2	298.2/74.1
C4-L-HSL	171.20	172.1/102.1	172.1/71.0	172.1/43.1
HHQ	243.34	244.0/159.0	244.0/172.0	244.0/130.0

An Agilent 1100 HPLC system (Agilent Waldbronn, Germany) was used for sample separation on a Nucleosil-C4 120A, 5µm column (100x4mm). A gradient of acetonitrile and 0.1% acetic acid (Table 2) was used by a total run time of 30 min. The ion source temperature was set to 400°C and a flow rate of 500µL/min was applied. The injection volume for all samples was 20 µL. A five-point calibration from 0 to 50 ng/mL was prepared for quantification of the extracted targets.

Table 2–Acetonitrile and acetic acid gradient

Time, min	Flow, µL/min	Acetonitrile Concentration, %
0.00	500	50
2.00	500	50
8.00	500	90
15.00	500	90
16.00	500	50
30.00	500	50

For the quantification of PQS, a separate UPLC-MS/MS method was developed. An Exion UPLC system (AB Sciex, Toronto, Canada) was used for sample separation on a Kinetex XB-C18 100A, 2.6 µm (100x2.1mm) at 45°C. A gradient (Table 3) of acetonitrile/water 95:5 v/v + 0.1% formic acid and water containing 2 mM picolinic acid + 0.1% formic acid was used, at a total run time of 3.40 min. The ion source temperature was set to 600°C and a flow rate of 900 to 1000 µL/min was applied. The injection volume for all samples was 4µL. A five-point calibration from 1 to 50 ng/mL was prepared for quantification of the extracted targets.

Table 3 –Gradient used for PQS determination.

Time, min	Flow, µL/min	Acetonitrile/water 95:5 v/v + 0.1% formic acid concentration, %
0.00	900	85.0
0.05	900	85.0
0.30	900	77.5
1.90	1000	45.0
2.20	1000	10.0
2.35	1000	10.0
2.45	900	85.0
3.40	900	85.0

For PQS, three mass transitions (one quantifier and two qualifiers) were selected (Table 4).

Table 4 LC-MS/MS analysis of PQS.

Target compound	Mw [g/mol]	m/z Quantifier	m/z Qualifier 1	m/z Qualifier 2
PQS	259.34	260.2/174.9	260.2/146.4	260.2/188.2

QS molecules determination using bacterial reporter strains

The expression of 3-o-C12-L-HSL and HHQ was determined using the PA14-R3 and PAO1 *pqsA* CTX-lux::*pqsA* bacteria reporters, respectively, and according to established protocols(*27, 28*). In short, PA14-R3 was streaked on LB plates, and colonies were further picked to inoculate LB medium. After overnight incubation (220 RPM, 37°C), the bacterial culture was further diluted in LB and re-grown for 2h. Optical density (OD600 nm) was determined and culture was diluted to OD600=0.045, in LB containing 50 mM of MOPS (Sigma). Diluted bacterial culture (180 µL) was transferred into transparent bottom 96 well black plates (Corning), and 20 µL of the positive control (3-o-C12-L-HSL at diverse concentrations) or the samples were added. The plate was incubated for 4h (100 RPM, 37°C) and further assayed for bioluminescence and OD600 in a TECAN200. Similarly, PAO1 *pqsA* CTX-lux::*pqsA* colonies were incubated overnight (220 RPM, 37°C) in LB containing 125 µg/mL tetracycline. After further dilution and 2h incubation (220 RPM, 37°C), OD600 was adjusted to 1 in LB containing the antibiotic. A dilution of 1:50 or 1:100 of the culture was placed in a transparent bottom 96 well black plate (Corning) and 100 µL of the positive control (HHQ at diverse concentrations) or the samples were added. The plate was incubated at 37°C (120 RPM) and bioluminescence and optical densities (OD600) were determined every 30 min. In both cases, luminescence values were normalized per cell density.

Degradation assays

In the 3-o-C12-L-HSL and HHQ degradation assays, A549 CRISPR Scramble and A549 CRISPR AhR-KO cells were stimulated with the respective QS molecule, and supernatants collected at different time points. The cell free supernatants were used to stimulate bacterial QS reporters, PA14-R3 and PAO1 *pqsA* CTX-lux::*pqsA* for the detection of 3-o-C12-L-HSL and HHQ, respectively. Simultaneous experiments were performed under conditions without cells to determine the natural decay of each compound in the cell medium. Relative QS levels were determined by comparison with the bioluminescence detected in the 'input' (i.e., cell medium containing the initial QS concentration used to stimulate the cells). HPLC experiments were performed using the protocol described above.

Microarray hybridization

Total RNA was isolated with Trizol (Invitrogen) following the manufacturer´s protocol using glycogen as co-precipitant. Quality control and quantification of total RNA was analysed using an Agilent 2100 Bioanalyzer (Agilent Technologies) and a NanoDrop 1000 UV-Vis spectrophotometer (Thermo Fisher Scientific). Microarray experiments were performed as single-color hybridization. Total RNA was amplified and labelled with the low input Quick-Amp Labeling Kit (Agilent Technologies). In brief, mRNA was reverse transcribed and amplified using an oligo-dT-T7 promoter primer and labelled with cyanine 3-CTP. After precipitation, purification, and quantification, 0.75 µg labelled cRNA was fragmented and hybridized to custom whole genome human 8 × 60K multipack microarrays (Agilent-048908) or 1.25 µg labelled cRNA was fragmented and hybridized to catalogue 4x44K Zebrafish (v3) gene expression microarrays (Agilent-026437) according to the supplier's protocol (Agilent Technologies). Scanning of microarrays was performed with either 3 µm resolution (8x60K) or extended dynamic range (XDR) and 5 µm resolution (4x44K) using a G2565CA high-resolution laser microarray scanner (Agilent Technologies). Microarray image data were processed with the Image Analysis/Feature Extraction software G2567AA v. A.11.5.1.1 (Agilent Technologies) using default settings and the GE1_1105_Oct12 extraction protocol. The extracted .txt files were further analysed using R and the associated BioConductor limma package(*58*). Microarray data have been deposited in the Gene Expression Omnibus (GEO; www.ncbi.nlm.nih.gov/geo/) of the National Center for Biotechnology Information and can be assessed with the GEO accession number GSE121101.

Microarray analysis

For differential gene expression analysis, the limma R package(*58*) was used. Contrasts were defined for comparison between each experimental condition and treatment with DMSO. In infection experiments, results were compared to non-infection controls. For comparison between treatments, the interaction between treatment (1-HP, 1-HP+3-o-C12-L-HSL, 3-o-C12-L-HSL or DMSO) and the experimental conditions in the presence or absence of CH223191 was tested.

Gene set enrichment analysis was performed using the tmod R package(*59*). Genes were ordered by the gene expression effect size metrics MSD(*60*). A custom gene set was defined for the xenobiotic metabolism based on current literature (Table S11) and enrichment was tested using the CERNO algorithm and the predefined module.

Homology modelling

A BLAST search with the sequence of hAhR PASB as a template revealed 58 hits in the Protein Data Bank (PDB) of experimental crystal structures. Based on sequence alignment, similarities as well as bound ligands of 7 crystal structures were selected for a multiple sequence alignment. This was then used to build a multiple template based homology model of hAhR PASB. X-ray complexes (PDB ID): 3F1O, 4F3L, 4GHI, 4GS9, 4H6J, 5TBM (chain A) and 4ZPR (chain B) were downloaded from the PDB and the respective chains were isolated. Modeller 9.17(*61*) was used to create the multiple template based homology model of hAhR. The resulting models were ranked by DOPE scoring(*62*). The best scoring model was selected for subsequent modelling activities. Then, model quality was checked and the Protein Preparation wizard included in Maestro11 software (Schrödinger, LLC, New York, NY, 2017) was used to adjust structural defects using default values. All ligands were downloaded from Pubchem and thereafter analysed by the Ligand Preparation Wizard to correct improper connectivity.

Docking studies

Molecular docking was carried out using Glide included in Maestro 11v0 software(*63*) (https://www.schrodinger.com/maestro). Glide docking methodologies use a series of hierarchical filters searching for possible ligand positions in the receptor binding-site. The first step in molecular docking via Maestro11v0 is to set up the receptor grid defining shape and properties of the receptor binding site, important for scoring the ligand poses in a later step. Ligand flexibility

is accounted for by exhaustive sampling of ligand torsions during the docking process. Suitable poses are selected in a next step for further refinement of torsional space in the field of the receptor. Finally, in a post-docking minimization the selected poses are minimized with full ligand flexibility. The docking results are ranked by GlideScore, an empirical scoring function yielding an estimate of the binding affinity and designed to maximize separation of compounds with strong binding affinity from those with low to no binding ability(*63*).

The receptor grid for the hAhR homology models was set up using default parameters. Flexible ligand docking was carried out in standard precision (SP). The Molecular Mechanics-Generalized Born Surface Area application MM-GBSA was used for rescoring the docking poses. MM-GBSA binding energies (ΔG^{Bind}) are approximate free binding energies of protein-ligand complexes, with a more negative value indicating stronger binding.

AhR binding studies - Radioactive labelled TCDD competition

Radioligand experiments were performed as described previously (*10*). In brief, livers from wild type (WT) and AhR knockout ($AhR^{-/-}$) mice were collected and minced in 3-fold (w/v) MDEG buffer (25 mM MOPS, 1 mM DTT, 1 mM EDTA and 10 % Glycerol, pH 7.5). Lysates were further homogenized using gentleMacs (Miltenyi), and subsequently ultracentrifuged at 100000 g for 1h. Cytosolic fraction was collected, protein concentration determined by Bradford reaction (Protein Assay Kit, Pierce) and further diluted to final concentration of 5 mg of cytosol protein/mL in MDEG buffer. The entire procedure was carried out at 4°C. Binding studies were performed by incubating the extracts 48h at 4°C with [^{3}H] TCDD and with or without an excess of unlabelled TCDD. After incubation, 30 µL of a charcoal Norit A suspension (100 mg/mL in previously prepared MDEG buffer) was added into 200 µl of the reaction mixture and incubated on ice for 15 min. Following centrifugation at 25000 g for 15 min at 4°C, 130 µL of the supernatant was removed and radioactivity was measured in a scintillation counter (Tri-Carb 3110TR, PerkinElmer). Specific binding was defined as the difference of radioactivity between AhR-proficient and AhR-deficient extracts. For competition assays, serial dilutions of competitor molecules (3-o-C12-L-HSL, C4-L-HSL, HHQ and PQS) were incubated together with [^{3}H]TCDD and the corresponding IC50 values determined. Bmax and K_d were calculated by nonlinear regression (GraphPad Prism version 7.0, San Diego, CA), fitting a saturation isotherm. IC50 values

were obtained by fitting a one-site competitive binding equation to the experimental data. K_i values were derived from IC50 using the Cheng-Prusoff equation.

AhR binding studies - Microscale Thermophoresis (MST)

A codon-optimized fragment of the human AhR encoding amino acid residues 23–475 was commercially synthesized (MWG Eurofins) and cloned into pET21b (Novagen). The pET30-EK/LIC-mARNT expression plasmid encoding the murine ARNT (residues 85-465) was a kind gift from Prof. Oliver Daumke (MDC Berlin). For protein expression, BL21(DE3) cells were co-transformed with both plasmids. Bacteria were grown in LB medium and expression was induced at an OD600 of 0.6 with 0.5 mM isopropyl-β-D-thiogalactopyranoside (IPTG), followed by an incubation over night at 16°C. Proteins were purified as previously described for other bHLH-PAS proteins(*64*). Briefly, cell pellets were resuspended in lysis buffer containing DNaseI (Serva) and Complete Protein Inhibitor Cocktail (Roche) and lysed using a French Cell Press. The clarified lysate was applied onto a HisTALON™ Superflow™ column (Clontech) and bound protein eluted with 300 mM imidazole. N-terminal 6xHis-tag was cleaved off with PreScission protease at 4°C. The protein complex was further purified on a HiTrap Heparin HP column (GE Healthcare), followed by SEC on a Superdex 200 10/300 GL equilibrated in 20 mM HEPES pH 8.0, 300 mM NaCl, 5% glycerol, and 5 mM DTT. Peak fractions containing the AhR-Arnt complex were pooled and concentrated using Amicon filter units (Millipore). Binding of ligands to the AhR-Arnt complex was assessed by microscale thermophoresis (MST) experiments using the Monolith® NT.LabelFree (NanoTemper Technologies GmbH). MST measurements were performed according to the manufacturer's instructions. In brief, a constant protein concentration of 250 nM (final) diluted in assay buffer including 0.1% Pluronic F-127 was used. After a short incubation at RT, the samples were centrifuged for 5 min at 16000xg to remove large aggregates and filled into NT. LabelFree Zero Background MST Premium coated capillaries (NanoTemper Technologies GmbH). Measurements were carried out at 22°C. MST traces were collected with an LED excitation power of 20% and a MST laser power of 20 or 40%. For analysing the interaction affinity, the dissociation constant K_d for each ligand was calculated using the NanoTemper Analysis software by the changes in the normalized fluorescence (ΔFnorm [‰]) versus the ligand concentration.

Zebrafish handling

Zebrafish and embryos were raised and maintained according to standard protocols(*65*). Experiments at the MPIIB were approved by and conducted in accordance with the guidelines set out by the State Agency for Health and Social Affairs (LaGeSo, Berlin, Germany).

Fertilized embryos were used for all experiments and kept in Embryo medium(*65*) (E3, 5 mM NaCl, 0.17 mM KCl, 0.33 mM $CaCl_2$, 0.33 mM $MgSO_4$) in an incubator at 28ºC. Of note, 0.00001 % Methylene Blue was added to the E3 in experiments not involving microscopy. In all experiments, 1dpf larvae were manually dechorionated under a Leica MZ6 Stereomicroscope or using Pronase (Sigma), following approved protocols(*65*). At 2dpf, zebrafish larvae were divided into the different experimental groups, at a density of 12 larvae per well of a 12 well plate (Corning) in 1.5mL of E3, unless stated otherwise.

Zebrafish larva exposure and infection experiments

In the larva exposure experiments, 2dpf AB strain larvae were exposed to the different ligands in water at 28 ºC at the indicated time points. In experiments using the AhR inhibitor CH223191 (SIGMA), larvae were pre-exposed to 5uM of the inhibitor for 2h prior to the start of the experiment and the inhibitor was kept during the experiment. In the infection by immersion experiments, 2dpf larvae were placed in water containing the different conditions of *P.aeruginosa*, containing the indicated CFU and bacterial growth conditions, and kept in the incubator at 28ºC for the indicated time points.

Zebrafish larva gene expression analysis

After the desired exposure to diverse ligands or infections, larvae were euthanized with Tricaine (MS-222, 300 µg/mL SIGMA) and placed in Trizol for RNA isolation. Further qRTPCR experiments were performed using Syber-green primers (Eurofins) listed in Table S8.

Zebrafish larva CYP1A enzymatic activity (EROD) and toxicity assessment

The EROD experiments were performed as described previously(*66*). Upon Cyp1a activation, non-fluorescent 7-ethoxyresorufin diffuses into the embryo and is O-deethylated into resorufin, a fluorescent product that can be measured(*66*). In brief, after *P.aeruginosa* or ligand exposure, 2dpf zebrafish larvae were washed and placed in medium containing 0.4 µg/mL of 7-ethoxyresorufin

(Cayman Chemical) for 5 min. Further, larvae were anesthetized with Tricaine (MS-222 168 µg/mL SIGMA), placed in black 96 well plates with clear bottom (Thermo Fisher Scientific) and imaged in an Array Scan TM XTI Live High Content Platform (Thermo Fisher Scientific). Brightfield images were used to identify the shape of the larvae and fluorescence (filters excitation: 549/15 nm, emission: 590-624 nm) was determined per larva as readout of CYP1A activation. Head-to-tail distances and straightness of individual larvae were determined to assess toxicity, using the Array Scan TM XTI Live High Content Platform (Thermo Fisher Scientific) software.

Zebrafish larva WB lysate preparation

Zebrafish larvae WB lysates were prepared as previously described(*67*). In brief, larvae were euthanized with Tricaine (MS-222, 300 µg/mL SIGMA) and kept on ice for 5 min. Deyolking was performed using 200 µL of deyolking buffer (55 mM NaCl, 1.8 mM KCl, 1.25 mM $NaHCO_3$ and Complete protease inhibitor cocktail (Roche)) and shaking for 5 min to dissolve the yolk. Samples were centrifuged for 30 sec, supernatants were discarded and pellets resuspended in 200 µL of RIPA buffer (Cell Signaling technology). After sonication, lysates were stored at -20°C until further use.

Zebrafish XRE determination

Promoter analysis to determine possible Xenobiotic Response Elements (XRE) was performed as previously described(*40*). In short, sequences of the different zebrafish genes, including the regions 0-5000 bp upstream of the untranslated region (UTR) and the UTRs (to include introns upstream of the start codon), were downloaded from Pubmed. Putative XRE were determined by identifying the consensus motifs, 5'-T/GNGCGTG-3'or its reverse complement, along the different sequences.

Mice handling

AhR-deficient mice (*AhR*$^{-/-}$, C57BL/6 background) were kindly provided by B. Stockinger (MRC, National Institute for Medical Research, London, UK). C57BL/6 (WT) and *AhR*$^{-/-}$ mice were bred in the Max Planck Institute for Infection Biology mouse facility. Mice were 8–12 weeks of age at the beginning of the experiments, matched for age and sex, and kept under specific pathogen-free conditions. Animal experiments were carried out according to institutional guidelines approved by

the local ethics committee of the German authorities (LaGeSo; Landesamtes für Verbraucherschutz und Lebensmittelsicherheit, project number G0257/12).

Mouse infection

Age- and gender-matched mice (all C57BL/6 background) were intratracheally infected with 2×10^6 CFU for *P.aeruginosa* PA14 (WT, 09480 and Δ*rsaL*) under light anaesthesia. Bacteria inoculum was streaked on LB agar plates for CFU enumeration. After 8h of infection, mice were sacrificed by cervical dislocation and the lungs were dissected and mechanically disrupted manually or using gentleMACS tubes (Miltenyi Biotec) in a gentleMACS Dissociator (Miltenyi Biotec), following manufacturer's instructions. Lung homogenates were plated on LB agar plates for CFU enumeration or stored at -20°C for further Bioplex analysis.

Flow cytometry analysis of mouse neutrophils

Mice were sacrificed by cervical dislocation. The lungs were dissected, placed into wells of a 6-well plate, diced into 1 mm pieces with scissors and incubated with collagenase and DNAse for 30 min at 37°C. The tissue was then gently forced through a 70 μm mesh and rinsed twice with complete medium. The cells were pelleted, and following lysis of red blood cells and another wash with medium, the cells were resuspended in Fc block and subsequently stained for flow cytometry (FACS). Following the staining, cells were washed in FACS buffer (PBS + 1% FCS) and resuspended in a Propidium Iodide (PI) solution. The gating strategy used to quantify neutrophils was as follows: single cells, $CD45^+$ PI^-, Siglec F^- $CD11c^-$, $Ly6G^+$ $CD11b^+$. The antibodies used for the FACS analysis are listed in Table S9.

Bacterial growth conditions and preparation

P.aeruginosa strains, listed in Table S10, were streaked on LB plates and incubated overnight at 37°C. The following day, 8 individual colonies of each strain were grown in liquid LB medium at 37°C overnight, shaking at 220 RPM. Cultures from the same bacterial strains were mixed and serial dilutions were made in order to reach the desired OD600 after 2h of further incubation (37°C, 220 RPM). Once the desired OD was reached, bacteria were spun and culture supernatants were filtered twice using 0.22 μm Spin-X centrifuge tube filters (Corning). The concentrations of different QS molecules were determined, as described above, and the supernatants stored at 4°C

or -20°C, depending on the following experiment. Pelleted bacteria were washed twice with PBS, passed 10 times through a syringe to obtain single colonies and the inocula prepared for further infection experiments according to the desired CFU. Inocula were streaked on LB plates for CFU enumeration.

In vitro infection and bacterial supernatant stimulation

For *in vitro* infection experiments, cells were infected with the different *P.aeruginosa* strains and gentamycin was added to the culture after 1h infection, to control extracellular bacterial growth(*10*). The filtered supernatants of *P.aeruginosa* were diluted in cell growth medium (DMEM or RPMI) and further used to stimulate the AhR reporter cell lines.

Statistical analysis

For *in vivo* experiments, animals were randomly assigned to the different experimental groups and group size was chosen to allow a significance threshold α of 0.05 with a power of 80% (β= 0.2). For *in vitro* studies, cells were randomly distributed in different culture well plate positions. Data are presented as mean+/-SD (for presentation of individual experiments, where n= number of biological replicates) or mean+/-SEM (for presentation of pooled experiments, where n=number of independent experiments), as mentioned in figure legends. Each individual experiment was performed with technical and/or biological replicates. Pooled experiments depict mean values of independent experiments. To compute P values, depending on sample distribution and variation, different tests were performed, as described in figure legends. Two-tailed Student's t-test or Mann-Whitney U-test were used to compare data from two groups and one-way or two-way ANOVA (randomized block design) to compare data from three or more groups. GraphPad Prism version 7.0 was used for analysis and differences were considered statistically significant at $P< 0.05$.

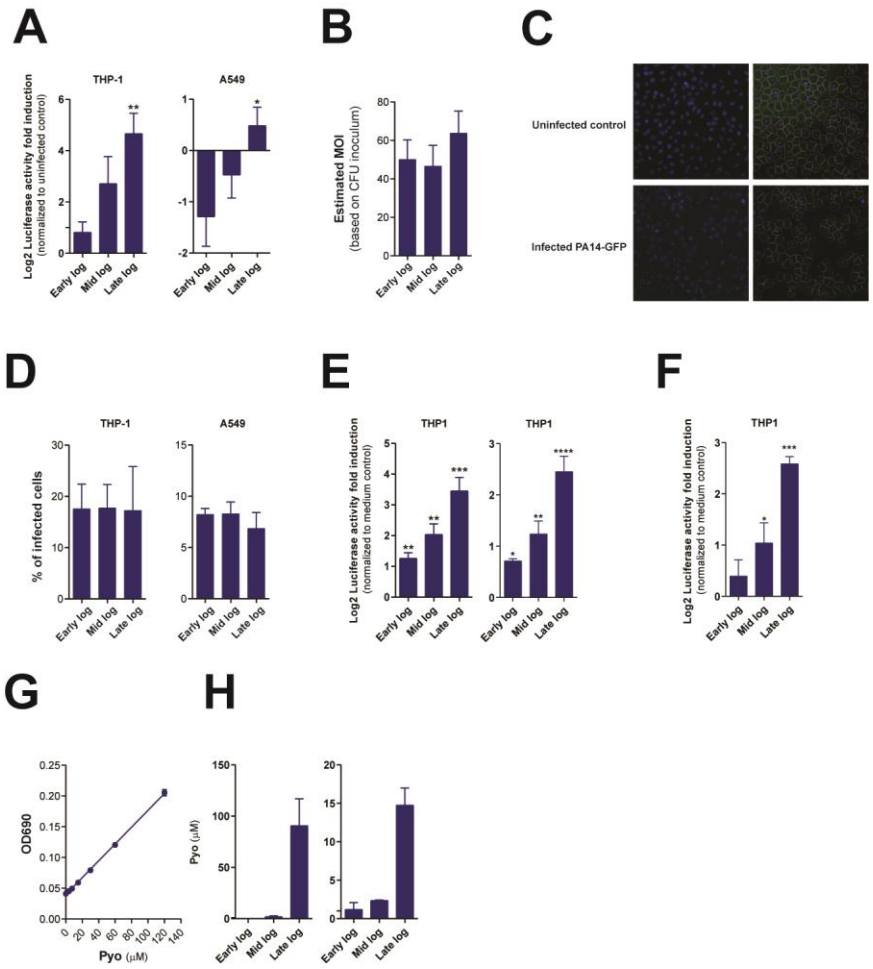

Fig. S1. ***P.aeruginosa*** **in vitro infection and Pyo expression kinetics. (A)** Luciferase activity of AhR reporter THP-1 and A549 cells upon 24h infection with *P.aeruginosa* PA14-WT strain grown in DMEM medium, at a multiplicity of infection (MOI) 50 (THP-1 (n=6) or A549 (n=3) independent experiments). **(B)** Multiplicity of infection (MOI) of *in vitro* infected cells (n=5 independent experiments). **(C,D)** Cells were infected for 1h with PA14-WT strain expressing GFP (PA14-WT-GFP) collected from different growth phases. **(C)** Representative images of A549 infected and non-infected cells. Nuclei depicted in blue and cell shape in yellow lines. Green dots (left) and Red dots (right) represent bacterial spots, total and localized within cell area, respectively. **(D)** Quantification of infected cells (THP-1 (n=2) or A549 (n=4) independent experiments). **(E,F)** THP-1 AhR reporter stimulation with filtered supernatants (1:25 diluted) from PA14 WT (**E left**, n=6 independent experiments), PA14 WT-GFP (**E right,** n=3 independent experiments) or PAO1 **(F**, n=3 independent experiments**)**, collected from different bacterial growth phases in DMEM medium. **(G,H)** Pyo concentration determined by spectrophotometry. **(G)** Standard curve (1 representative experiment out of at least 3 independent experiments) and **(H)** Pyo concentrations in supernatants of PA14-WT grown in LB (left, n=5 independent experiments) or DMEM medium (right, n=9 independent experiments), collected from different

bacterial growth phases. **(A,B,D,E,F, H)** Means +/- S.E.M. are depicted. **(G)** Means +/-S.D. are shown. **(A,B,D,E,F).** One-way ANOVA.* $p<0.05$, ** $P<0.01$, *** $p<0.001$ and ****$p<0.0001$.

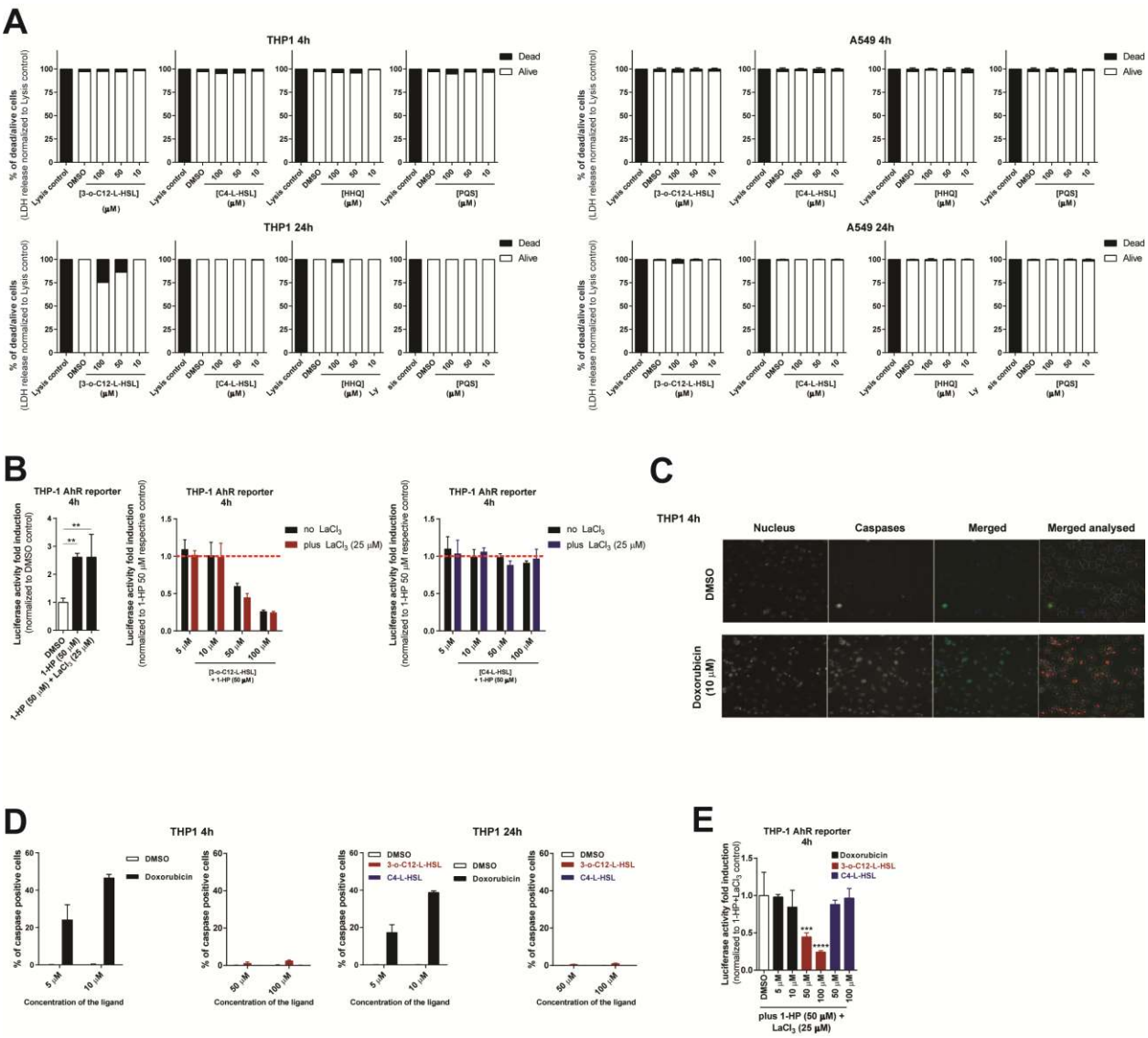

Fig. S2. Cell viability upon exposure to *P.aeruginosa* QS molecules. (A) Determination of the percentage of viable cells (THP-1 or A549) by lactate dehydrogenase release (LDH) after 4h or 24h incubation with various concentrations of QS molecules. Pooled data from: THP-1 (n=2) or A549 (n=4) independent experiments. **(B-E)** *Shiner et al* (80) reported that apoptosis induced by 3-o-C12-L-HSL can be blocked by Lanthanum chloride (LaCl3), leaving its immunomodulatory properties unaffected. **(B)** Luciferase activity of THP-1 AhR reporter cells upon incubation with 1-HP (50 µM) and various concentrations of 3-o-C12-L-HSL or C4-L-HSL, in presence or absence of Lanthanum chloride ($LaCl_3$, 25 µM). **(C,D)** Cell viability measured by Caspase 3/7 staining of THP-1 cells after stimulation for 4 or 24h with increasing concentrations of 3-o-C12-L-HSL or C4-L-HSL, or with Doxorubicin (10 µM). **(D,E)** Incubation of THP-1 AhR reporter for 4h with increasing concentrations of 3-o-C12-L-HSL, C4-L-HSL or Doxorubicin, in the presence of 1-HP (50 µM) and $LaCl_3$ (25 µM). Evaluation of **(D)** caspase 3/7 positive cells; **(E)** Luciferase AhR activity. **(B-E)**The presence or absence of $LaCl_3$ did neither affect AhR

activation induced by 1-HP, nor inhibition mediated by 3-o-C12-L-HSL **(B)**. Moreover, the presence of the apoptosis inducer Doxorubicin did not fully recapitulate the inhibition mediated by 3-o-C12-L-HSL **(C-E)**. **(A)** Data are pooled from at least 2 independent experiments. **(B-E)** Data from 1 representative experiment out of at least 3 independent experiments. **(A)** Means +/- S.E.M. are depicted. **(B-E)** Means +/- S.D. are depicted. **(B left panel, E)** One-way ANOVA. **(B middle or right panels)** Two-way ANOVA (blocking for each concentration). ** P<0.01, *** p<0.001 and ****p<0.0001.

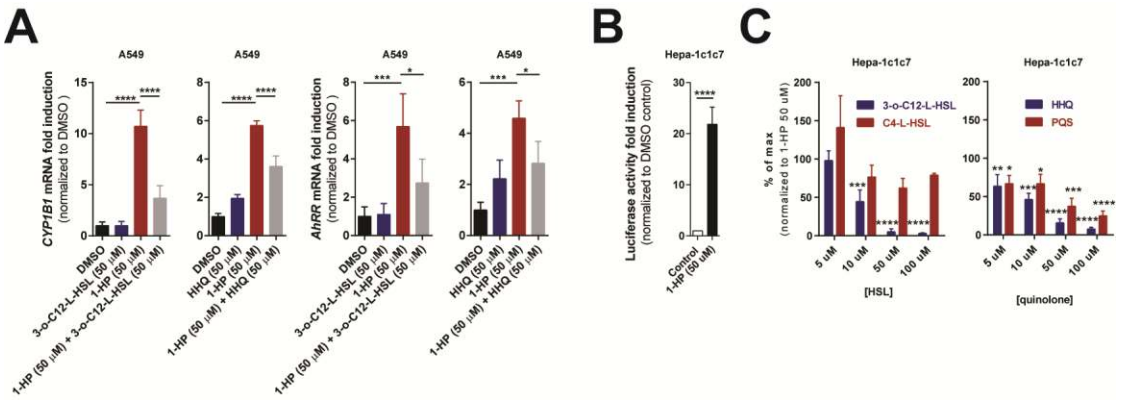

Fig. S3. AhR modulation by *P.aeruginosa* QS molecules. **(A)** *AhRR* and *CYP1B1* gene expression in A549 cells stimulated with QS molecules for 24h. Data from 1 representative experiment out of at least 3 independent experiments. **(B,C)** Luciferase activity of hepatocytic (Hepa-1c1c7) luciferase AhR reporter upon 4h stimulation with 1-HP (50 µM) in the presence or absence of different concentrations of QS molecules. Data are pooled from: B (n=8) or C (n=4) independent experiments. **(A)** Means **+/-**S.D. are depicted. **(B,C)** Means **+/-** S.E.M. are depicted. **(A-C)** One-way ANOVA. * p<0.05, ** P<0.01, *** p<0.001 and **** p<0.0001.

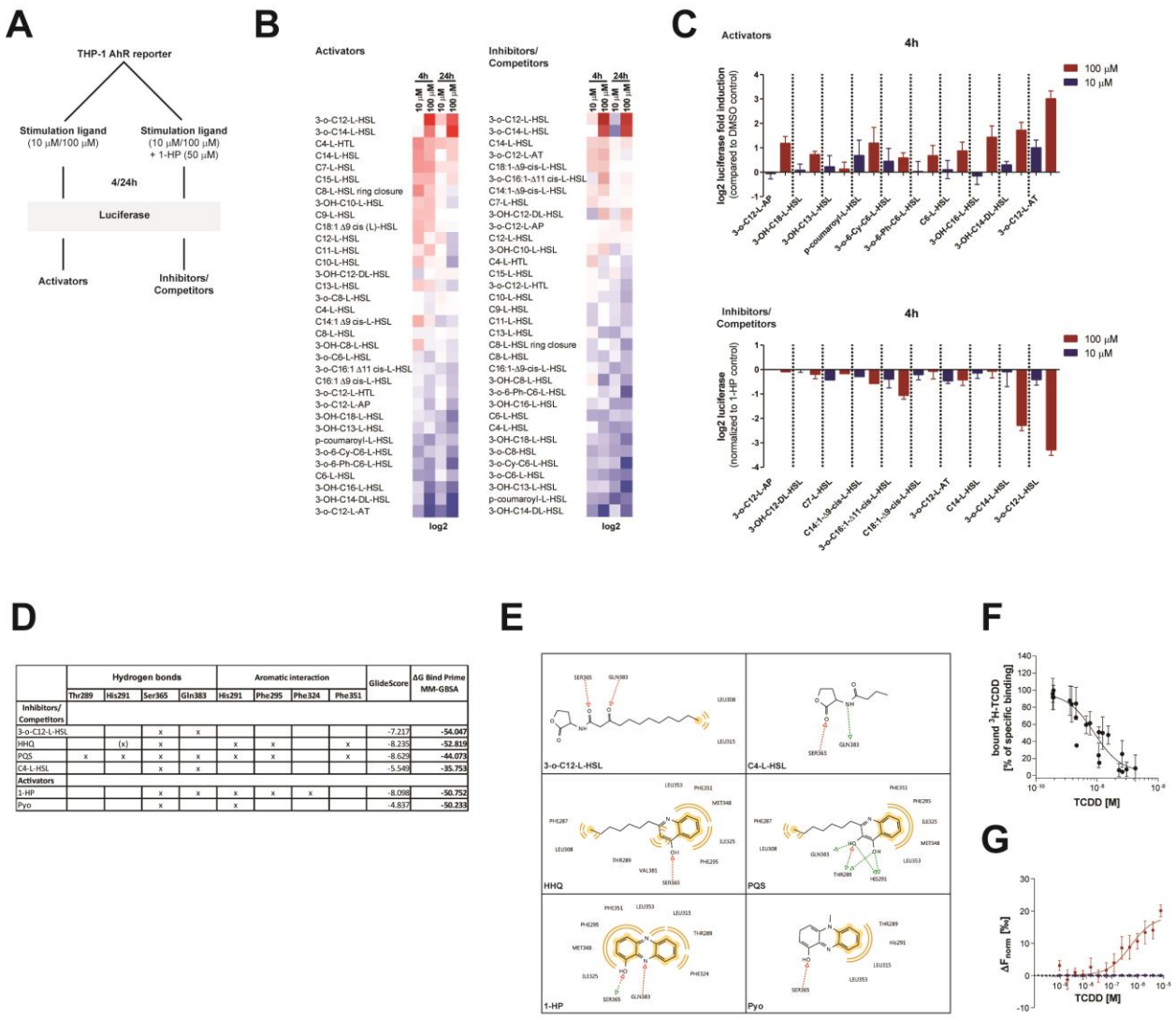

	Hydrogen bonds				Aromatic interaction				GlideScore	ΔG Bind Prime MM-GBSA
	Thr289	His291	Ser365	Gln383	His291	Phe295	Phe324	Phe351		
Inhibitors/ Competitors										
3-o-C12-L-HSL			x	x					-7.217	**-54.047**
HHQ		(x)	x		x	x		x	-8.235	**-52.819**
PQS	x	x	x	x	x	x		x	-8.629	**-44.073**
C4-L-HSL			x	x					-5.549	**-35.753**
Activators										
1-HP			x	x	x	x	x		-8.098	**-50.752**
Pyo			x		x				-4.837	**-50.233**

Fig. S4. AhR modulation by QS related molecules and AhR binding studies. (A) AhR modulation by QS related molecules and AhR binding studies. **(A)** Scheme of a Luciferase AhR reporter screen to evaluate QS related molecules capable of modulating AhR activity. **(B,C)** Identification of molecules capable of activating or inhibiting/competing AhR activity, in THP-1 AhR reporter cells, in presence or absence of 1-HP (50 µM). Data pooled from n=3-6 independent experiments. **(D)** Results for best scoring complexes for the hAhR homology model. Table indicates potential hydrogen bonds, aromatic interactions, as well as estimated binding affinity by GlideScore and ΔG^{bind}, calculated in Maestro 11v0 software. **(E)** Best docking pose for each of the investigated ligands as 2D-interaction plot (green dashed: hydrogen donor, red dashed: hydrogen acceptor, orange: hydrophobic interactions (plots drawn by LigandScout 4.1). **(F,G)** Binding of 2,3,7,8-Tetrachlorodibenzodioxin(TCDD) to AhR, measured by **(F)** displacement of radioactive[^{3}H] labelled TCDD([^{3}H]TCDD) from AhR in WT mouse liver cytosol (n=11 independent experiments) or **(G)** by Microscale Thermophoresis assay (n=4 independent experiments). **(C,F,G)** Means +/- S.E.M. are depicted.

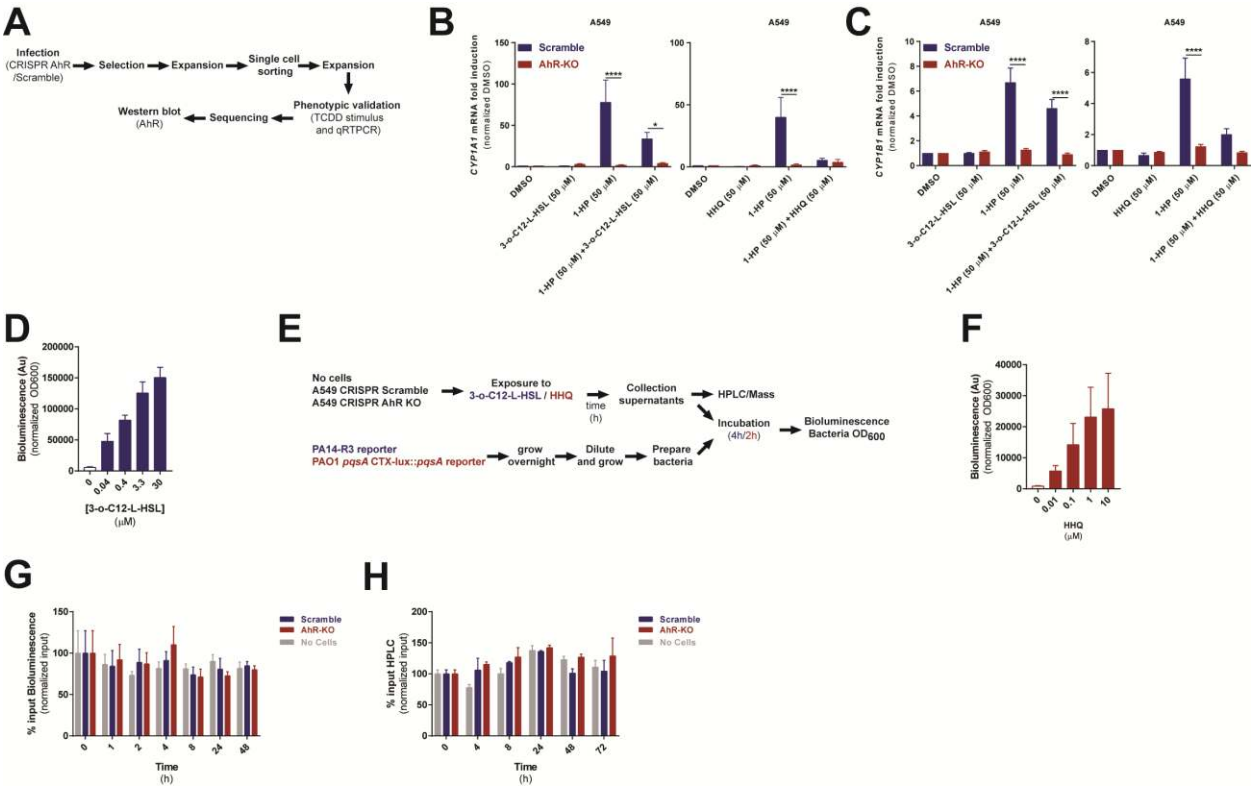

Fig. S5. AhR dependent responses to QS molecules. **(A)** Scheme of A549 CRISPR Scramble and A549 CRISPR AhR-KO cell line generation. **(B-C)** CYP1A1 **(B)** and CYP1B1 **(C)** gene expression in A549 CRISPR (Scramble and AhR-KO) cells upon 24h stimulation with *P.aeruginosa* QS molecules. Data pooled from: panels B, C left (n=7) or B, C right (n=5) independent experiments **(D)** Bioluminescence determination of PA14-R3 after incubation with increasing concentrations of 3-o-C12-L-HSL for 4h. Data from 1 representative experiment of at least 3 independent experiments**. (E)** Scheme of degradation studies performed using a bacterial PA14-R3 reporter strain to detect 3-o-C12-L-HSL and a PAO1 *pqsA* CTX-lux::*pqsA* bacterial reporter strain to detect HHQ, after exposure of A549 (CRISPR Scramble and CRISPR AhR-KO) to the respective QS molecules. **(F)** PAO1 *pqsA* CTX-lux::*pqsA* bioluminescence determination after incubation with increasing concentrations of HHQ for 2h. Data from 1 representative experiment of at least 3 independent experiments. **(G,H)** Degradation of HHQ (50 µM), measured in the supernatants of stimulated A549 CRISPR cells, compared to control without cells. HHQ expression levels detected by **(G)** bacterial PAO1 *pqsA* CTX-lux::*pqsA* bioluminescence reporter assay (n=1 experiment) or **(H)** HPLC (n=2 independent experiments). **(B,C, H)** Data depicted as Means +/- S.E.M. **(D,F,G)** Data depicted as Means +/- S.D. **(B,C,G,H)** Two-way ANOVA. * $p<0.05$ and **** $p<0.0001$.

A

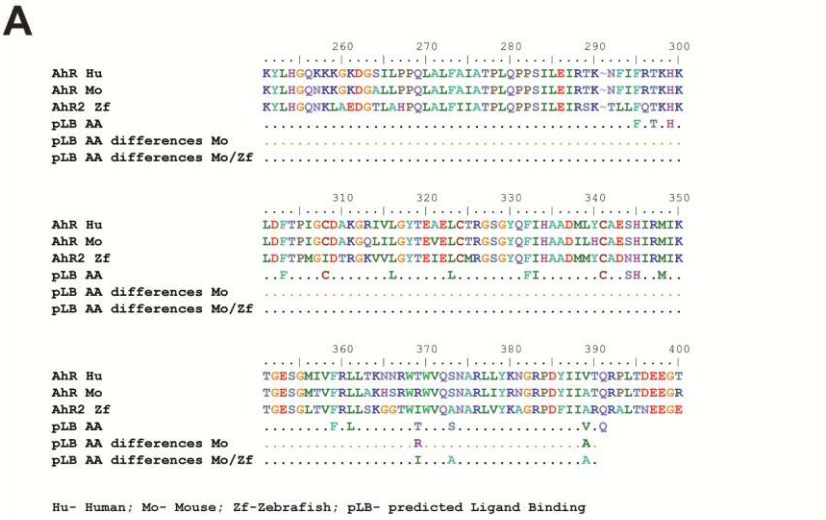

B

	AhR-human	AhR-mouse	AhR2-zebrafish
TCDD (MM-GBSA ΔG Bind [kcal/mol])	-42.43	-64.86	-66.19
CH-223191 (MM-GBSA ΔG Bind [kcal/mol])	-73.11	-70.24	-78.13

C

	AhR-human	AhR-mouse	AhR2-zebrafish
3-o-C12-L-HSL (MM-GBSA ΔG Bind [kcal/mol])	-54.05	-51.61	-51.55
C4-L-HSL (MM-GBSA ΔG Bind [kcal/mol])	-35.75	-39.12	-31.36
HHQ (MM-GBSA ΔG Bind [kcal/mol])	-52.82	-56.26	-45.99
PQS (MM-GBSA ΔG Bind [kcal/mol])	-44.07	-42.82	-46.04
1-HP (MM-GBSA ΔG Bind [kcal/mol])	-50.75	-46.73	-54.50
Pyo (MM-GBSA ΔG Bind [kcal/mol])	-50.23	-53.35	-49.31

Fig. S6. AhR homologues and ligand binding. (A) Alignment of the human (Hu), mouse (Mo) and zebrafish (Zf) AhR molecules indicating the aminoacids predicted to participate in ligand binding (pLB AA). Differences in conservation between the pLB AA among the different species are highlighted in the last rows. **(B, C)** Results for best scoring complexes for the hAhR homology model. Table indicates the estimated binding affinity by DG bind, calculated in Maestro 11v0 software. ΔG^{Bind} values were calculated starting from the same ligand pose as obtained for the human AhR. **(B)** TCDD as an example of an AhR agonist and CH223191 as an example of an AhR inhibitor. **(C)** *P.aeruginosa* QS molecules.

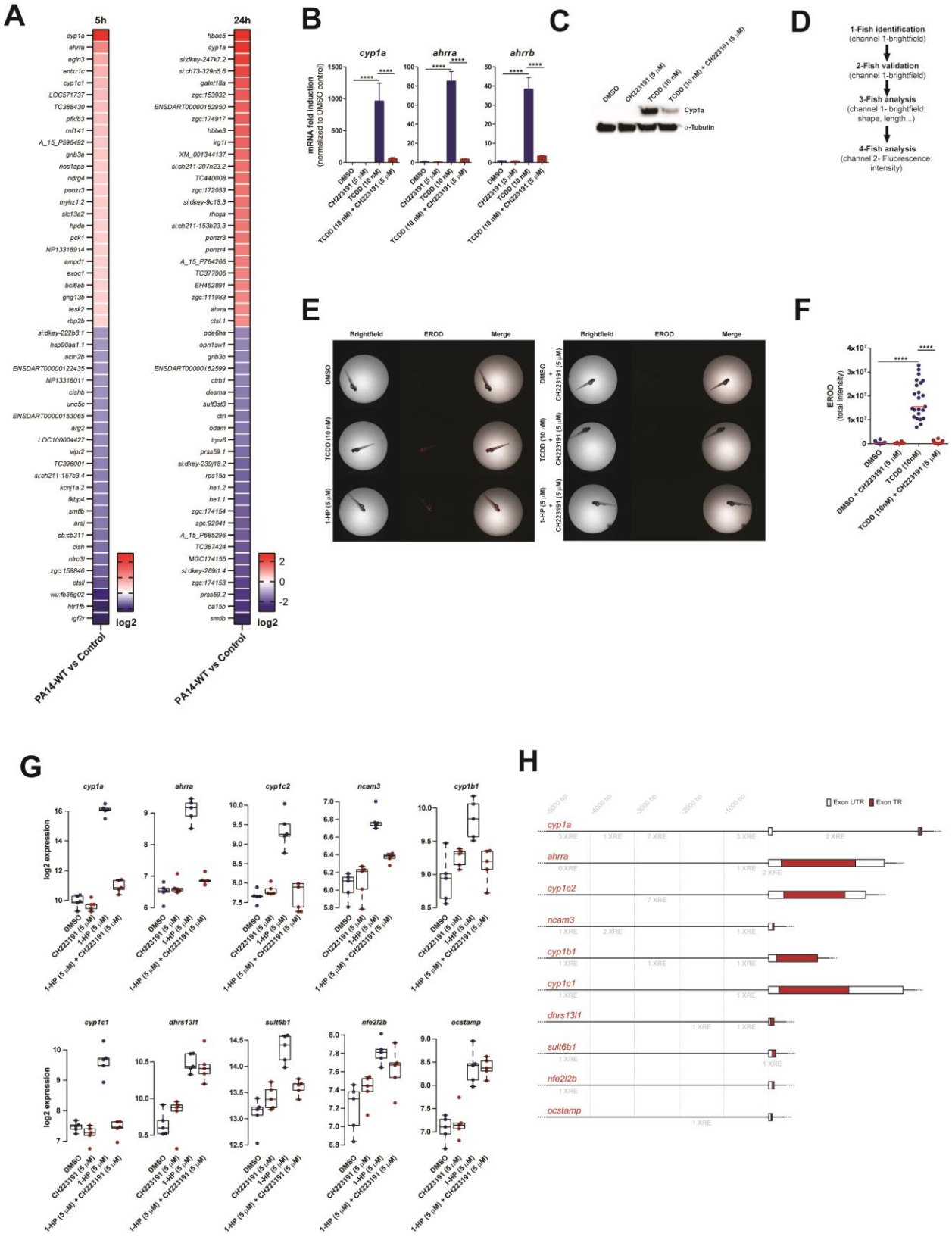

Fig. S7. AhR dependent responses in zebrafish larvae. (A) Microarray gene expression analysis of 2dpf zebrafish larvae upon 5h or 24h infection by immersion with $1x10^9$ CFU/mL of

P.aeruginosa PA14-WT, collected at mid log growth phase. **(B,C)** Gene expression analysis of *cyp1a*, *ahrra* and *ahrrb* transcripts from zebrafish larvae (2 days post-fertilization, dpf) treated (red) or untreated (blue) for 2h with 5 µM of the AhR inhibitor CH223191, followed by further 4h exposure with TCDD (10 nM) or DMSO vehicle control. Triplicates of 12 larvae depicted in each data point. One representative experiment out of at least 3 independent experiments. **(C)** Cyp1a protein expression detected by WB in 2dpf zebrafish larvae treated for 24h with DMSO, TCDD (10 nM), in the presence or absence of CH223191 (5 µM). **(D-F)** Cyp1a enzymatic assay (EROD) in 2dpf zebrafish larvae. **(D)** Scheme of the assay used to measure Cyp1a enzymatic activity. **(E,F)** **(E)** Representative images of Cyp1a enzymatic activity expressed as **(F)** total intensity of resorufin (EROD assay) detected per 2dpf larvae treated (red) or untreated (blue) for 2h with CH223191 (5 µM) followed by further 4h exposure with TCDD (10 nM) or DMSO vehicle control. Each data point represents a single larva. One representative experiment out of at least 3 independent experiments. **(G)** Microarray analysis of 2dpf larvae pre-exposed to DMSO or CH223191 (5 µM) for 2h, followed by 4h exposure to *P.aeruginosa* 1-HP (5 µM) or DMSO, in presence or absence of CH223191 (5µM). Data are pooled from 5 independent experiments, triplicates of 12 larvae depicted in each data point **(H)** *In silico* prediction of Xenobiotic Response Elements (XRE) in the promoter region of different genes. UTR-untranslated region; TR-translated region. **(B)** Means +/- S.D. are depicted. **(F)** Median is depicted. **(B, F)** One-way ANOVA. ****$p<0.0001$.

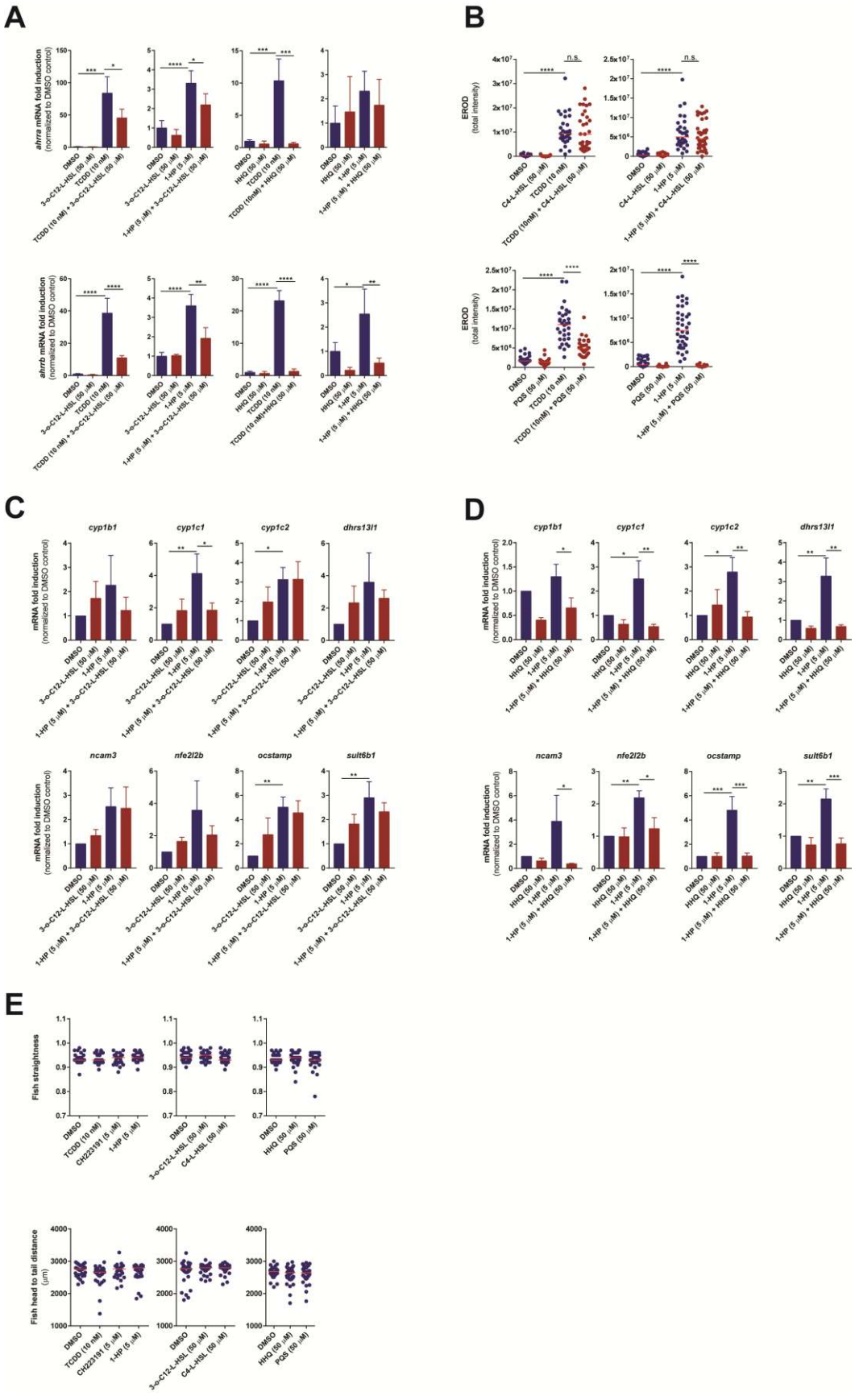
A
ahrra mRNA fold induction (normalized to DMSO control)
ahrrb mRNA fold induction (normalized to DMSO control)
DMSO
3-o-C12-L-HSL (50 μM)
TCDD (10 nM)
TCDD (10 nM) + 3-o-C12-L-HSL (50 μM)
1-HP (5 μM)
1-HP (5 μM) + 3-o-C12-L-HSL (50 μM)
HHQ (50 μM)
TCDD (10nM) + HHQ (50 μM)
1-HP (5 μM) + HHQ (50 μM)
B
EROD (total intensity)
n.s.
C4-L-HSL (50 μM)
TCDD (10nM) + C4-L-HSL (50 μM)
PQS (50 μM)
TCDD (10nM) + PQS (50 μM)
1-HP (5 μM) + C4-L-HSL (50 μM)
1-HP (5 μM) + PQS (50 μM)
C
cyp1b1
cyp1c1
cyp1c2
dhrs13l1
ncam3
nfe2l2b
ocstamp
sult6b1
mRNA fold induction (normalized to DMSO control)
D
E
Fish straightness
Fish head to tail distance (μm)
CH223191 (5 μM)

Fig. S8. AhR modulation in zebrafish larvae upon exposure to *P.aeruginosa* QS molecules. **(A,C,D)** Gene expression analysis or **(B)** Cyp1a enzymatic activity upon 4h exposure of 2dpf larvae to various *P.aeruginosa* QS molecules or TCDD. **(E)** Toxicity assessment of 2dpf zebrafish larvae upon exposure to different ligands, measured by straightness or total head to tail distance. **(A,B,E)** Data from 1 representative experiment out of at least 3 independent experiments. **(A)** Triplicates of 12 larvae depicted in each data point or **(B,E)** each data point represents a single larva. **(C,D)** Pooled data from n=5 independent experiments. **(A)** Means **+/-** S.D. are depicted. **(C,D)** Means +/- S.E.M. are depicted. **(B,E)** Medians are depicted. **(A-E)** One-way ANOVA. *p<0.05, ** p<0.01, *** p<0.001 and ****p<0.0001.

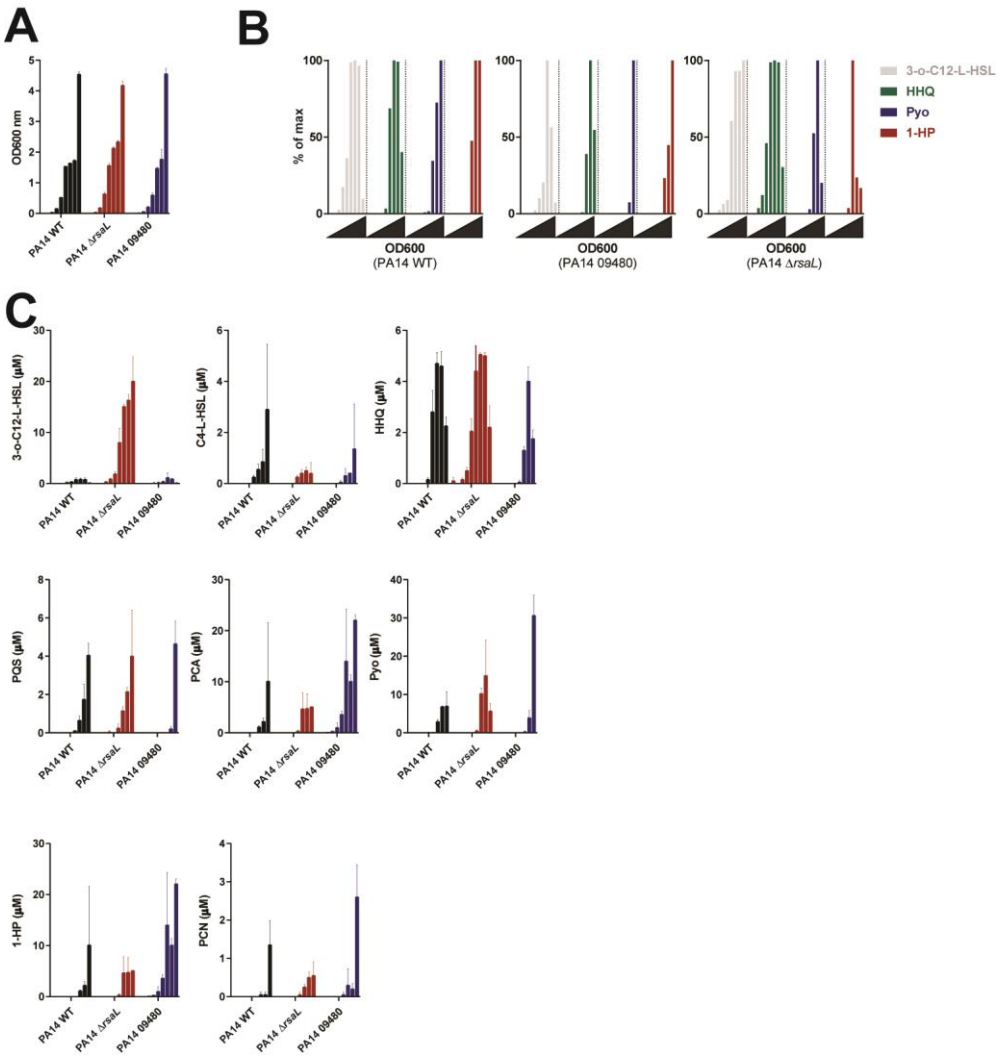

Fig. S9. *P.aeruginosa* QS expression dynamics (A) Growth curves of *P.aeruginosa* strains PA14-WT, PA14-Δ*rsaL* and PA14-09480 (n=2 independent experiments). **(B,C)** Kinetics of expression of different QS molecules in diverse *P.aeruginosa* strains, measured by HPLC (n=2 independent experiments).

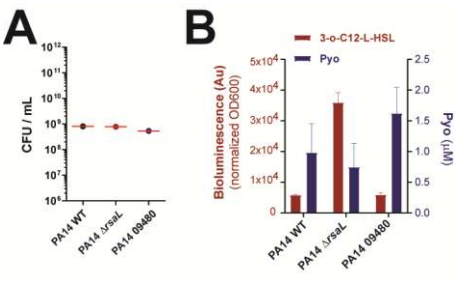

Fig. S10. *P.aeruginosa* infection of zebrafish larvae. (A) PA14 WT, PA14 Δ*rsaL* and PA14 09480 inoculum CFU administered to zebrafish by immersion. Data from 1 representative experiment of at least 3 independent experiments. **(B)** Expression of 3-o-C12-L-HSL and Pyo in the water of zebrafish larvae after 5h infection with different PA14 strains (n=7 independent experiments). **(A)** Means are depicted. **(B)** Means **+/-** S.E.M. are depicted.

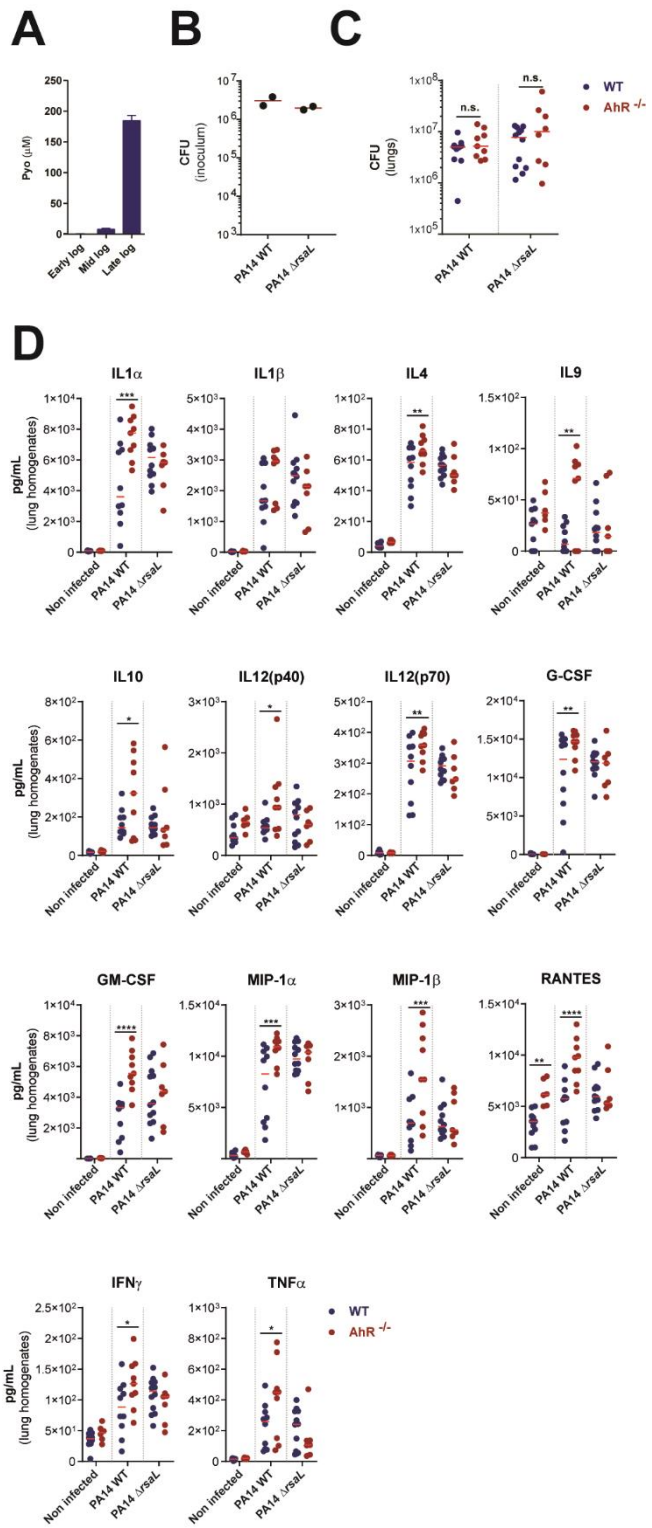

Fig. S11. *P.aeruginosa* infection of mice. (A) Pyocyanin (Pyo) concentrations in bacteria free supernatants of PA14-09480 strain grown in LB. **(B-D)** AhR deficient (*AhR* $^{-/-}$) and proficient (WT) mice were infected intratracheally for 8h with PA14 WT and PA14 Δ*rsaL* strains. **(B)** PA14 WT and PA14 Δ *rsaL* inoculum CFU administered to mice. Each dot represents the CFU from

each experiment. **(C)** Bacterial counts in the lungs of infected mice. Each dot represents 1 mouse **(D)** Cytokine and chemokine protein levels in lung homogenates after infection. Each dot represents 1 mouse. **(A-D)** Data are pooled from 2 independent experiments. **(A)**Means **+/-** S.E.M are depicted. **(B-D)** Medians are shown. **(C)** Mann-Whitney U-test. **(D)** Two-way ANOVA. n.s.- not significant, * $p<0.05$, ** $p<0.01$, *** $p<0.001$ and $p<0.0001$.

Table S1.

List of QS molecules and analogues tested.

Bacteria	C4-L-HSL	C6-L-HSL	C7-L-HSL	C8-L-HSL	C9-L-HSL	C10-L-HSL	C11-L-HSL	C12-L-HSL	C13-L-HSL	C14-L-HSL	C15-L-HSL	3-OH-C8-L-HSL	3-OH-C10-L-HSL	3-OH-C12-DL-HSL	3-OH-C14-DL-HSL	3-OH-C16-L-HSL	3-o-C6-L-HSL	3-o-C8-L-HSL	3-o-C12-L-HSL	3-o-C14-L-HSL	C14:1-Δ9-cis-L-HSL	C16:1-Δ9-cis-L-HSL	C18:1-Δ9-cis-L-HSL	3-o-C16:1-Δ11-cis-L-HSL	p-coumaroyl-L-HSL	HHQ	PQS	3-OH-C13-L-HSL	3-OH-C18-L-HSL	C4-L-HTL	3-o-6-Ph-C6-L-HSL	3-o-C12-L-HTL	3-o-C12-L-AP	3-o-C12-L-AT	3-o-6-Cy-L-HSL	C8-HSL ring closure
Acidithibacillus ferroxidans								■		■		■	■	■	■	■			■	■															
Aeromonas allosaccharophila	■	■																																	
Aeromonas bivalvium	■	■	■	■																															
Aeromonas caviae	■	■																																	
Aeromonas hydrophila	■	■																																	
Aeromonas jandaci	■	■																																	
Aeromonas salmonicida	■	■																																	
Aeromonas sobria		■																																	
Aeromonas trota	■	■	■																																
Aeromonas veronii	■	■	■	■																															
Agrobacterium tumefaciens																		■																	
Agrobacterium vitis																					■			■											
Bradyrhizobium spp																									■										
Burkholderia cepacia		■		■																															
Burkholderia cenocepacia		■		■																						■									
Burkholderia mallei				■		■						■	■																						
Burkholderia pseudomallei				■		■		■				■	■		■					■															
Burkholderia vietnamiensis		■		■		■		■																											
Burkholderia kururiensis																	■	■	■	■															
Burkholderia xenovorans												■					■	■	■	■															
Burkholderia unamae				■													■	■	■	■															
Burkholderia thailandiensis				■								■	■																						
Chromobacterium violaceum		■																																	
Dinoroseobacter shibae				■																			■												
Erwinia psidii R.IBSBF 435T			■																																
Pectobacterium carovotorum (former Erwinia carotovora)			■	■	■	■						■					■	■																	
Pantoea agglomerans pv. Gypsophilae	■	■																																	
Pantoea stewartii (former Erwinia stewartii)																	■																		
Phaeobacter inhibens													■																						
Pseudomonas aeruginosa	■	■		■			■											■	■	■						■	■								
Pseudomonas aureofaciens		■																																	
Pseudomonas clororaphis		■															■																		
Pseudomonas fluorescens		■		■		■												■																	
Pseudomonas fuscovaginae						■		■											■																	
Pseudomonas helianthi		■															■																		
Pseudomonas corrugata		■		■													■																		
Pseudomonas putida																	■	■	■																
Pseudomonas savastanoi		■															■	■																	
Pseudomonas syringae		■															■	■																	
Pseudomonas tomato	■	■															■	■																	
Rhizobium leguminosarum bv. Viciae		■	■	■								■						■		■															
Rhodopseudomonas palustris																									■										
Ruegeria sp. strain KLH1														■	■						■														
Serratia liquefaciens	■	■																																	
Serratia ATCC 39006	■	■																																	
Serratia marcescens SS-1		■	■	■													■																		
Serratia proteamaculans B5a																	■																		
Silicibacter pomeroyi																									■										
Vibrio anguillarum		■																																	
Vibrio fisheri				■													■																		
Vibrio harveyi																																			
Sinorhizobium melliloti				■				■		■										■		■													
Yersinia enterocolitica		■															■		■	■															
Yersinia pestis		■		■													■	■																	
Yersinia pseudotuberculosis	■	■	■	■		■		■	■	■	■	■	■	■	■		■	■	■	■															
	Expressed by bacteria																											Not expressed by bacteria							

References: 68-84

Table S2.

List of genes differentially expressed upon 5h infection of zebrafish larvae (2 days post fertilization) with PA14-WT.

Sequence Name(s)	Sequence Description	Log_2FC (PA14-WT vs Control)	p-Value
cyp1a	ref|Danio rerio cytochrome P450, family 1, subfamily A (cyp1a), mRNA [NM_131879]	5.07	3.24E-25
cyp1a	ref|Danio rerio cytochrome P450, family 1, subfamily A (cyp1a), mRNA [NM_131879]	3.34	1.48E-19
cyp1a	ref|Danio rerio cytochrome P450, family 1, subfamily A (cyp1a), mRNA [NM_131879]	2.43	2.69E-16
ahrra	ref|Danio rerio aryl-hydrocarbon receptor repressor a (ahrra), mRNA [NM_001035265]	2.30	1.62E-17
egln3	ref|Danio rerio egl-9 family hypoxia-inducible factor 3 (egln3), mRNA [NM_213310]	1.55	4.57E-06
antxr1c	ens|ANTXR cell adhesion molecule 1c [Source:ZFIN;Acc:ZDB-GENE-090514-5] [ENSDART00000093113]	1.38	4.04E-03
cyp1c1	ref|Danio rerio cytochrome P450, family 1, subfamily C, polypeptide 1 (cyp1c1), mRNA [NM_001020610]	1.28	6.47E-08
LOC571737	ens|high affinity cGMP-specific 3',5'-cyclic phosphodiesterase 9A-like [Source:NCBI gene;Acc:571737] [ENSDART00000181584]	1.23	2.10E-03
cyp1c1	ref|Danio rerio cytochrome P450, family 1, subfamily C, polypeptide 1 (cyp1c1), mRNA [NM_001020610]	1.18	1.14E-05
TC388430	tc|Rep: Forkhead box protein G1 - Homo sapiens (Human), partial (4%) [TC388430]	1.17	1.04E-04
pfkfb3	ref|Danio rerio 6-phosphofructo-2-kinase/fructose-2,6-biphosphatase 3 (pfkfb3), mRNA [NM_213397]	1.13	2.65E-06
rnf141	ref|Danio rerio ring finger protein 141 (rnf141), mRNA [NM_001007290]	1.12	3.22E-03
A_15_P596492	Unknown	1.01	1.90E-06

gnb3a	ref|Danio rerio guanine nucleotide binding protein (G protein), beta polypeptide 3a (gnb3a), mRNA [NM_001002437]	0.99	8.50E-03
egln3	ref|Danio rerio egl-9 family hypoxia-inducible factor 3 (egln3), mRNA [NM_213310]	0.98	5.26E-04
nos1apa	ens|nitric oxide synthase 1 (neuronal) adaptor protein a [Source:ZFIN;Acc:ZDB-GENE-081024-1] [ENSDART00000148997]	0.95	1.59E-02
ndrg4	ref|Danio rerio NDRG family member 4 (ndrg4), mRNA [NM_001045173]	0.91	1.57E-02
ponzr3	ref|Danio rerio plac8 onzin related protein 3 (ponzr3), mRNA [NM_001327984]	0.91	3.84E-02
myhz1.2	ref|Danio rerio myosin, heavy polypeptide 1.2, skeletal muscle (myhz1.2), mRNA [NM_001161446]	0.91	9.44E-04
slc13a2	ref|Danio rerio solute carrier family 13 (sodium-dependent dicarboxylate transporter), member 2 (slc13a2), mRNA [NM_213452]	0.88	1.69E-04
hpda	ref|Danio rerio 4-hydroxyphenylpyruvate dioxygenase a (hpda), mRNA [NM_201167]	0.87	2.01E-03
pck1	ref|Danio rerio phosphoenolpyruvate carboxykinase 1 (soluble) (pck1), mRNA [NM_214751]	0.84	5.14E-04
NP13318914	tc|GB|XM_001919200.1|XP_001919235.1 hypothetical protein [NP13318914]	0.83	2.61E-03
ampd1	ref|Danio rerio adenosine monophosphate deaminase 1 (isoform M) (ampd1), mRNA [NM_200893]	0.83	4.55E-03
exoc1	ref|Danio rerio exocyst complex component 1 (exoc1), mRNA [NM_199597]	0.83	1.65E-02
bcl6ab	ref|Danio rerio B cell CLL/lymphoma 6ab (bcl6ab), mRNA [NM_001100074]	0.82	9.10E-06
gng13b	ref|Danio rerio guanine nucleotide binding protein (G protein), gamma 13b (gng13b), mRNA [NM_001002400]	0.82	2.20E-03
pck1	ref|Danio rerio phosphoenolpyruvate carboxykinase 1 (soluble) (pck1), mRNA [NM_214751]	0.80	2.89E-03
tesk2	ref|Danio rerio testis associated actin remodelling kinase 2 (tesk2), mRNA [NM_001110476]	0.80	4.19E-03

rbp2b	ref|Danio rerio retinol binding protein 2b, cellular (rbp2b), mRNA [NM_001002307]	0.79	9.14E-03
slc13a2	ref|Danio rerio solute carrier family 13 (sodium-dependent dicarboxylate transporter), member 2 (slc13a2), mRNA [NM_213452]	0.79	6.46E-05
ponzr4	ref|Danio rerio plac8 onzin related protein 4 (ponzr4), mRNA [NM_001327980]	0.79	4.82E-02
ponzr4	ref|Danio rerio plac8 onzin related protein 4 (ponzr4), mRNA [NM_001327980]	0.79	2.90E-02
zgc:136908	ref|Danio rerio zgc:136908 (zgc:136908), mRNA [NM_001039928]	0.79	2.89E-04
p4ha1b	Unknown	0.78	1.47E-04
EH438071	gb|FDR103-P00018-DEPE-F_K13 FDR103 Danio rerio cDNA clone FDR103-P00018-BR_K13 5', mRNA sequence [EH438071]	0.78	8.42E-03
si:dkey-47k20.8	ens|si:dkey-47k20.8 [Source:ZFIN;Acc:ZDB-GENE-060503-359] [ENSDART00000140043]	0.77	2.99E-03
eef1db	ref|Danio rerio eukaryotic translation elongation factor 1 delta b (guanine nucleotide exchange protein) (eef1db), transcript variant 1, mRNA [NM_001161414]	0.77	5.76E-05
si:busm1-266f07.2	ref|Danio rerio si:busm1-266f07.2 (si:busm1-266f07.2), mRNA [NM_001004521]	0.76	1.43E-03
myhz1.1	ref|Danio rerio myosin, heavy polypeptide 1.1, skeletal muscle (myhz1.1), transcript variant 1, mRNA [NM_001115089]	0.76	2.00E-03
gnb3a	ref|Danio rerio guanine nucleotide binding protein (G protein), beta polypeptide 3a (gnb3a), mRNA [NM_001002437]	0.75	2.71E-02
six7	ref|Danio rerio SIX homeobox 7 (six7), mRNA [NM_131354]	0.75	3.37E-03
znf395a	ref|Danio rerio zinc finger protein 395a (znf395a), mRNA [NM_001080054]	0.75	2.33E-04
slco2a1	ref|Danio rerio solute carrier organic anion transporter family, member 2A1 (slco2a1), mRNA [NM_001089582]	0.74	3.71E-06
hif1an	ref|Danio rerio hypoxia inducible factor 1 subunit alpha inhibitor (hif1an), mRNA [NM_201496]	0.74	1.16E-05

aqp9a	ref|Danio rerio aquaporin 9a (aqp9a), mRNA [NM_001033096]	0.74	7.46E-03
gpr39	ref|Danio rerio G protein-coupled receptor 39 (gpr39), mRNA [NM_200417]	0.73	3.41E-02
zgc:174917	ref|Danio rerio zgc:174917 (zgc:174917), mRNA [NM_001105590]	0.73	3.77E-02
aqp9a	ref|Danio rerio aquaporin 9a (aqp9a), mRNA [NM_001033096]	0.72	6.51E-03
zgc:158404	ref|Danio rerio zgc:158404 (zgc:158404), mRNA [NM_001080565]	0.72	8.62E-03
grifin	ref|Danio rerio galectin-related inter-fiber protein (grifin), mRNA [NM_001003430]	0.72	1.56E-02
ampd1	ref|Danio rerio adenosine monophosphate deaminase 1 (isoform M) (ampd1), mRNA [NM_200893]	0.72	6.49E-03
tsc22d3	ref|Danio rerio TSC22 domain family, member 3 (tsc22d3), transcript variant 1, mRNA [NM_200569]	0.72	2.38E-02
klhl31	gb|Danio rerio kelch-like 31 (Drosophila) (klhl31), mRNA [NM_001003727]	0.72	6.73E-06
podn	ens|podocan [Source:ZFIN;Acc:ZDB-GENE-100922-117] [ENSDART00000181882]	0.72	1.35E-03
mpeg1.2	ref|Danio rerio macrophage expressed 1, tandem duplicate 2 (mpeg1.2), mRNA [NM_001020586]	0.72	1.25E-02
TC388430	tc|Rep: Forkhead box protein G1 - Homo sapiens (Human), partial (4%) [TC388430]	0.71	8.15E-06
uox	ref|Danio rerio urate oxidase (uox), mRNA [NM_001002332]	0.71	2.61E-02
myhz1.2	ref|Danio rerio myosin, heavy polypeptide 1.2, skeletal muscle (myhz1.2), mRNA [NM_001161446]	0.71	1.20E-03
EH438071	gb|FDR103-P00018-DEPE-F_K13 FDR103 Danio rerio cDNA clone FDR103-P00018-BR_K13 5', mRNA sequence [EH438071]	0.71	1.41E-02
akt1s1	ens|AKT1 substrate 1 (proline-rich) [Source:ZFIN;Acc:ZDB-GENE-030131-482] [ENSDART00000157320]	0.71	1.19E-07
sult6b1	ref|Danio rerio sulfotransferase family, cytosolic, 6b, member 1 (sult6b1), mRNA [NM_214686]	0.71	1.46E-05

ENSDART00000165967	ens|si:dkey-3h2.3 [Source:ZFIN;Acc:ZDB-GENE-070705-465] [ENSDART00000165967]	0.70	5.45E-03
ctps1b	ref|Danio rerio CTP synthase 1b (ctps1b), mRNA [NM_001111247]	0.70	2.38E-03
kdm5ba	ref|Danio rerio lysine (K)-specific demethylase 5Ba (kdm5ba), mRNA [NM_001347607]	0.70	1.46E-05
pdk2b	ref|Danio rerio pyruvate dehydrogenase kinase, isozyme 2b (pdk2b), mRNA [NM_200996]	0.70	3.48E-03
cyp24a1	ref|Danio rerio cytochrome P450, family 24, subfamily A, polypeptide 1 (cyp24a1), mRNA [NM_001089458]	0.70	2.14E-02
ucp1	ref|Danio rerio uncoupling protein 1 (ucp1), mRNA [NM_199523]	0.69	1.20E-03
ccl20a.3	ref|Danio rerio chemokine (C-C motif) ligand 20a, duplicate 3 (ccl20a.3), mRNA [NM_001136254]	0.69	3.53E-02
ENSDART00000162027	tc|GB|XM_001343781.2|XP_001343817.2 similar to protease, serine 27 [NP13317523]	0.69	5.56E-03
dhrs13l1	ref|Danio rerio dehydrogenase/reductase (SDR family) member 13 like 1 (dhrs13l1), mRNA [NM_205648]	0.68	1.17E-04
syt5b	ref|Danio rerio synaptotagmin Vb (syt5b), mRNA [NM_001020546]	0.68	1.12E-02
znf395a	ref|Danio rerio zinc finger protein 395a (znf395a), mRNA [NM_001080054]	0.68	2.03E-04
dhrs13l1	ref|Danio rerio dehydrogenase/reductase (SDR family) member 13 like 1 (dhrs13l1), mRNA [NM_205648]	0.68	6.34E-03
g6pca.2	ref|Danio rerio glucose-6-phosphatase a, catalytic subunit, tandem duplicate 2 (g6pca.2), mRNA [NM_001163806]	0.67	7.93E-04
sult6b1	ref|Danio rerio sulfotransferase family, cytosolic, 6b, member 1 (sult6b1), mRNA [NM_214686]	0.67	4.89E-08
kdm7aa	ref|Danio rerio lysine (K)-specific demethylase 7Aa (kdm7aa), mRNA [NM_001346151]	0.66	6.13E-04
zgc:92606	ref|Danio rerio zgc:92606 (zgc:92606), mRNA [NM_001002707]	0.66	1.02E-03
ENSDART00000067461	ens|si:ch211-152c2.3 [Source:ZFIN;Acc:ZDB-GENE-030131-9914] [ENSDART00000067461]	0.66	2.43E-04

slc25a55b	ref|Danio rerio solute carrier family 25, member 55b (slc25a55b), mRNA [NM_001003448]	0.66	6.32E-05
cyp1c2	ref|Danio rerio cytochrome P450, family 1, subfamily C, polypeptide 2 (cyp1c2), mRNA [NM_001114849]	0.66	9.84E-03
tsc22d3	ref|Danio rerio TSC22 domain family, member 3 (tsc22d3), transcript variant 2, mRNA [NM_001348480]	0.66	1.10E-03
aldocb	ref|Danio rerio aldolase C, fructose-bisphosphate, b (aldocb), mRNA [NM_194384]	0.66	9.03E-04
agt	ref|Danio rerio angiotensinogen (agt), mRNA [NM_198063]	0.65	1.06E-02
p4ha1b	ref|Danio rerio prolyl 4-hydroxylase, alpha polypeptide I b (p4ha1b), mRNA [NM_214691]	0.65	5.62E-03
soul4	tc|Rep: Predicted protein - Monosiga brevicollis MX1, partial (37%) [TC434991]	0.65	1.26E-05
si:ch211-11n16.2	ens|si:ch211-11n16.2 [Source:ZFIN;Acc:ZDB-GENE-041008-77] [ENSDART00000160145]	0.65	3.22E-03
rdh8b	ref|Danio rerio retinol dehydrogenase 8b (rdh8b), mRNA [NM_200788]	0.65	3.15E-03
prr33	ens|proline rich 33 [Source:ZFIN;Acc:ZDB-GENE-030131-5326] [ENSDART00000156828]	0.65	1.85E-02
tcp11l2	ref|Danio rerio t-complex 11, testis-specific-like 2 (tcp11l2), mRNA [NM_213020]	0.64	1.30E-06
eno2	ref|Danio rerio enolase 2 (eno2), mRNA [NM_001003848]	0.64	4.57E-03
kif5aa	ref|Danio rerio kinesin family member 5A, a (kif5aa), mRNA [NM_001199776]	0.64	1.11E-04
bcl6ab	ref|Danio rerio B cell CLL/lymphoma 6ab (bcl6ab), mRNA [NM_001100074]	0.64	3.04E-05
myhz1.1	ref|Danio rerio myosin, heavy polypeptide 1.1, skeletal muscle (myhz1.1), transcript variant 1, mRNA [NM_001115089]	0.64	1.36E-02
iffo1a	ens|intermediate filament family orphan 1a [Source:ZFIN;Acc:ZDB-GENE-060503-418] [ENSDART00000091615]	0.63	9.11E-03
tsc22d2	ref|Danio rerio TSC22 domain family 2 (tsc22d2), mRNA [NM_200109]	0.63	4.32E-06

slc35g2b	ref|Danio rerio solute carrier family 35, member G2b (slc35g2b), mRNA [NM_001013563]	0.63	1.57E-03
rgma	tc|GB|BC165864.1|AAI65864.1 Unknown (protein for MGC:192952) [NP13228499]	0.63	2.36E-04
tmem59l	ref|Danio rerio transmembrane protein 59-like (tmem59l), mRNA [NM_213337]	0.63	2.12E-05
slc12a7b	ens|solute carrier family 12 (potassium/chloride transporter), member 7b [Source:ZFIN;Acc:ZDB-GENE-030829-61] [ENSDART00000134251]	0.62	8.26E-04
mfsd4ab	ref|Danio rerio major facilitator superfamily domain containing 4Ab (mfsd4ab), mRNA [NM_001114416]	0.62	9.36E-03
clpxb	ens|caseinolytic mitochondrial matrix peptidase chaperone subunit b [Source:ZFIN;Acc:ZDB-GENE-130404-1] [ENSDART00000153827]	0.62	1.17E-02
slc7a8a	ref|Danio rerio solute carrier family 7 (amino acid transporter light chain, L system), member 8a (slc7a8a), mRNA [NM_001271897]	0.62	2.39E-03
bcl6aa	ref|Danio rerio B cell CLL/lymphoma 6aa (bcl6aa), mRNA [NM_200734]	0.62	1.12E-02
opn6a	ref|Danio rerio opsin 6, group member a (opn6a), mRNA [NM_001079657]	0.62	7.50E-03
ethe1	ref|Danio rerio ethylmalonic encephalopathy 1 (ethe1), mRNA [NM_212929]	0.61	3.43E-03
myhz2	Unknown	0.61	5.71E-03
myhz1.1	ref|Danio rerio myosin, heavy polypeptide 1.1, skeletal muscle (myhz1.1), transcript variant 1, mRNA [NM_001115089]	0.61	1.93E-02
brip1	ref|Danio rerio BRCA1 interacting protein C-terminal helicase 1 (brip1), mRNA [NM_001110296]	0.61	1.80E-02
BC154660	Unknown	0.61	1.04E-04
ppdpfa	gb|FDR103-P00062-DEPE-R_K11 FDR103 Danio rerio cDNA clone FDR103-P00062-BR_K11 3', mRNA sequence [EH479777]	0.61	1.28E-02
mpeg1.3	ref|Danio rerio macrophage expressed 1, tandem duplicate 3 (mpeg1.3), mRNA [NM_001123310]	0.61	1.32E-03

mybpc2b	ref|Danio rerio myosin binding protein C, fast type b (mybpc2b), mRNA [NM_001013511]	0.61	2.24E-04
castor2	ref|Danio rerio cytosolic arginine sensor for mTORC1 subunit 2 (castor2), mRNA [NM_199780]	0.61	1.20E-03
ryr3	ens|ryanodine receptor 3 [Source:ZFIN;Acc:ZDB-GENE-041001-165] [ENSDART00000172634]	0.61	2.10E-02
crx	ref|Danio rerio cone-rod homeobox (crx), mRNA [NM_152940]	0.60	7.93E-03
rpe65a	ref|Danio rerio retinal pigment epithelium-specific protein 65a (rpe65a), mRNA [NM_200751]	0.60	3.91E-02
zgc:92606	ref|Danio rerio zgc:92606 (zgc:92606), mRNA [NM_001002707]	0.60	1.39E-03
lin7b	ref|Danio rerio lin-7 homolog B (C. elegans) (lin7b), mRNA [NM_001020733]	0.60	2.52E-03
abi1a	ref|Danio rerio abl-interactor 1a (abi1a), mRNA [NM_001328427]	0.60	1.41E-02
ENSDART00000092493	ens|protein tyrosine phosphatase, receptor type, t [Source:ZFIN;Acc:ZDB-GENE-101028-4] [ENSDART00000092493]	0.60	8.33E-03
orc4	ref|Danio rerio origin recognition complex, subunit 4 (orc4), mRNA [NM_213183]	-0.60	2.23E-03
EH440809	gb|FDR103-P00026-DEPE-F_E19 FDR103 Danio rerio cDNA clone FDR103-P00026-BR_E19 5', mRNA sequence [EH440809]	-0.60	2.33E-03
odc1	ref|Danio rerio ornithine decarboxylase 1 (odc1), mRNA [NM_131801]	-0.61	4.25E-03
tma7	ref|Danio rerio translation machinery associated 7 homolog (tma7), mRNA [NM_001159834]	-0.61	1.29E-02
zgc:153665	ref|Danio rerio zgc:153665 (zgc:153665), mRNA [NM_001077463]	-0.61	2.14E-03
mrpl16	ref|Danio rerio mitochondrial ribosomal protein L16 (mrpl16), mRNA [NM_001007764]	-0.61	3.24E-03
anxa1b	ref|Danio rerio annexin A1b (anxa1b), mRNA [NM_181759]	-0.61	3.73E-03
rnasel3	ref|Danio rerio ribonuclease like 3 (rnasel3), mRNA [NM_001099453]	-0.61	4.50E-03

znf410	ref|Danio rerio zinc finger protein 410 (znf410), mRNA [NM_205653]	-0.61	1.22E-02
naalad2	ref|Danio rerio N-acetylated alpha-linked acidic dipeptidase 2 (naalad2), mRNA [NM_200277]	-0.61	1.53E-04
psma5	ref|Danio rerio proteasome subunit alpha 5 (psma5), mRNA [NM_205708]	-0.62	1.16E-05
si:ch73-347e22.8	ens|si:ch73-347e22.8 [Source:ZFIN;Acc:ZDB-GENE-030131-8455] [ENSDART00000168968]	-0.62	2.43E-04
hells	ref|Danio rerio helicase, lymphoid specific (hells), mRNA [NM_001037101]	-0.62	3.58E-03
zgc:194839	ref|Danio rerio zgc:194839 (zgc:194839), mRNA [NM_001123324]	-0.62	1.38E-03
mboat1	ens|membrane bound O-acyltransferase domain containing 1 [Source:ZFIN;Acc:ZDB-GENE-041114-98] [ENSDART00000141860]	-0.63	3.06E-04
wu:fc14h11	gb|AGENCOURT_16619286 NIH_ZGC_7 Danio rerio cDNA clone IMAGE:7052511 5', mRNA sequence [CK028151]	-0.63	3.35E-02
ca15c	ref|Danio rerio carbonic anhydrase XV c (ca15c), mRNA [NM_001077333]	-0.63	5.14E-04
tomm20a	ref|Danio rerio translocase of outer mitochondrial membrane 20 (tomm20a), mRNA [NM_213036]	-0.63	4.33E-02
hsp90aa1.1	ref|Danio rerio heat shock protein 90, alpha (cytosolic), class A member 1, tandem duplicate 1 (hsp90aa1.1), mRNA [NM_131328]	-0.63	4.37E-03
anxa3a	ens|annexin A3a [Source:ZFIN;Acc:ZDB-GENE-040912-58] [ENSDART00000192044]	-0.63	5.22E-04
mboat1	ens|membrane bound O-acyltransferase domain containing 1 [Source:ZFIN;Acc:ZDB-GENE-041114-98] [ENSDART00000141860]	-0.63	2.16E-05
si:ch211-201h21.5	ref|Danio rerio si:ch211-201h21.5 (si:ch211-201h21.5), mRNA [NM_001030089]	-0.63	9.29E-04
NP13316691	tc|GB|XM_001344782.2|XP_001344818.2 similar to predicted protein [NP13316691]	-0.63	2.66E-02

si:ch211-131k2.3	ref|Danio rerio si:ch211-131k2.3 (si:ch211-131k2.3), mRNA [NM_001326711]	-0.63	2.83E-04
imp3	ref|Danio rerio IMP3, U3 small nucleolar ribonucleoprotein, homolog (yeast) (imp3), mRNA [NM_001291357]	-0.64	4.22E-04
si:dkey-172k15.13	ens|si:dkey-172k15.3 [Source:ZFIN;Acc:ZDB-GENE-131121-97] [ENSDART00000155070]	-0.64	3.40E-03
sfrp1b	ref|Danio rerio secreted frizzled-related protein 1b (sfrp1b), mRNA [NM_001083571]	-0.64	1.13E-02
ENSDART00000153065	ens|si:ch211-57i17.2 [Source:ZFIN;Acc:ZDB-GENE-041014-258] [ENSDART00000153065]	-0.64	3.87E-02
si:ch73-269m23.5	ens|si:ch73-269m23.5 [Source:ZFIN;Acc:ZDB-GENE-110411-68] [ENSDART00000148669]	-0.64	4.76E-03
BI673044	gb|ft33c11.y1 Gong zebrafish testis Danio rerio cDNA clone IMAGE:5152508 5', mRNA sequence [BI673044]	-0.64	1.34E-02
odc1	ref|Danio rerio ornithine decarboxylase 1 (odc1), mRNA [NM_131801]	-0.65	3.58E-03
elovl8b	ref|Danio rerio ELOVL fatty acid elongase 8b (elovl8b), transcript variant 1, mRNA [NM_001024438]	-0.65	1.16E-03
orc3	ref|Danio rerio origin recognition complex, subunit 3 (orc3), mRNA [NM_212727]	-0.65	1.72E-05
ucp3	ref|Danio rerio uncoupling protein 3 (ucp3), mRNA [NM_200353]	-0.65	4.88E-02
zgc:77739	ref|Danio rerio zgc:77739 (zgc:77739), mRNA [NM_200896]	-0.65	3.69E-02
gbgt1l4	ref|Danio rerio globoside alpha-1,3-N-acetylgalactosaminyltransferase 1, like 4 (gbgt1l4), mRNA [NM_200125]	-0.65	4.57E-03
rpa2	ref|Danio rerio replication protein A2 (rpa2), mRNA [NM_131711]	-0.66	2.49E-04
capn9	ref|Danio rerio calpain 9 (capn9), mRNA [NM_001003501]	-0.66	5.52E-05
fthl31	ref|Danio rerio ferritin, heavy polypeptide-like 31 (fthl31), mRNA [NM_001020531]	-0.66	3.89E-03
wu:fj88f11	gb|FDR306-P00011-DEPE-F_K17 FDR306 Danio rerio cDNA clone	-0.66	3.65E-03

	FDR306-P00011-BR_K17 5', mRNA sequence [EH582267]		
arf2b	ref|Danio rerio ADP-ribosylation factor 2b (arf2b), mRNA [NM_201480]	-0.66	3.55E-02
si:ch211-244o22.2	ref|Danio rerio si:ch211-244o22.2 (si:ch211-244o22.2), mRNA [NM_001082823]	-0.67	1.49E-06
LOC791500	ens|zgc:153921 [Source:ZFIN;Acc:ZDB-GENE-060929-816] [ENSDART00000011111]	-0.67	1.58E-02
cldne	ref|Danio rerio claudin e (cldne), mRNA [NM_131765]	-0.67	1.87E-04
krt99	ref|Danio rerio keratin 99 (krt99), mRNA [NM_001017588]	-0.68	6.18E-03
smx5	ref|Danio rerio smx5 (smx5), mRNA [NM_131496]	-0.68	1.68E-04
gch2	ref|Danio rerio GTP cyclohydrolase 2 (gch2), mRNA [NM_131667]	-0.69	1.25E-02
narf	ens|nuclear prelamin A recognition factor [Source:ZFIN;Acc:ZDB-GENE-040718-31] [ENSDART00000007053]	-0.69	1.31E-03
pmm2	ref|Danio rerio phosphomannomutase 2 (pmm2), mRNA [NM_200084]	-0.69	3.93E-04
socs1a	ref|Danio rerio suppressor of cytokine signaling 1a (socs1a), mRNA [NM_001003467]	-0.69	2.61E-05
si:ch1073-126c3.2	ref|Danio rerio si:ch1073-126c3.2 (si:ch1073-126c3.2), mRNA [NM_001144786]	-0.69	2.63E-02
TC418621	ref|PREDICTED: Danio rerio uncharacterized LOC100537502 (LOC100537502), mRNA [XM_003200273]	-0.70	3.56E-02
uhrf1	ref|Danio rerio ubiquitin-like with PHD and ring finger domains 1 (uhrf1), mRNA [NM_213077]	-0.70	3.20E-04
pcna	Unknown	-0.70	1.97E-02
ly6m5	ens|lymphocyte antigen 6 family member M5 [Source:ZFIN;Acc:ZDB-GENE-131127-265] [ENSDART00000170587]	-0.70	1.89E-02
dao.1	ref|Danio rerio D-amino-acid oxidase, tandem duplicate 1 (dao.1), mRNA [NM_001033740]	-0.70	1.08E-02
zgc:153284	ref|Danio rerio zgc:153284 (zgc:153284), transcript variant 1, mRNA [NM_001291936]	-0.70	8.06E-05

zgc:153665	ref|Danio rerio zgc:153665 (zgc:153665), mRNA [NM_001077463]	-0.70	9.51E-04
il4r.1	ref|Danio rerio interleukin 4 receptor, tandem duplicate 1 (il4r.1), mRNA [NM_001013282]	-0.71	1.98E-02
EE697538	gb|AGENCOURT_90073624 NIH_ZGC_29 Danio rerio cDNA clone IMAGE:8815158 5', mRNA sequence [EE697538]	-0.71	1.30E-03
scel	ref|Danio rerio sciellin (scel), mRNA [NM_001005304]	-0.71	1.52E-03
dhfr	ref|Danio rerio dihydrofolate reductase (dhfr), mRNA [NM_131775]	-0.71	1.34E-04
rrm2	ref|Danio rerio ribonucleotide reductase M2 polypeptide (rrm2), mRNA [NM_131450]	-0.71	4.21E-04
TC431279	tc|Rep: Predicted protein - Monosiga brevicollis MX1, partial (3%) [TC431279]	-0.71	1.31E-02
il4r.2	ens|interleukin 4 receptor, tandem duplicate 1 [Source:ZFIN;Acc:ZDB-GENE-050227-5] [ENSDART00000157463]	-0.71	2.69E-02
A_15_P460125	Unknown	-0.72	1.44E-03
rpf2	ref|Danio rerio ribosome production factor 2 homolog (rpf2), mRNA [NM_214748]	-0.73	2.18E-03
cyp2y3	ref|Danio rerio cytochrome P450, family 2, subfamily Y, polypeptide 3 (cyp2y3), mRNA [NM_001020822]	-0.73	3.59E-05
socs1a	ref|Danio rerio suppressor of cytokine signaling 1a (socs1a), mRNA [NM_001003467]	-0.73	3.12E-05
perp	ref|Danio rerio PERP, TP53 apoptosis effector (perp), mRNA [NM_001256207]	-0.73	3.78E-04
si:dkeyp-69e1.8	ref|Danio rerio si:dkeyp-69e1.8 (si:dkeyp-69e1.8), mRNA [NM_001127520]	-0.74	3.86E-05
cgref1	ens|cell growth regulator with EF-hand domain 1 [Source:ZFIN;Acc:ZDB-GENE-131121-137] [ENSDART00000155002]	-0.75	1.23E-02
cish	ref|Danio rerio cytokine inducible SH2-containing protein (cish), mRNA [NM_001076617]	-0.76	1.85E-08
ENSDART00000153065	ens|si:ch211-57i17.2 [Source:ZFIN;Acc:ZDB-GENE-041014-258] [ENSDART00000153065]	-0.76	2.96E-02

or109-5	ref|Danio rerio odorant receptor, family D, subfamily 109, member 5 (or109-5), mRNA [NM_001130807]	-0.76	3.80E-02
chrac1	tc|GB|BC164918.1|AAI64918.1 zgc:110753 protein [NP13229156]	-0.77	1.01E-03
si:ch211-157c3.4	ref|Danio rerio si:ch211-157c3.4 (si:ch211-157c3.4), mRNA [NM_001164368]	-0.78	2.72E-04
zgc:162193	ref|Danio rerio zgc:162193 (zgc:162193), mRNA [NM_001089327]	-0.78	1.02E-04
zgc:101716	Unknown	-0.79	1.40E-02
frg1	ref|Danio rerio FSHD region gene 1 (frg1), mRNA [NM_001017793]	-0.79	2.15E-02
kcnj1a.2	ref|Danio rerio potassium inwardly-rectifying channel, subfamily J, member 1a, tandem duplicate 2 (kcnj1a.2), mRNA [NM_001014312]	-0.80	3.55E-07
NP9868346	tc|GB|XM_688888.1|XP_693980.1 hypothetical protein [NP9868346]	-0.80	2.20E-03
DV599636	gb|AGENCOURT_61885554 NIH_ZGC_14 Danio rerio cDNA clone IMAGE:8152191 5', mRNA sequence [DV599636]	-0.81	9.48E-03
kcnj1a.5	ref|Danio rerio potassium inwardly-rectifying channel, subfamily J, member 1a, tandem duplicate 5 (kcnj1a.5), mRNA [NM_001045169]	-0.81	2.00E-05
si:ch211-131k2.3	ref|Danio rerio si:ch211-131k2.3 (si:ch211-131k2.3), mRNA [NM_001326711]	-0.81	2.53E-04
ntrk1	ref|Danio rerio neurotrophic tyrosine kinase, receptor, type 1 (ntrk1), mRNA [NM_001301356]	-0.82	4.58E-03
pkn1a	gb|CT725606 ZF_mu Danio rerio cDNA clone ZF_mu_212o05 3', mRNA sequence [CT725606]	-0.83	1.97E-03
cishb	ref|Danio rerio cytokine inducible SH2-containing protein b (cishb), mRNA [NM_001114554]	-0.83	3.75E-07
fosab	ref|Danio rerio v-fos FBJ murine osteosarcoma viral oncogene homolog Ab (fosab), mRNA [NM_205569]	-0.83	1.85E-03
zgc:174938	ref|Danio rerio zgc:174938 (zgc:174938), mRNA [NM_001105700]	-0.83	1.13E-03

si:dkey-147f3.4	tc|Rep: LOC553461 protein - Danio rerio (Zebrafish) (Brachydanio rerio), complete [TC373254]	-0.85	8.37E-03
gch2	ref|Danio rerio GTP cyclohydrolase 2 (gch2), mRNA [NM_131667]	-0.86	1.50E-03
cst14b.1	ref|Danio rerio cystatin 14b, tandem duplicate 1 (cst14b.1), mRNA [NM_001077274]	-0.87	5.19E-04
swi5	ref|Danio rerio SWI5 homologous recombination repair protein (swi5), mRNA [NM_001326527]	-0.87	1.53E-02
ENSDART00000073440	ens|DnaJ heat shock protein family (Hsp40) member A4 [Source:HGNC Symbol;Acc:HGNC:14885] [ENSDART00000073440]	-0.88	8.00E-03
zgc:174938	ref|Danio rerio zgc:174938 (zgc:174938), mRNA [NM_001105700]	-0.88	1.58E-03
si:ch211-201h21.5	ref|Danio rerio si:ch211-201h21.5 (si:ch211-201h21.5), mRNA [NM_001030089]	-0.88	1.33E-05
si:dkey-52p2.5	ref|Danio rerio si:dkey-52p2.5 (si:dkey-52p2.5), mRNA [NM_001327887]	-0.89	3.41E-03
si:zfos-2330d3.8	ens|microfibril associated protein 4 [Source:HGNC Symbol;Acc:HGNC:7035] [ENSDART00000171552]	-0.90	2.20E-02
si:ch211-157c3.4	ref|Danio rerio si:ch211-157c3.4 (si:ch211-157c3.4), mRNA [NM_001164368]	-0.91	4.66E-04
cish	ref|Danio rerio cytokine inducible SH2-containing protein (cish), mRNA [NM_001076617]	-0.92	1.94E-07
ENSDART00000193104	gb|CT661491 ZF_mu Danio rerio cDNA clone ZF_mu_122f15 5', mRNA sequence [CT661491]	-0.92	2.29E-03
tsga10	ref|Danio rerio testis specific, 10 (tsga10), mRNA [NM_001077289]	-0.92	8.67E-03
si:busm1-172k9.2	gb|CT661491 ZF_mu Danio rerio cDNA clone ZF_mu_122f15 5', mRNA sequence [CT661491]	-0.94	1.66E-02
si:dkey-222b8.1	ens|si:dkey-222b8.1 [Source:ZFIN;Acc:ZDB-GENE-060503-248] [ENSDART00000139040]	-0.95	2.53E-04
hsp90aa1.1	ref|Danio rerio heat shock protein 90, alpha (cytosolic), class A member 1,	-0.95	2.09E-04

	tandem duplicate 1 (hsp90aa1.1), mRNA [NM_131328]		
actn2b	ref|Danio rerio actinin, alpha 2b (actn2b), mRNA [NM_001037573]	-0.96	2.98E-02
ENSDART00000122435	tc|GB|XM_001345917.2|XP_001345953.2 similar to GTPase, IMAP family member 8 [NP13315638]	-0.97	2.34E-03
NP13316011	tc|GB|XM_001921709.1|XP_001921744.1 similar to polyprotein [NP13316011]	-0.97	5.31E-03
zgc:158846	ref|Danio rerio zgc:158846 (zgc:158846), mRNA [NM_001083023]	-0.98	4.44E-03
cishb	ref|Danio rerio cytokine inducible SH2-containing protein b (cishb), mRNA [NM_001114554]	-1.00	1.29E-05
unc5c	ref|Danio rerio unc-5 netrin receptor C (unc5c), mRNA [NM_001099984]	-1.02	2.14E-03
ENSDART00000153065	ens|si:ch211-57i17.2 [Source:ZFIN;Acc:ZDB-GENE-041014-258] [ENSDART00000153065]	-1.02	7.44E-03
arg2	ref|Danio rerio arginase 2 (arg2), mRNA [NM_199611]	-1.05	6.80E-08
LOC100004427	ens|serine protease 27-like [Source:NCBI gene;Acc:100004427] [ENSDART00000162248]	-1.05	2.90E-03
cish	ref|Danio rerio cytokine inducible SH2-containing protein (cish), mRNA [NM_001076617]	-1.06	4.11E-06
si:ch211-157c3.4	ref|Danio rerio si:ch211-157c3.4 (si:ch211-157c3.4), mRNA [NM_001164368]	-1.08	1.53E-06
vipr2	ref|Danio rerio vasoactive intestinal peptide receptor 2 (vipr2), mRNA [NM_131779]	-1.09	1.90E-03
TC396001	Unknown	-1.13	1.99E-02
si:ch211-157c3.4	ref|Danio rerio si:ch211-157c3.4 (si:ch211-157c3.4), mRNA [NM_001164368]	-1.15	3.40E-05
kcnj1a.2	tc|Rep: Zgc:113361 - Danio rerio (Zebrafish) (Brachydanio rerio), complete [TC369963]	-1.16	9.58E-08
fkbp4	ref|Danio rerio FK506 binding protein 4 (fkbp4), mRNA [NM_201469]	-1.16	1.27E-04
smtlb	ref|Danio rerio somatolactin beta (smtlb), mRNA [NM_001037674]	-1.20	3.94E-03

arsj	gb|PREDICTED: Danio rerio hypothetical protein LOC559800 (LOC559800), mRNA [XM_683173]	-1.20	5.60E-03
sb:cb311	gb|ZF101-P00078-DEPE-F3_A22 GISZF101 Danio rerio cDNA clone IMAGE:7163616 5', mRNA sequence [CK697995]	-1.28	2.24E-02
cish	ref|Danio rerio cytokine inducible SH2-containing protein (cish), mRNA [NM_001076617]	-1.29	1.13E-09
nlrc3l	ens|NLR family, CARD domain containing 3-like [Source:ZFIN;Acc:ZDB-GENE-121214-346] [ENSDART00000186320]	-1.33	1.64E-03
zgc:158846	ref|Danio rerio zgc:158846 (zgc:158846), mRNA [NM_001083023]	-1.44	1.20E-02
ctsll	ref|Danio rerio cathepsin L, like (ctsll), mRNA [NM_001005999]	-1.58	4.11E-03
wu:fb36g02	gb|ZF101-P00073-DEPE-F2_G05 GISZF101 Danio rerio cDNA clone IMAGE:7161823 5', mRNA sequence [CK696476]	-2.00	2.91E-03
htr1fb	ens|5-hydroxytryptamine (serotonin) receptor 1Fb [Source:ZFIN;Acc:ZDB-GENE-090312-140] [ENSDART00000075626]	-2.32	2.18E-03
igf2r	ref|Danio rerio insulin-like growth factor 2 receptor (igf2r), mRNA [NM_001039627]	-2.38	1.13E-03

Table S3.

List of genes differentially expressed upon 24h infection of zebrafish larvae (2 days post fertilization) with PA14-WT.

Sequence Name(s)	Sequence Description	Log_2FC (PA14-WT vs Control)	p-Value
hbae5	ref|Danio rerio hemoglobin, alpha embryonic 5 (hbae5), mRNA [NM_001326701]	2.78	3.70E-06
cyp1a	ref|Danio rerio cytochrome P450, family 1, subfamily A (cyp1a), mRNA [NM_131879]	2.55	2.63E-14
hbae5	ref|Danio rerio hemoglobin, alpha embryonic 5 (hbae5), mRNA [NM_001326701]	2.53	1.02E-05
si:dkey-247k7.2	ens|si:dkey-247k7.2 [Source:ZFIN;Acc:ZDB-GENE-031118-45] [ENSDART00000158821]	2.25	1.21E-07
si:ch73-329n5.6	ens|si:ch73-329n5.6 [Source:NCBI gene;Acc:101883339] [ENSDART00000193110]	2.10	4.93E-08
galnt18a	ref|Danio rerio UDP-N-acetyl-alpha-D-galactosamine:polypeptide N-acetylgalactosaminyltransferase 18a (galnt18a), mRNA [NM_001130648]	1.87	1.79E-03
zgc:153932	ref|Danio rerio zgc:153932 (zgc:153932), mRNA [NM_001083007]	1.81	1.11E-05
ENSDART00000152950	gb|PREDICTED: Danio rerio hypothetical protein LOC100005636 (LOC100005636), mRNA [XM_001922840]	1.76	5.38E-05
zgc:174917	ref|Danio rerio zgc:174917 (zgc:174917), mRNA [NM_001105590]	1.75	5.78E-06
hbbe3	Unknown	1.75	2.58E-03
irg1l	ref|Danio rerio immunoresponsive gene 1, like (irg1l), mRNA [NM_001077607]	1.68	1.14E-04
XM_001344137	gb|PREDICTED: Danio rerio hypothetical protein LOC100005016 (LOC100005016), mRNA [XM_001344137]	1.59	9.98E-04
zgc:153932	ref|Danio rerio zgc:153932 (zgc:153932), mRNA [NM_001083007]	1.55	8.31E-05

si:ch211-207n23.2	ens|si:ch211-207n23.2 [Source:ZFIN;Acc:ZDB-GENE-131121-310] [ENSDART00000155153]	1.52	1.46E-04
hbbe3	ref|Danio rerio hemoglobin beta embryonic-3 (hbbe3), mRNA [NM_001015058]	1.52	4.92E-03
TC440008	ref|PREDICTED: Danio rerio uncharacterized LOC568930 (LOC568930), transcript variant X1, mRNA [XM_017358590]	1.50	4.76E-05
zgc:172053	ref|Danio rerio zgc:172053 (zgc:172053), mRNA [NM_001111242]	1.48	6.36E-05
si:dkey-9c18.3	ens|si:dkey-9c18.3 [Source:ZFIN;Acc:ZDB-GENE-121214-321] [ENSDART00000152356]	1.47	4.94E-02
rhcga	ref|Danio rerio Rh family, C glycoprotein a (rhcga), mRNA [NM_001089577]	1.47	2.62E-02
si:ch211-153b23.3	ens|si:ch211-153b23.3 [Source:ZFIN;Acc:ZDB-GENE-141216-408] [ENSDART00000165275]	1.45	6.69E-04
ponzr3	ref|Danio rerio plac8 onzin related protein 3 (ponzr3), mRNA [NM_001327984]	1.44	1.59E-03
XM_001344137	gb|PREDICTED: Danio rerio hypothetical protein LOC100005016 (LOC100005016), mRNA [XM_001344137]	1.43	8.36E-03
zgc:172053	ref|Danio rerio zgc:172053 (zgc:172053), mRNA [NM_001111242]	1.39	9.96E-05
ponzr4	ref|Danio rerio plac8 onzin related protein 4 (ponzr4), mRNA [NM_001327980]	1.37	1.05E-03
A_15_P764266	Unknown	1.35	1.93E-05
TC377006	tc|Rep: LOC571499 protein - Danio rerio (Zebrafish) (Brachydanio rerio), partial (49%) [TC377006]	1.31	3.56E-04
cyp1a	ref|Danio rerio cytochrome P450, family 1, subfamily A (cyp1a), mRNA [NM_131879]	1.29	2.23E-07
EH452891	gb|FDR103-P00059-DEPE-F_J01 FDR103 Danio rerio cDNA clone FDR103-P00059-BR_J01 5', mRNA sequence [EH452891]	1.29	5.44E-04
zgc:111983	ref|Danio rerio zgc:111983 (zgc:111983), mRNA [NM_001017803]	1.27	1.60E-05
ahrra	ref|Danio rerio aryl-hydrocarbon receptor repressor a (ahrra), mRNA [NM_001035265]	1.22	3.79E-09

ctsl.1	ref|Danio rerio cathepsin L.1 (ctsl.1), mRNA [NM_001002368]	1.20	9.37E-04
AW174830	gb|fe06b07.y1 Zebrafish WashU MPIMG EST Danio rerio cDNA clone IMAGE:3738037 5' similar to TR:O88486 O88486 CYTOPLASMIC DYNEIN INTERMEDIATE CHAIN 1B. [1] ;contains element PTR5 repetitive element ;, mRNA sequence [AW174830]	1.18	3.75E-03
ponzr4	ref|Danio rerio plac8 onzin related protein 4 (ponzr4), mRNA [NM_001327980]	1.17	1.75E-03
TC378867	ref|PREDICTED: Danio rerio sushi, nidogen and EGF-like domain-containing protein 1 (LOC108179106), mRNA [XM_001341787]	1.14	5.89E-04
LOC100005948	ref|PREDICTED: Danio rerio uncharacterized LOC100005948 (LOC100005948), mRNA [XM_001344808]	1.14	2.87E-03
ccl20a.3	ref|Danio rerio chemokine (C-C motif) ligand 20a, duplicate 3 (ccl20a.3), mRNA [NM_001136254]	1.10	1.18E-03
si:ch211-153b23.3	ens|si:ch211-153b23.3 [Source:ZFIN;Acc:ZDB-GENE-141216-408] [ENSDART00000165275]	1.09	2.02E-03
zgc:111983	ref|Danio rerio zgc:111983 (zgc:111983), mRNA [NM_001017803]	1.09	1.76E-04
ctsl.1	ref|Danio rerio cathepsin L.1 (ctsl.1), mRNA [NM_001002368]	1.08	1.24E-03
NP13322337	tc|GB|XM_001344530.2|XP_001344566.2 similar to Uromodulin precursor (Tamm-Horsfall urinary glycoprotein) (THP) [NP13322337]	1.03	1.06E-04
mpeg1.2	ref|Danio rerio macrophage expressed 1, tandem duplicate 2 (mpeg1.2), mRNA [NM_001020586]	1.02	5.94E-04
alas2	ref|Danio rerio aminolevulinate, delta-, synthase 2 (alas2), mRNA [NM_131682]	1.01	2.01E-02
cyp26a1	ref|Danio rerio cytochrome P450, family 26, subfamily A, polypeptide 1 (cyp26a1), mRNA [NM_131146]	1.01	2.00E-02
irg1l	ref|Danio rerio immunoresponsive gene 1, like (irg1l), mRNA [NM_001077607]	1.01	4.45E-04
egln3	ref|Danio rerio egl-9 family hypoxia-inducible factor 3 (egln3), mRNA [NM_213310]	1.00	1.53E-03

cox4i1l	ens|cytochrome c oxidase subunit 4I1, like [Source:ZFIN;Acc:ZDB-GENE-130814-2] [ENSDART00000105691]	1.00	1.50E-05
zgc:111983	ref|Danio rerio zgc:111983 (zgc:111983), mRNA [NM_001017803]	0.98	1.57E-03
hsp70.1	ref|Danio rerio heat shock cognate 70-kd protein, tandem duplicate 1 (hsp70.1), mRNA [NM_001362359]	0.95	3.86E-02
tbx16l	ref|Danio rerio T-box 16, like (tbx16l), mRNA [NM_131052]	0.94	2.53E-04
prss60.2	Unknown	0.94	1.73E-05
A_15_P671586	Unknown	0.91	1.73E-02
sult5a1	ref|Danio rerio sulfotransferase family 5A, member 1 (sult5a1), mRNA [NM_001076656]	0.91	1.28E-02
si:dkeyp-34c12.1	ref|Danio rerio si:dkeyp-34c12.1 (si:dkeyp-34c12.1), transcript variant 2, mRNA [NM_001104944]	0.90	1.81E-02
prss60.2	ref|Danio rerio serine protease 60.2 (prss60.2), mRNA [NM_001105601]	0.90	5.42E-04
zgc:158404	ref|Danio rerio zgc:158404 (zgc:158404), mRNA [NM_001080565]	0.89	1.50E-03
wu:fb93c02	gb|fb93c02.x1 Zebrafish WashU MPIMG EST Danio rerio cDNA clone IMAGE:3719426 3', mRNA sequence [AI584407]	0.89	2.96E-03
cyp26a1	ref|Danio rerio cytochrome P450, family 26, subfamily A, polypeptide 1 (cyp26a1), mRNA [NM_131146]	0.89	4.36E-02
rfesd	ref|Danio rerio Rieske (Fe-S) domain containing (rfesd), mRNA [NM_001017740]	0.89	9.98E-03
eevs	ens|2-epi-5-epi-valiolone synthase [Source:ZFIN;Acc:ZDB-GENE-131121-365] [ENSDART00000122423]	0.88	8.48E-05
LOC100535095	ref|Danio rerio uncharacterized LOC100535095 (LOC100535095), long non-coding RNA [NR_138558]	0.87	5.00E-03
tmem176l.2	ens|transmembrane protein 176l.2 [Source:ZFIN;Acc:ZDB-GENE-080829-12] [ENSDART00000132926]	0.87	5.31E-03
mfsd4ab	ref|Danio rerio major facilitator superfamily domain containing 4Ab (mfsd4ab), mRNA [NM_001114416]	0.85	6.04E-04
foxq1a	ref|Danio rerio forkhead box Q1a (foxq1a), mRNA [NM_001243344]	0.85	3.42E-04

lgals1l1	tc|GB|BC164225.1|AAI64225.1 lgals1l1 protein [NP13225910]	0.85	1.37E-02
cyp1a	ref|Danio rerio cytochrome P450, family 1, subfamily A (cyp1a), mRNA [NM_131879]	0.83	6.93E-05
zgc:172053	ref|Danio rerio zgc:172053 (zgc:172053), mRNA [NM_001111242]	0.79	4.29E-03
lgals3bpb	ref|Danio rerio lectin, galactoside-binding, soluble, 3 binding protein b (lgals3bpb), mRNA [NM_212873]	0.79	3.13E-03
ero1a	ref|Danio rerio endoplasmic reticulum oxidoreductase alpha (ero1a), mRNA [NM_200350]	0.78	1.73E-06
TC388923	ref|PREDICTED: Danio rerio uncharacterized LOC108179107 (LOC108179107), transcript variant X1, mRNA [XM_009306955]	0.77	5.86E-04
ENSDART00000146748	ens|si:dkey-21e2.3 [Source:ZFIN;Acc:ZDB-GENE-050208-618] [ENSDART00000146748]	0.77	6.43E-03
p4ha1b	ref|Danio rerio prolyl 4-hydroxylase, alpha polypeptide I b (p4ha1b), mRNA [NM_214691]	0.77	1.25E-03
slc7a3b	ens|solute carrier family 7 (cationic amino acid transporter, y+ system), member 3b [Source:ZFIN;Acc:ZDB-GENE-120813-6] [ENSDART00000087918]	0.77	3.91E-03
mmp13a	ref|Danio rerio matrix metallopeptidase 13a (mmp13a), mRNA [NM_001290479]	0.76	3.20E-02
pck1	ref|Danio rerio phosphoenolpyruvate carboxykinase 1 (soluble) (pck1), mRNA [NM_214751]	0.76	4.72E-03
cyp26c1	ref|Danio rerio cytochrome P450, family 26, subfamily C, polypeptide 1 (cyp26c1), mRNA [NM_001029951]	0.75	2.03E-03
zgc:162608	ref|Danio rerio zgc:162608 (zgc:162608), mRNA [NM_001089487]	0.75	7.22E-03
zgc:162608	ref|Danio rerio zgc:162608 (zgc:162608), mRNA [NM_001089487]	0.75	5.94E-03
LOC108179106	ens|si:ch73-329n5.2 [Source:ZFIN;Acc:ZDB-GENE-131121-66] [ENSDART00000180059]	0.75	1.36E-05
LOC571499	ens|si:ch73-329n5.1 [Source:ZFIN;Acc:ZDB-GENE-131121-475] [ENSDART00000166273]	0.74	2.58E-05

myl9b	ref|Danio rerio myosin, light chain 9b, regulatory (myl9b), mRNA [NM_213212]	0.73	2.51E-02
p4ha1b	Unknown	0.72	3.98E-04
fundc2	ref|Danio rerio fun14 domain containing 2 (fundc2), mRNA [NM_001005954]	0.72	3.30E-03
elf3	ens|E74-like factor 3 (ets domain transcription factor, epithelial-specific) [Source:ZFIN;Acc:ZDB-GENE-030131-8760] [ENSDART00000149460]	0.72	1.46E-03
TC379404	tc|Rep: Secretogranin III - Danio rerio (Zebrafish) (Brachydanio rerio), partial (92%) [TC379404]	0.71	2.29E-03
cxcl19	ref|Danio rerio chemokine (C-X-C motif) ligand 19 (cxcl19), mRNA [NM_001113651]	0.71	2.21E-03
hspa8	ref|Danio rerio heat shock protein 8 (hspa8), mRNA [NM_001110403]	0.70	3.40E-04
stau1	ref|Danio rerio staufen double-stranded RNA binding protein 1 (stau1), mRNA [NM_205561]	0.68	9.88E-04
zgc:111983	Unknown	0.68	3.78E-02
sult6b1	ref|Danio rerio sulfotransferase family, cytosolic, 6b, member 1 (sult6b1), mRNA [NM_214686]	0.68	2.69E-05
bcas2	ref|Danio rerio BCAS2, pre-mRNA processing factor (bcas2), mRNA [NM_001007774]	0.68	1.74E-02
dnase1l1l	ref|Danio rerio deoxyribonuclease I-like 1-like (dnase1l1l), mRNA [NM_001002403]	0.67	3.04E-02
eif3ea	ref|Danio rerio eukaryotic translation initiation factor 3, subunit E, a (eif3ea), mRNA [NM_200839]	0.67	9.65E-06
TC377034	ref|PREDICTED: Danio rerio uncharacterized LOC100536887 (LOC100536887), mRNA [XM_003201704]	0.67	1.87E-02
stc1l	ref|Danio rerio stanniocalcin 1, like (stc1l), mRNA [NM_200539]	0.67	8.55E-03
cyp1b1	ref|Danio rerio cytochrome P450, family 1, subfamily B, polypeptide 1 (cyp1b1), transcript variant 3, mRNA [NM_001145708]	0.67	2.15E-03

ENSDART00000162027	tc|GB|XM_001343781.2|XP_001343817.2 similar to protease, serine 27 [NP13317523]	0.67	6.78E-03
pfkfb3	ref|Danio rerio 6-phosphofructo-2-kinase/fructose-2,6-biphosphatase 3 (pfkfb3), mRNA [NM_213397]	0.67	2.57E-03
TC454255	tc|Rep: Copia-type polyprotein - Arabidopsis thaliana (Mouse-ear cress), partial (10%) [TC454255]	0.67	3.26E-02
BC054571	gb|FDR103-P00060-DEPE-F_O04 FDR103 Danio rerio cDNA clone FDR103-P00060-BR_O04 5', mRNA sequence [EH453373]	0.66	1.66E-04
cyp1c2	ref|Danio rerio cytochrome P450, family 1, subfamily C, polypeptide 2 (cyp1c2), mRNA [NM_001114849]	0.65	1.04E-02
lrrn1	ref|Danio rerio leucine rich repeat neuronal 1 (lrrn1), mRNA [NM_001130694]	0.65	1.48E-05
CT648970	gb|CT648970 ZF_mu Danio rerio cDNA clone ZF_mu_101c10 5', mRNA sequence [CT648970]	0.65	1.87E-02
snx4	ref|Danio rerio sorting nexin 4 (snx4), mRNA [NM_001014346]	0.65	3.47E-04
fam114a1	ref|Danio rerio family with sequence similarity 114, member A1 (fam114a1), mRNA [NM_001089478]	0.65	3.38E-02
prtga	tc|Rep: Protogenin A precursor - Danio rerio (Zebrafish) (Brachydanio rerio), complete [TC366174]	0.65	3.24E-04
zgc:163057	ref|Danio rerio zgc:163057 (zgc:163057), mRNA [NM_001082834]	0.65	1.44E-02
noxo1a	ref|Danio rerio NADPH oxidase organizer 1a (noxo1a), mRNA [NM_001077584]	0.65	3.65E-04
egln3	ref|Danio rerio egl-9 family hypoxia-inducible factor 3 (egln3), mRNA [NM_213310]	0.65	1.78E-02
fut9d	ref|Danio rerio fucosyltransferase 9d (fut9d), mRNA [NM_001077246]	0.63	4.15E-03
cyp1c1	ref|Danio rerio cytochrome P450, family 1, subfamily C, polypeptide 1 (cyp1c1), mRNA [NM_001020610]	0.63	1.14E-02
serbp1a	ref|Danio rerio SERPINE1 mRNA binding protein 1a (serbp1a), mRNA [NM_214714]	0.63	1.33E-05

pnp4b	ref|Danio rerio purine nucleoside phosphorylase 4b (pnp4b), mRNA [NM_205643]	0.63	3.32E-02
pkhd1l1	ref|Danio rerio polycystic kidney and hepatic disease 1 (autosomal recessive)-like 1 (pkhd1l1), mRNA [NM_001318128]	0.62	7.17E-04
slc2a15b	ref|Danio rerio solute carrier family 2 (facilitated glucose transporter), member 15b (slc2a15b), mRNA [NM_001020494]	0.62	2.77E-02
chd4b	ens|chromodomain helicase DNA binding protein 4a [Source:ZFIN;Acc:ZDB-GENE-041111-187] [ENSDART00000005453]	0.62	1.33E-02
emg1	tc|Rep: LOC553478 protein - Danio rerio (Zebrafish) (Brachydanio rerio), complete [TC376782]	0.62	1.69E-02
zgc:158404	ref|Danio rerio zgc:158404 (zgc:158404), mRNA [NM_001080565]	0.62	1.52E-02
tbx16l	ref|Danio rerio T-box 16, like (tbx16l), mRNA [NM_131052]	0.62	4.19E-03
tcnbb	ref|Danio rerio si:ch211-117m20.5 (si:ch211-117m20.5), mRNA [NM_001252649]	0.61	2.72E-04
serpinh1a	ref|Danio rerio serpin peptidase inhibitor, clade H (heat shock protein 47), member 1a (serpinh1a), mRNA [NM_001110374]	0.61	3.12E-04
vcanb	ref|Danio rerio versican b (vcanb), mRNA [NM_214688]	0.60	2.34E-04
pdia3	ref|Danio rerio protein disulfide isomerase family A, member 3 (pdia3), mRNA [NM_001199737]	0.60	2.80E-05
g6pca.1	ref|Danio rerio glucose-6-phosphatase a, catalytic subunit, tandem duplicate 1 (g6pca.1), transcript variant 1, mRNA [NM_001003512]	0.60	3.63E-02
gstm.1	ref|Danio rerio glutathione S-transferase mu, tandem duplicate 1 (gstm.1), mRNA [NM_212676]	-0.60	1.54E-05
gnat1	ref|Danio rerio guanine nucleotide binding protein (G protein), alpha transducing activity polypeptide 1 (gnat1), mRNA [NM_131868]	-0.60	1.94E-02
cyp2k16	ref|Danio rerio cytochrome P450, family 2, subfamily K, polypeptide16 (cyp2k16), mRNA [NM_001005963]	-0.61	6.28E-05

ckmt2a	ref|Danio rerio creatine kinase, mitochondrial 2a (sarcomeric) (ckmt2a), transcript variant 1, mRNA [NM_001308608]	-0.61	3.39E-02
si:dkeyp-110c7.4	ens|si:dkeyp-110c7.4 [Source:ZFIN;Acc:ZDB-GENE-070705-532] [ENSDART00000164279]	-0.61	4.54E-07
si:ch211-195b11.3	ref|Danio rerio si:ch211-195b11.3 (si:ch211-195b11.3), mRNA [NM_001291900]	-0.61	3.82E-05
krt15	ref|Danio rerio keratin 15 (krt15), mRNA [NM_213523]	-0.61	3.78E-04
itih3a	ref|Danio rerio inter-alpha-trypsin inhibitor heavy chain 3a (itih3a), mRNA [NM_001020588]	-0.61	2.73E-02
ucmab	ref|Danio rerio upper zone of growth plate and cartilage matrix associated b (ucmab), mRNA [NM_212934]	-0.61	1.78E-03
matn3a	ref|Danio rerio matrilin 3a (matn3a), transcript variant 1, mRNA [NM_001004007]	-0.61	7.19E-03
krt15	ref|Danio rerio keratin 15 (krt15), mRNA [NM_213523]	-0.61	5.47E-04
tmem237a	ref|Danio rerio transmembrane protein 237a (tmem237a), mRNA [NM_001319136]	-0.61	4.57E-03
tnni2a.1	ref|Danio rerio troponin I type 2a (skeletal, fast), tandem duplicate 1 (tnni2a.1), mRNA [NM_001007365]	-0.61	1.57E-02
aqp8b	ref|Danio rerio aquaporin 8b (aqp8b), mRNA [NM_001114910]	-0.61	1.13E-03
cishb	ref|Danio rerio cytokine inducible SH2-containing protein b (cishb), mRNA [NM_001114554]	-0.61	4.29E-03
ccl34b.1	ref|Danio rerio chemokine (C-C motif) ligand 34b, duplicate 1 (ccl34b.1), mRNA [NM_001115054]	-0.61	1.55E-03
prph2a	ref|Danio rerio peripherin 2a (retinal degeneration, slow) (prph2a), mRNA [NM_131566]	-0.62	5.42E-03
zgc:112146	ref|Danio rerio zgc:112146 (zgc:112146), mRNA [NM_001017731]	-0.62	5.50E-04
mgst2	ref|Danio rerio microsomal glutathione S-transferase 2 (mgst2), mRNA [NM_001045302]	-0.62	2.61E-03

jac10	ref|Danio rerio jacalin 10 (jac10), mRNA [NM_001110036]	-0.62	1.49E-02
cpb1	ref|Danio rerio carboxypeptidase B1 (tissue) (cpb1), transcript variant 2, mRNA [NM_001110021]	-0.62	2.24E-04
klhdc3	gb|AGENCOURT_21025036 NIH_ZGC_8 Danio rerio cDNA clone IMAGE:7242183 5', mRNA sequence [CN174295]	-0.62	9.22E-03
apbb1ip	ref|Danio rerio amyloid beta (A4) precursor protein-binding, family B, member 1 interacting protein (apbb1ip), mRNA [NM_200634]	-0.62	1.28E-02
rbp2a	ref|Danio rerio retinol binding protein 2a, cellular (rbp2a), mRNA [NM_153004]	-0.63	4.27E-02
gucy2d	ref|Danio rerio guanylate cyclase 2D, retinal (gucy2d), mRNA [NM_131866]	-0.63	5.35E-03
sv2ba	ref|Danio rerio synaptic vesicle glycoprotein 2Ba (sv2ba), mRNA [NM_001082995]	-0.63	7.68E-03
A_15_P156651	Unknown	-0.63	1.07E-02
si:ch211-240l19.5	ref|Danio rerio si:ch211-240l19.5 (si:ch211-240l19.5), mRNA [NM_001030152]	-0.63	2.66E-04
LOC110437731	ens|haptoglobin [Source:ZFIN;Acc:ZDB-GENE-030131-1259] [ENSDART00000149010]	-0.63	9.37E-03
ezra	ref|Danio rerio ezrin a (ezra), mRNA [NM_001020490]	-0.64	2.95E-03
crybgx	ref|Danio rerio crystallin beta gamma X (crybgx), mRNA [NM_001033722]	-0.64	4.17E-02
cnga3a	ens|cyclic nucleotide gated channel alpha 3a [Source:ZFIN;Acc:ZDB-GENE-090611-2] [ENSDART00000149833]	-0.64	1.59E-03
gngt2a	Unknown	-0.64	9.93E-03
grk7a	ref|Danio rerio G protein-coupled receptor kinase 7a (grk7a), mRNA [NM_001031841]	-0.65	2.11E-03
csnk1a1	ref|Danio rerio casein kinase 1, alpha 1 (csnk1a1), mRNA [NM_152951]	-0.65	7.62E-03
krt96	ref|Danio rerio keratin 96 (krt96), mRNA [NM_001199952]	-0.65	2.26E-03
cplx4a	ref|Danio rerio complexin 4a (cplx4a), mRNA [NM_001077300]	-0.65	1.51E-02
cgref1	ens|cell growth regulator with EF-hand domain 1 [Source:ZFIN;Acc:ZDB-	-0.65	2.94E-02

	GENE-131121-137] [ENSDART00000155002]		
zgc:113232	ref|Danio rerio zgc:113232 (zgc:113232), transcript variant 2, mRNA [NM_001127513]	-0.65	5.21E-03
col9a1b	ref|Danio rerio collagen, type IX, alpha 1b (col9a1b), mRNA [NM_213264]	-0.65	9.73E-05
si:dkey-96g2.1	ens|si:dkey-96g2.1 [Source:ZFIN;Acc:ZDB-GENE-131121-563] [ENSDART00000155131]	-0.65	6.92E-07
matn3a	ref|Danio rerio matrilin 3a (matn3a), transcript variant 1, mRNA [NM_001004007]	-0.66	2.36E-02
zgc:110789	ref|Danio rerio zgc:110789 (zgc:110789), mRNA [NM_001013335]	-0.66	3.98E-02
arr3a	ref|Danio rerio arrestin 3a, retinal (X-arrestin) (arr3a), mRNA [NM_001002405]	-0.66	4.09E-02
sult2st2	ref|Danio rerio sulfotransferase family 2, cytosolic sulfotransferase 2 (sult2st2), mRNA [NM_001078169]	-0.66	1.19E-02
si:dkey-266f7.4	ref|Danio rerio si:dkey-266f7.4 (si:dkey-266f7.4), mRNA [NM_001100018]	-0.66	4.96E-03
LOC560627	ens|cytosolic 5'-nucleotidase 1A [Source:NCBI gene;Acc:560627] [ENSDART00000184275]	-0.66	4.05E-02
mboat1	ens|membrane bound O-acyltransferase domain containing 1 [Source:ZFIN;Acc:ZDB-GENE-041114-98] [ENSDART00000141860]	-0.66	1.08E-05
epd	ref|Danio rerio ependymin (epd), mRNA [NM_131005]	-0.66	1.39E-02
prph2a	ref|Danio rerio peripherin 2a (retinal degeneration, slow) (prph2a), mRNA [NM_131566]	-0.66	8.98E-04
acmsd	ref|Danio rerio aminocarboxymuconate semialdehyde decarboxylase (acmsd), mRNA [NM_001089494]	-0.67	9.51E-03
csnk2a1	ref|Danio rerio casein kinase 2, alpha 1 polypeptide (csnk2a1), mRNA [NM_131252]	-0.67	2.57E-03
aqp8b	ref|Danio rerio aquaporin 8b (aqp8b), mRNA [NM_001114910]	-0.67	1.58E-04
stoml3b	ref|Danio rerio stomatin (EPB72)-like 3b (stoml3b), mRNA [NM_001017825]	-0.67	1.17E-03

ela2l	ref|Danio rerio elastase 2 like (ela2l), mRNA [NM_199886]	-0.67	3.28E-02
zgc:77748	ref|Danio rerio zgc:77748 (zgc:77748), mRNA [NM_200858]	-0.67	3.23E-03
zgc:193726	ref|Danio rerio zgc:193726 (zgc:193726), mRNA [NM_001135973]	-0.68	6.61E-03
erp27	tc|Rep: Chromosome undetermined SCAF12091, whole genome shotgun sequence - Tetraodon nigroviridis (Green puffer), partial (71%) [TC377954]	-0.68	5.03E-03
crip1	ref|Danio rerio cysteine-rich protein 1 (crip1), transcript variant 2, mRNA [NM_001166582]	-0.68	4.15E-03
trpv6	ref|Danio rerio transient receptor potential cation channel, subfamily V, member 6 (trpv6), mRNA [NM_001001849]	-0.68	8.87E-07
cpb1	ref|Danio rerio carboxypeptidase B1 (tissue) (cpb1), transcript variant 2, mRNA [NM_001110021]	-0.68	2.31E-04
NP13322978	tc|GB|XM_001919422.1|XP_001919457.1 similar to pol polyprotein [NP13322978]	-0.68	1.16E-03
A_15_P201336	Unknown	-0.68	3.77E-04
crygm2f	ref|Danio rerio crystallin, gamma M2f (crygm2f), mRNA [NM_001110106]	-0.69	6.07E-03
guk1b	ref|Danio rerio guanylate kinase 1b (guk1b), mRNA [NM_200724]	-0.69	7.43E-03
mustn1b	ref|Danio rerio musculoskeletal, embryonic nuclear protein 1b (mustn1b), mRNA [NM_001197053]	-0.69	3.21E-02
fabp2	ref|Danio rerio fatty acid binding protein 2, intestinal (fabp2), mRNA [NM_131431]	-0.70	1.36E-03
si:dkey-188i13.6	ref|Danio rerio si:dkey-188i13.6 (si:dkey-188i13.6), mRNA [NM_001327855]	-0.70	2.05E-03
socs1a	ref|Danio rerio suppressor of cytokine signaling 1a (socs1a), mRNA [NM_001003467]	-0.70	6.27E-05
cish	ref|Danio rerio cytokine inducible SH2-containing protein (cish), mRNA [NM_001076617]	-0.70	2.41E-05
cyp2p9	ref|Danio rerio cytochrome P450, family 2, subfamily P, polypeptide 9 (cyp2p9), mRNA [NM_200620]	-0.70	2.93E-02
psma4	ref|Danio rerio proteasome subunit alpha 4 (psma4), mRNA [NM_214697]	-0.70	3.35E-03

itln3	ref|Danio rerio intelectin 3 (itln3), mRNA [NM_001159584]	-0.70	2.55E-04
or126-2	ref|Danio rerio odorant receptor, family E, subfamily 126, member 2 (or126-2), mRNA [NM_001128397]	-0.71	1.86E-03
ngs	ref|Danio rerio notochord granular surface (ngs), mRNA [NM_001128765]	-0.71	1.75E-03
arl3l2	ref|Danio rerio ADP-ribosylation factor-like 3, like 2 (arl3l2), mRNA [NM_200719]	-0.71	2.51E-05
sncga	ref|Danio rerio synuclein, gamma a (sncga), mRNA [NM_001017567]	-0.71	2.07E-04
tmem237b	ref|Danio rerio transmembrane protein 237b (tmem237b), mRNA [NM_001004636]	-0.71	7.45E-03
lmnl3	ref|Danio rerio lamin L3 (lmnl3), mRNA [NM_152973]	-0.72	4.24E-02
stm	ref|Danio rerio starmaker (stm), mRNA [NM_198817]	-0.72	5.20E-04
arr3a	ref|Danio rerio arrestin 3a, retinal (X-arrestin) (arr3a), mRNA [NM_001002405]	-0.72	3.46E-02
sult1st6	ref|Danio rerio sulfotransferase family 1, cytosolic sulfotransferase 6 (sult1st6), mRNA [NM_001002599]	-0.72	9.50E-06
cts12	ens|cathepsin 12 [Source:ZFIN;Acc:ZDB-GENE-050208-336] [ENSDART00000062749]	-0.73	1.30E-04
kcnh3	ens|potassium voltage-gated channel, subfamily H (eag-related), member 3 [Source:ZFIN;Acc:ZDB-GENE-070912-23] [ENSDART00000146284]	-0.73	2.93E-03
zgc:112492	ref|Danio rerio zgc:112492 (zgc:112492), mRNA [NM_001017658]	-0.73	2.59E-04
zgc:172079	ref|Danio rerio zgc:172079 (zgc:172079), mRNA [NM_001113340]	-0.73	7.67E-04
pkp1b	ens|plakophilin 1b [Source:ZFIN;Acc:ZDB-GENE-030131-417] [ENSDART00000074605]	-0.74	8.78E-07
nme2a	ref|Danio rerio NME/NM23 nucleoside diphosphate kinase 2a (nme2a), mRNA [NM_199970]	-0.74	2.18E-02
zgc:112302	ref|Danio rerio zgc:112302 (zgc:112302), mRNA [NM_001025187]	-0.74	1.32E-04
fads2	ref|Danio rerio fatty acid desaturase 2 (fads2), mRNA [NM_131645]	-0.74	2.60E-04

stm	ref|Danio rerio starmaker (stm), mRNA [NM_198817]	-0.74	2.92E-03
matn3a	ref|Danio rerio matrilin 3a (matn3a), transcript variant 1, mRNA [NM_001004007]	-0.74	2.23E-04
sagb	ref|Danio rerio S-antigen; retina and pineal gland (arrestin) b (sagb), mRNA [NM_001033749]	-0.75	2.77E-03
opn1mw2	ref|Danio rerio opsin 1 (cone pigments), medium-wave-sensitive, 2 (opn1mw2), mRNA [NM_182891]	-0.75	3.03E-03
matn3a	tc|Rep: Matrilin-3a precursor - Danio rerio (Zebrafish) (Brachydanio rerio), complete [TC370620]	-0.75	4.34E-03
trappc13	ref|Danio rerio trafficking protein particle complex 13 (trappc13), transcript variant 2, mRNA [NM_199538]	-0.75	1.23E-02
TC387531	tc|Rep: Chromosome undetermined SCAF14702, whole genome shotgun sequence - Tetraodon nigroviridis (Green puffer), partial (56%) [TC387531]	-0.75	1.18E-02
cish	ref|Danio rerio cytokine inducible SH2-containing protein (cish), mRNA [NM_001076617]	-0.75	5.20E-04
rgs9a	ref|Danio rerio regulator of G protein signaling 9a (rgs9a), mRNA [NM_001327800]	-0.76	1.60E-03
cbln13	ref|Danio rerio cerebellin 13 (cbln13), mRNA [NM_001123061]	-0.76	5.28E-04
rho	ref|Danio rerio rhodopsin (rho), mRNA [NM_131084]	-0.76	1.21E-02
cst14b.1	ref|Danio rerio cystatin 14b, tandem duplicate 1 (cst14b.1), mRNA [NM_001077274]	-0.76	2.03E-03
syt5a	ref|Danio rerio synaptotagmin Va (syt5a), mRNA [NM_001103137]	-0.76	1.38E-02
si:ch211-81a5.8	ref|Danio rerio si:ch211-81a5.8 (si:ch211-81a5.8), mRNA [NM_001044935]	-0.77	5.27E-03
pdcb	ref|Danio rerio phosducin b (pdcb), mRNA [NM_001025464]	-0.77	9.89E-03
tm4sf4	ref|Danio rerio transmembrane 4 L six family member 4 (tm4sf4), mRNA [NM_001003489]	-0.77	9.47E-03
duox	ens|dual oxidase [Source:ZFIN;Acc:ZDB-GENE-091117-14] [ENSDART00000090727]	-0.77	4.09E-03

apmap	ref|Danio rerio adipocyte plasma membrane associated protein (apmap), mRNA [NM_212608]	-0.77	5.47E-03
olfm1a	ref|Danio rerio olfactomedin 1a (olfm1a), transcript variant 2, mRNA [NM_001327880]	-0.77	9.74E-03
LOC100331497	ref|Danio rerio U2 small nuclear ribonucleoprotein auxiliary factor 35 kDa subunit-related protein 1-like (LOC100331497), mRNA [NM_001327888]	-0.78	8.16E-04
s100a11	ref|Danio rerio S100 calcium binding protein A11 (s100a11), mRNA [NM_001282183]	-0.78	3.50E-05
aldoca	ref|Danio rerio aldolase C, fructose-bisphosphate, a (aldoca), mRNA [NM_001029952]	-0.78	4.33E-06
NP13317243	tc|GB|XM_001922300.1|XP_001922335.1 similar to serine hydrolase-like [NP13317243]	-0.78	2.05E-03
zgc:77748	ref|Danio rerio zgc:77748 (zgc:77748), mRNA [NM_200858]	-0.80	8.89E-05
anxa2b	Unknown	-0.80	5.93E-04
EH440526	gb|FDR103-P00025-DEPE-F_I03 FDR103 Danio rerio cDNA clone FDR103-P00025-BR_I03 5', mRNA sequence [EH440526]	-0.81	1.14E-04
si:dkey-21e2.15	ens|si:dkey-21e2.15 [Source:ZFIN;Acc:ZDB-GENE-050208-780] [ENSDART00000132386]	-0.81	1.36E-03
vil1	ref|Danio rerio villin 1 (vil1), mRNA [NM_200238]	-0.81	2.38E-03
hoxc12a	ref|Danio rerio homeobox C12a (hoxc12a), mRNA [NM_001110759]	-0.81	3.15E-03
fbp2	ref|Danio rerio fructose-1,6-bisphosphatase 2 (fbp2), mRNA [NM_001004008]	-0.82	4.49E-03
NP13318126	tc|GB|XM_001920642.1|XP_001920677.1 similar to butyrophilin, subfamily 2, member A2 [NP13318126]	-0.82	8.91E-03
si:ch73-288o11.5	ens|si:ch73-288o11.5 [Source:ZFIN;Acc:ZDB-GENE-131121-416] [ENSDART00000154123]	-0.82	2.36E-10
gng13a	ref|Danio rerio guanine nucleotide binding protein (G protein), gamma 13a	-0.82	1.47E-04

	(gng13a), transcript variant 1, mRNA [NM_001166125]		
si:dkey-21e2.15	ens|si:dkey-21e2.15 [Source:ZFIN;Acc:ZDB-GENE-050208-780] [ENSDART00000137976]	-0.83	4.07E-04
mtif3	ref|Danio rerio mitochondrial translational initiation factor 3 (mtif3), mRNA [NM_001326363]	-0.83	2.25E-02
pdcb	ref|Danio rerio phosducin b (pdcb), mRNA [NM_001025464]	-0.83	2.04E-03
stm	ref|Danio rerio starmaker (stm), mRNA [NM_198817]	-0.84	2.87E-05
zgc:172065	ref|Danio rerio zgc:172065 (zgc:172065), mRNA [NM_001114719]	-0.84	2.98E-03
anxa2b	ref|Danio rerio annexin A2b (anxa2b), mRNA [NM_001105600]	-0.84	4.95E-05
pdia2	ref|Danio rerio protein disulfide isomerase family A, member 2 (pdia2), mRNA [NM_001320534]	-0.85	7.73E-04
gnat2	ref|Danio rerio guanine nucleotide binding protein (G protein), alpha transducing activity polypeptide 2 (gnat2), mRNA [NM_131869]	-0.85	1.13E-02
si:dkey-52d15.2	ens|si:dkey-52d15.2 [Source:NCBI gene;Acc:100006993] [ENSDART00000142311]	-0.85	2.38E-02
cpb1	ref|Danio rerio carboxypeptidase B1 (tissue) (cpb1), transcript variant 2, mRNA [NM_001110021]	-0.85	5.77E-05
aasdhppt	ref|Danio rerio aminoadipate-semialdehyde dehydrogenase-phosphopantetheinyl transferase (aasdhppt), mRNA [NM_001033729]	-0.86	1.77E-02
fabp10a	ref|Danio rerio fatty acid binding protein 10a, liver basic (fabp10a), mRNA [NM_152960]	-0.86	2.54E-02
prf1.1	ref|Danio rerio perforin 1.1 (prf1.1), mRNA [NM_001317762]	-0.86	6.16E-04
slc38a11	ref|Danio rerio solute carrier family 38, member 11 (slc38a11), mRNA [NM_001017644]	-0.86	2.71E-04
zgc:112160	ref|Danio rerio zgc:112160 (zgc:112160), mRNA [NM_001017724]	-0.86	3.90E-03
si:ch1073-303d10.1	ens|si:ch1073-303d10.1 [Source:ZFIN;Acc:ZDB-GENE-141216-327] [ENSDART00000171854]	-0.87	3.54E-03

zgc:158846	ref|Danio rerio zgc:158846 (zgc:158846), mRNA [NM_001083023]	-0.87	1.08E-02
zgc:165515	ref|Danio rerio zgc:165515 (zgc:165515), mRNA [NM_001099227]	-0.87	1.45E-02
si:dkeyp-73d8.6	ref|Danio rerio si:dkeyp-73d8.6 (si:dkeyp-73d8.6), mRNA [NM_001130644]	-0.87	3.45E-03
scpp5	ref|Danio rerio secretory calcium-binding phosphoprotein 5 (scpp5), mRNA [NM_001145236]	-0.87	6.39E-03
ela3l	ref|Danio rerio elastase 3 like (ela3l), mRNA [NM_001024408]	-0.88	3.39E-05
si:ch211-285j22.3	ref|Danio rerio si:ch211-285j22.3 (si:ch211-285j22.3), long non-coding RNA [NR_120357]	-0.88	9.01E-03
cish	ref|Danio rerio cytokine inducible SH2-containing protein (cish), mRNA [NM_001076617]	-0.88	4.18E-06
zgc:193593	ref|Danio rerio zgc:193593 (zgc:193593), mRNA [NM_001128717]	-0.88	9.40E-03
spaca4l	ens|sperm acrosome associated 4 like [Source:ZFIN;Acc:ZDB-GENE-101011-2] [ENSDART00000188868]	-0.88	4.51E-02
prph2a	ref|Danio rerio peripherin 2a (retinal degeneration, slow) (prph2a), mRNA [NM_131566]	-0.88	5.19E-03
TC382187	tc|Rep: Zgc:158224 protein - Danio rerio (Zebrafish) (Brachydanio rerio), complete [TC382187]	-0.89	6.76E-04
ppa1a	ref|Danio rerio pyrophosphatase (inorganic) 1a (ppa1a), mRNA [NM_200733]	-0.89	1.50E-03
rcvrn3	ref|Danio rerio recoverin 3 (rcvrn3), mRNA [NM_200825]	-0.90	8.89E-03
si:ch211-103n10.5	ens|si:ch211-103n10.5 [Source:ZFIN;Acc:ZDB-GENE-030131-5155] [ENSDART00000188165]	-0.91	7.57E-03
cpa4	ref|Danio rerio carboxypeptidase A4 (cpa4), mRNA [NM_001002217]	-0.91	3.20E-03
si:ch73-306e8.2	ens|si:ch73-306e8.2 [Source:ZFIN;Acc:ZDB-GENE-131121-409] [ENSDART00000153515]	-0.91	2.20E-10
rp1l1b	ens|retinitis pigmentosa 1-like 1b [Source:ZFIN;Acc:ZDB-GENE-091204-67] [ENSDART00000151881]	-0.91	1.18E-03
anxa1b	ref|Danio rerio annexin A1b (anxa1b), mRNA [NM_181759]	-0.92	3.76E-05

ENSDART00000134017	ens|si:dkey-17e16.15 [Source:ZFIN;Acc:ZDB-GENE-091204-295] [ENSDART00000134017]	-0.93	1.01E-03
syt5a	ref|Danio rerio synaptotagmin Va (syt5a), mRNA [NM_001103137]	-0.93	6.24E-03
EH440526	gb|FDR103-P00025-DEPE-F_I03 FDR103 Danio rerio cDNA clone FDR103-P00025-BR_I03 5', mRNA sequence [EH440526]	-0.93	6.79E-05
sgcg	ens|sarcoglycan, gamma [Source:ZFIN;Acc:ZDB-GENE-030724-2] [ENSDART00000144381]	-0.93	2.29E-02
opn1mw2	ref|Danio rerio opsin 1 (cone pigments), medium-wave-sensitive, 2 (opn1mw2), mRNA [NM_182891]	-0.94	6.87E-03
cpa4	ref|Danio rerio carboxypeptidase A4 (cpa4), mRNA [NM_001002217]	-0.95	1.97E-03
hmgb2a	ref|Danio rerio high mobility group box 2a (hmgb2a), mRNA [NM_001037424]	-0.95	4.12E-02
si:dkey-78l4.8	ens|si:dkey-78l4.8 [Source:ZFIN;Acc:ZDB-GENE-060503-270] [ENSDART00000136576]	-0.96	2.87E-03
cbx5	ref|Danio rerio chromobox homolog 5 (HP1 alpha homolog, Drosophila) (cbx5), mRNA [NM_001080184]	-0.96	1.60E-02
guca1c	ref|Danio rerio guanylate cyclase activator 1C (guca1c), mRNA [NM_194393]	-0.97	2.71E-04
selenoe	ref|Danio rerio selenoprotein e (selenoe), mRNA [NM_001195784]	-0.97	1.98E-03
ppa2	ref|Danio rerio pyrophosphatase (inorganic) 2 (ppa2), mRNA [NM_205662]	-0.97	1.22E-02
pde6hb	ref|Danio rerio phosphodiesterase 6H, cGMP-specific, cone, gamma, paralog b (pde6hb), mRNA [NM_200837]	-0.97	6.84E-03
prss1	ref|Danio rerio serine protease 1 (prss1), mRNA [NM_131708]	-0.97	1.09E-02
grk7a	ref|Danio rerio G protein-coupled receptor kinase 7a (grk7a), mRNA [NM_001031841]	-0.98	1.27E-02
arr3b	ref|Danio rerio arrestin 3b, retinal (X-arrestin) (arr3b), mRNA [NM_200792]	-0.98	1.33E-02
si:ch211-285j22.3	ref|Danio rerio si:ch211-285j22.3 (si:ch211-285j22.3), long non-coding RNA [NR_120357]	-0.98	3.20E-03

rbp3	ref|Danio rerio retinol binding protein 3 (rbp3), mRNA [NM_131451]	-0.98	2.42E-03
slc25a3a	ref|Danio rerio solute carrier family 25 (mitochondrial carrier; phosphate carrier), member 3a (slc25a3a), transcript variant 2, mRNA [NM_200715]	-0.99	3.63E-03
ctrb1	ref|Danio rerio chymotrypsinogen B1 (ctrb1), mRNA [NM_212618]	-0.99	1.89E-03
tcnba	ref|Danio rerio transcobalamin like (tcnl), mRNA [NM_001128735]	-0.99	3.62E-04
galns	ref|Danio rerio galactosamine (N-acetyl)-6-sulfatase (galns), mRNA [NM_001080641]	-1.00	5.48E-03
opn1lw2	ref|Danio rerio opsin 1 (cone pigments), long-wave-sensitive, 2 (opn1lw2), mRNA [NM_001002443]	-1.01	1.12E-02
gnat2	ref|Danio rerio guanine nucleotide binding protein (G protein), alpha transducing activity polypeptide 2 (gnat2), mRNA [NM_131869]	-1.02	4.10E-02
aqp8a.2	ref|Danio rerio aquaporin 8a, tandem duplicate 2 (aqp8a.2), mRNA [NM_001080182]	-1.02	1.58E-03
arr3b	ref|Danio rerio arrestin 3b, retinal (X-arrestin) (arr3b), mRNA [NM_200792]	-1.03	6.60E-03
si:ch211-119o8.7	ref|Danio rerio si:ch211-119o8.7 (si:ch211-119o8.7), mRNA [NM_001114899]	-1.03	2.14E-03
zgc:195245	ref|Danio rerio zgc:195245 (zgc:195245), mRNA [NM_001126422]	-1.04	5.57E-04
prph2b	ref|Danio rerio peripherin 2b (retinal degeneration, slow) (prph2b), mRNA [NM_131567]	-1.04	5.25E-03
grk7a	ref|Danio rerio G protein-coupled receptor kinase 7a (grk7a), mRNA [NM_001031841]	-1.04	4.89E-04
pdcb	ref|Danio rerio phosducin b (pdcb), mRNA [NM_001025464]	-1.06	1.04E-02
guca1c	ref|Danio rerio guanylate cyclase activator 1C (guca1c), mRNA [NM_194393]	-1.08	1.83E-04
pde6c	ref|Danio rerio phosphodiesterase 6C, cGMP-specific, cone, alpha prime (pde6c), mRNA [NM_200871]	-1.09	2.93E-02

opn1sw2	ref|Danio rerio opsin 1 (cone pigments), short-wave-sensitive 2 (opn1sw2), mRNA [NM_131192]	-1.10	1.02E-02
ela2	ref|Danio rerio elastase 2 (ela2), mRNA [NM_001139464]	-1.11	8.39E-03
sult3st4	ref|Danio rerio sulfotransferase family 3, cytosolic sulfotransferase 4 (sult3st4), mRNA [NM_001308830]	-1.14	1.66E-09
tgm1l4	ref|Danio rerio transglutaminase 1 like 4 (tgm1l4), mRNA [NM_001030096]	-1.14	1.62E-04
tmsb4x	ref|Danio rerio thymosin beta 4 X-linked (tmsb4x), mRNA [NM_001130697]	-1.14	1.01E-03
pde6hb	ref|Danio rerio phosphodiesterase 6H, cGMP-specific, cone, gamma, paralog b (pde6hb), mRNA [NM_200837]	-1.15	2.72E-03
cpa5	ref|Danio rerio carboxypeptidase A5 (cpa5), mRNA [NM_199271]	-1.15	7.67E-04
cpa5	ref|Danio rerio carboxypeptidase A5 (cpa5), mRNA [NM_199271]	-1.17	2.07E-04
gnb3b	ref|Danio rerio guanine nucleotide binding protein (G protein), beta polypeptide 3b (gnb3b), mRNA [NM_213202]	-1.19	1.03E-02
ctrl	ref|Danio rerio chymotrypsin-like (ctrl), mRNA [NM_001004582]	-1.19	1.86E-03
gnat2	ref|Danio rerio guanine nucleotide binding protein (G protein), alpha transducing activity polypeptide 2 (gnat2), mRNA [NM_131869]	-1.19	1.17E-02
rcvrn3	ref|Danio rerio recoverin 3 (rcvrn3), mRNA [NM_200825]	-1.21	6.51E-03
tgm1l4	ref|Danio rerio transglutaminase 1 like 4 (tgm1l4), mRNA [NM_001030096]	-1.21	5.99E-05
setdb1a	ref|Danio rerio SET domain, bifurcated 1a (setdb1a), mRNA [NM_001044767]	-1.22	1.15E-02
prss1	ref|Danio rerio serine protease 1 (prss1), mRNA [NM_131708]	-1.23	2.74E-04
apoda.2	ref|Danio rerio apolipoprotein Da, duplicate 2 (apoda.2), transcript variant 1, mRNA [NM_001201348]	-1.24	2.84E-04
sult3st3	ref|Danio rerio sulfotransferase family 3, cytosolic sulfotransferase 3 (sult3st3), mRNA [NM_001082876]	-1.26	9.71E-09
gnb3b	ref|Danio rerio guanine nucleotide binding protein (G protein), beta	-1.28	8.94E-03

	polypeptide 3b (gnb3b), mRNA [NM_213202]		
opn1mw1	ref|Danio rerio opsin 1 (cone pigments), medium-wave-sensitive, 1 (opn1mw1), mRNA [NM_131253]	-1.29	1.47E-02
grk1b	ref|Danio rerio G protein-coupled receptor kinase 1 b (grk1b), mRNA [NM_001017711]	-1.31	3.65E-03
opn1mw1	ref|Danio rerio opsin 1 (cone pigments), medium-wave-sensitive, 1 (opn1mw1), mRNA [NM_131253]	-1.31	1.69E-02
gnb3b	ref|Danio rerio guanine nucleotide binding protein (G protein), beta polypeptide 3b (gnb3b), mRNA [NM_213202]	-1.31	1.08E-02
pde6ha	ref|Danio rerio phosphodiesterase 6H, cGMP-specific, cone, gamma, paralog a (pde6ha), transcript variant 2, mRNA [NM_200785]	-1.35	3.49E-02
opn1sw1	ref|Danio rerio opsin 1 (cone pigments), short-wave-sensitive 1 (opn1sw1), mRNA [NM_131319]	-1.37	2.81E-03
opn1sw1	ref|Danio rerio opsin 1 (cone pigments), short-wave-sensitive 1 (opn1sw1), mRNA [NM_131319]	-1.38	4.60E-03
gnb3b	ref|Danio rerio guanine nucleotide binding protein (G protein), beta polypeptide 3b (gnb3b), mRNA [NM_213202]	-1.38	5.45E-03
gnb3b	ref|Danio rerio guanine nucleotide binding protein (G protein), beta polypeptide 3b (gnb3b), mRNA [NM_213202]	-1.39	3.81E-03
ENSDART00000162599	ens|phosphodiesterase 6H, cGMP-specific, cone, gamma, paralog a [Source:ZFIN;Acc:ZDB-GENE-040426-1754] [ENSDART00000162599]	-1.39	3.05E-02
ctrb1	ref|Danio rerio chymotrypsinogen B1 (ctrb1), mRNA [NM_212618]	-1.41	9.17E-04
prss59.1	ref|Danio rerio serine protease 59, tandem duplicate 1 (prss59.1), mRNA [NM_199605]	-1.48	4.49E-04
desma	ref|Danio rerio desmin a (desma), transcript variant 2, mRNA [NM_001328376]	-1.49	5.74E-03

sult3st3	ref|Danio rerio sulfotransferase family 3, cytosolic sulfotransferase 3 (sult3st3), mRNA [NM_001082876]	-1.50	4.70E-08
ctrl	ref|Danio rerio chymotrypsin-like (ctrl), mRNA [NM_001004582]	-1.53	1.75E-03
odam	ref|Danio rerio odontogenic, ameloblast associated (odam), mRNA [NM_001145243]	-1.53	1.11E-03
trpv6	ref|Danio rerio transient receptor potential cation channel, subfamily V, member 6 (trpv6), mRNA [NM_001001849]	-1.54	1.12E-13
si:dkey-269i1.4	ref|Danio rerio si:dkey-269i1.4 (si:dkey-269i1.4), mRNA [NM_001105680]	-1.59	3.28E-04
si:dkey-269i1.4	ref|Danio rerio si:dkey-269i1.4 (si:dkey-269i1.4), mRNA [NM_001105680]	-1.62	2.61E-04
prss59.1	ref|Danio rerio serine protease 59, tandem duplicate 1 (prss59.1), mRNA [NM_199605]	-1.64	2.15E-04
he1.2	ref|Danio rerio hatching enzyme 1, tandem dupliate 2 (he1.2), mRNA [NM_213635]	-1.65	5.79E-04
zgc:174154	ref|Danio rerio si:dkey-269i1.3 (si:dkey-269i1.3), mRNA [NM_001327979]	-1.66	4.83E-04
zgc:92041	ref|Danio rerio zgc:92041 (zgc:92041), mRNA [NM_001003737]	-1.67	1.31E-05
he1.2	ref|Danio rerio hatching enzyme 1, tandem dupliate 2 (he1.2), mRNA [NM_213635]	-1.72	3.37E-04
si:dkey-269i1.4	ref|Danio rerio si:dkey-269i1.4 (si:dkey-269i1.4), mRNA [NM_001105680]	-1.73	3.73E-04
si:dkey-239j18.2	ref|Danio rerio si:dkey-239j18.2 (si:dkey-239j18.2), mRNA [NM_001287203]	-1.77	1.53E-04
rps15a	ref|Danio rerio ribosomal protein S15a (rps15a), mRNA [NM_212762]	-1.77	1.47E-03
he1.2	*ref|Danio rerio hatching enzyme 1, tandem dupliate 2 (he1.2), mRNA [NM_213635]*	*-1.78*	*5.90E-04*
he1.1	*ref|Danio rerio hatching enzyme 1, tandem duplicate 1 (he1.1), mRNA [NM_001045174]*	*-1.79*	*3.56E-04*
MGC174155	*ref|Danio rerio Cathepsin L1-like (MGC174155), mRNA [NM_001103118]*	*-1.79*	*6.48E-04*
MGC174155	*ref|Danio rerio Cathepsin L1-like (MGC174155), mRNA [NM_001103118]*	*-1.80*	*4.06E-04*
zgc:174154	*ref|Danio rerio si:dkey-269i1.3 (si:dkey-269i1.3), mRNA [NM_001327979]*	*-1.80*	*2.12E-04*

zgc:174154	*ref|Danio rerio si:dkey-269i1.3 (si:dkey-269i1.3), mRNA [NM_001327979]*	*-1.82*	*3.04E-04*
zgc:92041	*ref|Danio rerio zgc:92041 (zgc:92041), mRNA [NM_001003737]*	*-1.83*	*2.69E-05*
A_15_P685296	*Unknown*	*-1.86*	*2.06E-04*
MGC174155	*ref|Danio rerio Cathepsin L1-like (MGC174155), mRNA [NM_001103118]*	*-1.86*	*1.44E-04*
TC387424	*tc|Rep: MGC174857 protein - Danio rerio (Zebrafish) (Brachydanio rerio), complete [TC387424]*	*-1.90*	*1.66E-05*
MGC174155	*ref|Danio rerio Cathepsin L1-like (MGC174155), mRNA [NM_001103118]*	*-1.91*	*1.47E-04*
MGC174155	*ref|Danio rerio Cathepsin L1-like (MGC174155), mRNA [NM_001103118]*	*-1.93*	*9.98E-05*
si:dkey-269i1.4	*ref|Danio rerio si:dkey-269i1.4 (si:dkey-269i1.4), mRNA [NM_001105680]*	*-1.97*	*1.87E-04*
zgc:174153	*ref|Danio rerio zgc:174153 (zgc:174153), mRNA [NM_001111192]*	*-2.11*	*1.65E-05*
prss59.2	*ref|Danio rerio serine protease 59, tandem duplicate 2 (prss59.2), mRNA [NM_001281994]*	*-2.25*	*1.61E-04*
ca15b	*ref|Danio rerio carbonic anhydrase XVb (ca15b), mRNA [NM_213182]*	*-2.29*	*2.44E-03*
smtlb	*ref|Danio rerio somatolactin beta (smtlb), mRNA [NM_001037674]*	*-2.97*	*2.02E-09*

Table S4.

Differentially induced genes upon 4h larval exposure to 1-HP (5 µM), in the presence or absence of CH223191 (5µM).

		1-HP vs DMSO		1-HP + CH223191 vs DMSO	
Sequence Name(s)	**Sequence Description**	**q-value**	**Log_2 Fold Change**	**q-value**	**Log_2 Fold Change**
ahrra	ref|Danio rerio aryl-hydrocarbon receptor repressor a (ahrra), mRNA [NM_001035265]	3.55E-13	2.56	9.38E-01	0.22
cyp1a	ref|Danio rerio cytochrome P450, family 1, subfamily A (cyp1a), mRNA [NM_131879]	3.65E-20	6.11	1.09E-01	1.27
cyp1a	ref|Danio rerio cytochrome P450, family 1, subfamily A (cyp1a), mRNA [NM_131879]	9.42E-15	3.93	8.42E-01	0.47
cyp1a	ref|Danio rerio cytochrome P450, family 1, subfamily A (cyp1a), mRNA [NM_131879]	1.33E-14	3.38	9.46E-01	0.23
cyp1b1	ref|Danio rerio cytochrome P450, family 1, subfamily B, polypeptide 1 (cyp1b1), transcript variant 3, mRNA [NM_001145708]	4.41E-02	0.90	9.78E-01	-0.11
cyp1c1	ref|Danio rerio cytochrome P450, family 1, subfamily C, polypeptide 1 (cyp1c1), mRNA [NM_001020610]	8.89E-10	2.16	9.51E-01	0.20
cyp1c1	ref|Danio rerio cytochrome P450, family 1, subfamily C, polypeptide 1 (cyp1c1), mRNA [NM_001020610]	1.96E-11	2.41	9.86E-01	0.08
cyp1c2	ref|Danio rerio cytochrome P450, family 1, subfamily C, polypeptide 2 (cyp1c2), mRNA [NM_001114849]	2.39E-07	1.70	9.77E-01	-0.11
dhrs13l1	ref|Danio rerio dehydrogenase/reductase (SDR family) member 13 like 1 (dhrs13l1), mRNA [NM_205648]	2.62E-02	0.83	7.13E-01	0.66
ncam3	ens|neural cell adhesion molecule 3 [Source:ZFIN;Acc:ZDB-GENE-131127-340] [ENSDART00000156921]	2.03E-05	0.75	7.80E-01	0.26

ncam3	ens|neural cell adhesion molecule 3 [Source:ZFIN;Acc:ZDB-GENE-131127-340] [ENSDART00000156921]	2.62E-02	1.10	9.88E-01	-0.08
nfe2l2b	ens|nuclear factor, erythroid 2-like 2b [Source:ZFIN;Acc:ZDB-GENE-120320-3] [ENSDART00000122221]	3.73E-02	0.95	9.55E-01	0.18
ocstamp	ref|Danio rerio osteoclast stimulatory transmembrane protein (ocstamp), mRNA [NM_001014340]	2.23E-04	1.32	1.76E-02	1.19
sult6b1	ref|Danio rerio sulfotransferase family, cytosolic, 6b, member 1 (sult6b1), mRNA [NM_214686]	1.68E-05	1.26	9.40E-01	0.19
sult6b1	ref|Danio rerio sulfotransferase family, cytosolic, 6b, member 1 (sult6b1), mRNA [NM_214686]	4.94E-03	1.17	8.49E-01	0.38

Table S5.
Differentially induced genes upon 4h larval exposure to 1-HP (5 μM), in the presence or absence of 3-o-C12-L-HSL (50 μM)).

		1-HP vs DMSO		**1-HP+ 3-o-C12-L-HSL vs DMSO**	
Sequence Name(s)	**Sequence Description**	**q-value**	**Log_2 Fold Change**	**q-value**	**Log_2 Fold Change**
cyp1a	ref|Danio rerio cytochrome P450, family 1, subfamily A (cyp1a), mRNA [NM_131879]	3.65E-20	6.11	5.73E-16	4.63
cyp1a	ref|Danio rerio cytochrome P450, family 1, subfamily A (cyp1a), mRNA [NM_131879]	9.42E-15	3.93	1.18E-09	2.71
cyp1a	ref|Danio rerio cytochrome P450, family 1, subfamily A (cyp1a), mRNA [NM_131879]	1.33E-14	3.38	1.87E-08	2.14
ahrra	ref|Danio rerio aryl-hydrocarbon receptor repressor a (ahrra), mRNA [NM_001035265]	3.55E-13	2.56	1.95E-06	1.45
cyp1c1	ref|Danio rerio cytochrome P450, family 1, subfamily C, polypeptide 1 (cyp1c1), mRNA [NM_001020610]	1.96E-11	2.41	4.38E-05	1.34
cyp1c1	ref|Danio rerio cytochrome P450, family 1, subfamily C,	8.89E-10	2.16	2.21E-04	1.23

	polypeptide 1 (cyp1c1), mRNA [NM_001020610]				
cyp1c2	ref|Danio rerio cytochrome P450, family 1, subfamily C, polypeptide 2 (cyp1c2), mRNA [NM_001114849]	2.39E-07	1.70	2.25E-03	1.02
ocstamp	ref|Danio rerio osteoclast stimulatory transmembrane protein (ocstamp), mRNA [NM_001014340]	2.23E-04	1.32	6.83E-08	1.89
sult6b1	ref|Danio rerio sulfotransferase family, cytosolic, 6b, member 1 (sult6b1), mRNA [NM_214686]	1.68E-05	1.26	7.62E-03	0.81
sult6b1	ref|Danio rerio sulfotransferase family, cytosolic, 6b, member 1 (sult6b1), mRNA [NM_214686]	4.94E-03	1.17	9.25E-03	0.99
ncam3	ens|neural cell adhesion molecule 3 [Source:ZFIN;Acc:ZDB-GENE-131127-340] [ENSDART00000156921]	2.62E-02	1.10	2.01E-02	0.95
nfe2l2b	ens|nuclear factor, erythroid 2-like 2b [Source:ZFIN;Acc:ZDB-GENE-120320-3] [ENSDART00000122221]	3.73E-02	0.95	3.71E-05	1.37
cyp1b1	ref|Danio rerio cytochrome P450, family 1, subfamily B, polypeptide 1 (cyp1b1), transcript variant 3, mRNA [NM_001145708]	4.41E-02	0.90	6.99E-01	0.27
dhrs13l1	ref|Danio rerio dehydrogenase/reductase (SDR family) member 13 like 1 (dhrs13l1), mRNA [NM_205648]	2.62E-02	0.83	1.57E-04	1.06
ncam3	ens|neural cell adhesion molecule 3 [Source:ZFIN;Acc:ZDB-GENE-131127-340] [ENSDART00000156921]	2.03E-05	0.75	1.08E-04	0.67

Table S6.

CRISPR sequences used in this study.

Target Gene	Vector	CRISPR sequence	Source
AhR	pLv-U6g-EPCG	AGTCGGTCTCTATGCCGCTTGG	Sigma-Aldrich
Scramble Control	pLv-U6g-EPCG		Sigma-Aldrich

Table S7.

List of molecules used in this study.

Name	Abbreviation name	Source	Reference	Storage
2,3,7,8-Tetrachlorodibenzo-p-dioxin [^{3}H(G)]	[^{3}H] TCDD	Hartmann Analytical	ART1642	-20°C
1-Hydroxyphenazine	1-HP	TCI chemicals	H0289	RT
N-6-Cyclohexyl-3-oxohexanoyl-L-homoserinelactone	3-o-6-Cy-C6-L-HSL	University of Nottingham	39	-20°C
N-6-Phenyl-3-oxohexanoyl-L-homoserinelactone	3-o-6-Ph-C6-L-HSL	University of Nottingham	40	-20°C
3-3-Oxododecanoylamin)-L-2-pyrrolidone	3-o-C12-L-AP	University of Nottingham	37	-20°C
2-3-Oxododecanoylamino-thiazole	3-o-C12-L-AT	University of Nottingham	38	-20°C
N-3-Oxododecanoyl-L-homoserinelactone	3-o-C12-L-HSL	Biomol	Cay10007895	-20°C
N-3-Oxododecanoyl-L-homocysteinethiolactone	3-o-C12-L-HTL	University of Nottingham	36	-20°C
N-3-Oxotetradecanoyl-L-homoserinelactone	3-o-C14-L-HSL	Sigma-Aldrich	O9264	-20°C
N-3-Oxo-hexadec-11(Z)-enoyl-L-homoserine lactone	3-o-C16:1-Δ11-cis-L-HSL	Biomol	Cay10011238	-20°C
N-3-Oxohexanoyl-L-homoserinelactone	3-o-C6-L-HSL	Sigma-Aldrich	K3007	-20°C
N-3-Oxooctanoyl-L-homoserinelactone	3-o-C8-L-HSL	Biomol	Cay10011206	-20°C
N-3-Hydroxydecanoyl-L-homoserinelactone	3-OH-C10-L-HSL	Biomol	Cay9001147	-20°C
N-3-Hydroxydodecanoyl-DL-homoserinelactone	3-OH-C12-DL-HSL	Sigma-Aldrich	53727	-20°C
N-3-Hydroxytridecanoyl-L-homoserinelactone	3-OH-C13-L-HSL	University of Nottingham	23	-20°C
N-3-Hydroxytetradecanoyl-DL-homoserinelactone	3-OH-C14-DL-HSL	Sigma-Aldrich	51481	-20°C
N-3-Hydroxyhexadecanoyl-L-homoserinelactone	3-OH-C16-L-HSL	University of Nottingham	28	-20°C
N-3-Hydroxyoctadecanoyl-L-homoserinelactone	3-OH-C18-L-HSL	University of Nottingham	32	-20°C
N-3-Hydroxyoctanoyl-L-homoserinelactone	3-OH-C8-L-HSL	Biomol	Cay9001150	-20°C
N-Decanoyl-L-homoserinelactone	C10-L-HSL	Biomol	Cay10011201	-20°C

N-Undecanoyl-L-homoserinelactone	C11-L-HSL	Biomol	Cay16827	-20°C
N-Dodecanoyl-L-homoserinelactone	C12-L-HSL	Biomol	Cay10011203	-20°C
N-Tridecanoyl-L-homoserinelactone	C13-L-HSL	Biomol	Cay13093	-20°C
N-cis-Tetradec-9Z-enoyl-L-homoserinelactone	C14:1-Δ9-cis-L-HSL	Biomol	Cay10012672	-20°C
N-Tetradecanoyl-L-homoserinelactone	C14-L-HSL	Biomol	Cay10011200	-20°C
N-Pentadecanoyl-L-homoserinelactone	C15-L-HSL	Biomol	Cay13094	-20°C
N-cis-Hexadec-9Z-enoyl-L-homoserinelactone	C16:1-Δ9-cis-L-HSL	Biomol	Cay10012673	-20°C
N-cis-Octadec-9-enoyl-L-homoserinelactone	C18:1-Δ9-cis-L-HSL	Biomol	Cay10012674	-20°C
N-Butyryl-L-homoserinelactone	C4-L-HSL	Biomol	Cay10007898	-20°C
N-Butyryl-L-homocysteinethiolactone	C4-L-HTL	Biomol	Cay10011204	-20°C
N-hexanoyl-L-homoserinelactone	C6-L-HSL	Biomol	Cay10007896	-20°C
N-Heptanoyl-L-homoserinelactone	C7-L-HSL	Biomol	Cay10011198	-20°C
N-Octanoyl-L-homoserinelactone	C8-L-HSL	Biomol	Cay10011199	-20°C
N-Phenylacetyl-L-homoserinelactone	C8-L-HSL ring closure	Biomol	Cay9001737	-20°C
N-Nonanoyl-L-homoserinelactone	C9-L-HSL	Biomol	Cay16868	-20°C
2-Methyl-2H-pyrazole-3-carboxylic acid (2-methyl-4-o-tolylazo-phenyl)-amide	CH223191	Sigma-Aldrich	C8124	4°C
2-Heptyl-4-quinolone	HHQ	Sigma-Aldrich	SML0747	-20°C
N-p-Coumaroyl-L-homoserine lactone	p-coumaroyl-L-HSL	Sigma-Aldrich	7077	-20°C
2-Heptyl-3-hydroxy-4(1H)quinolone	PQS	Sigma-Aldrich	94398	-20°C
Pyocyanin	Pyo	Sigma-Aldrich	P0046	-20°C
2,3,7,8-Tetrachlorodibenzo-p-dioxin	TCDD	Sigma-Aldrich	48599	4°C

Table S8.

List of primers and probes used in this study.

Gene	Primer sequence	Organism
AhRR	F-GCGCCTCAGTGTCAGTTACC	human
	R-CTCCTGCACGACTTGGAAGAA	
CYP1A1	F-ACATGCTGACCCTGGGAAAG	human
	R-GGTGTGGAGCCAATTCGGAT	
CYP1B1	F-GGGACCGTCTGCCTTGTATG	human
	R-GGTGGCATGAGGAATAGTGACA	
GAPDH	F-CATGAGAAGTATGACAACAGCCT	human
	R-AGTCCTTCCACGATACCAAAGT	
IL-1b	F-CTCGCCAGTGAAATGATGGCT	human
	R-GTCGGAGATTCGTAGCTGGAT	
IL-8	F-TTTTGCCAAGGAGTGCTAAAGA	human
	R-AACCCTCTGCACCCAGTTTTC	
ahRRa	F-GCCGCTGGCATATAACATGAGC	zebrafish
	R-TGACGCTGTGTTCACGTCACTG	
ahRRb	F-GACTACCTGGGATTTCATCAGACG	zebrafish
	R-GAGCCGTCACAACATCCTCATC	
β-actin	F-CGAGCAGGAGATGGGAACC	zebrafish
	R-CAACGGAAACGCTCATTGC	
cyp1a	F-GCATTACGATACGTTCGATAAGGAC	zebrafish
	R-GCTCCGAATAGGTCATTGACGAT	
cyp1b1	F-AGGGGGTGATTTCGGATACAG	zebrafish
	R-AAATCACAAGTGTGAACGCTCT	
cyp1c1	F-GGGCAAATGCCACACATCAC	zebrafish
	R-TTCCTTATCGCCGCATCTCC	
cyp1c2	F-GCGCTCATTGCATCGTTCAT	zebrafish
	R-CAAAGGGTCCCGGAAGTCTC	
dhrs13l1	F-AGAAGCTCGGTCTGGGATCT	zebrafish
	R-ACTGAACCTGGATGGAGACTG	
ncam3	F-CCCCAGTCAGTTCAGCATGT	zebrafish
	R-AGTAGCTAATGGGGGAGCCT	
nfe2l2b	F-AGAAGCAGGGTTTCGGTGAG	zebrafish
	R-TGGATCGGGGAGGTTAGGTT	
sultb1	F-AAACCCGAAAGACACGCTGG	zebrafish
	R-CCCCAACTAACATCACCAGTCA	

Table S9.

List of antibodies used on this study.

Protein	Company	Ref.	Dilution	Incubation conditions	Application	Fluorochrome
Human β-actin	Abcam	ab6276	1/24000	1h, RT	WB	
Human AhR	Santa Cruz	sc-85682	1/500	overnight, 4°C	WB	
IgG mouse	Cell Signaling	7076	1/5000	1h, RT	WB	
Zebrafish CYP1A	Biosense laboratories	C10-7	1/1000	overnight, 4°C	WB	
Zebrafish α-tubulin	Sigma-Aldrich	T6199	1/1000	overnight, 4°C	WB	
Mouse CD45	Biolegend	104	1/100	15 min, 4°C	Flow cytometry	Alexa 700
Mouse Siglec F	BD Pharmingen	E50-2440	1/100	15 min, 4°C	Flow cytometry	Pacific Blue
Mouse CD11c	Biolegend	N418	1/400	15 min, 4°C	Flow cytometry	APC
Mouse Ly6G	Biolegend	1A8	1/100	15 min, 4°C	Flow cytometry	PerCP Cy5.5
Mouse CD11b	BD Pharmingen	M1/70	1/200	15 min, 4°C	Flow cytometry	PeCy7

Table S10.

List of bacteria used in this study.

Target Gene	Medium used	Antibiotic used	Source	References
PA14 WT	LB		Burkhard Tuemmler (Medizinsche Hoschule Hannover, Germany)	10
PA14 WT-GFP	LB	Carbenicillin 300 µg/mL	Fred Ausubel (Harvard Medical School/Massachussets General Hospital, Boston, USA)	85
PA14 09480	LB		Burkhard Tuemmler (Medizinsche Hoschule Hannover, Germany)	10
PA14 Δ*rsaL*	LB		Livia Leoni (University Roma Tre, Rome, Italy)	27,41
PA14 R3	LB		Livia Leoni (University Roma Tre, Rome, Italy)	27
PAO1	LB		Burkhard Tuemmler (Medizinsche Hoschule Hannover, Germany)	10
PAO1 *pqsA* CTX-lux::*pqsA*	LB	Tetracycline 125 µg/mL	Paul Williams (University of Nottingham, Nottingham, UK)	28

Table S11.

Custom gene set used for xenobiotic metabolism gene enrichment analysis.

ZFIN ID	gene name
ZDB-GENE-030529-3	*adh8a*
ZDB-GENE-020531-2	*ahr1a*
ZDB-GENE-050922-1	*ahr1b*
ZDB-GENE-990714-16	*ahr2*
ZDB-GENE-051018-1	*ahrra*
ZDB-GENE-051018-2	*ahrrb*
ZDB-GENE-030131-9732	*apobb.1*
ZDB-GENE-060126-7	*arnt*
ZDB-GENE-050522-215	*atp6v0a1b*
ZDB-GENE-031219-5	*ca2*
ZDB-GENE-011210-1	*casp3a*
ZDB-GENE-020530-2	*cox2a*
ZDB-GENE-041014-323	*cox2b*
ZDB-GENE-030131-1132	*cpb1*
ZDB-GENE-040426-2148	*cyb5a*
ZDB-GENE-990415-43	*cyp19a1a*
ZDB-GENE-001103-4	*cyp19a1b*
ZDB-GENE-011219-1	*cyp1a*
ZDB-GENE-030902-1	*cyp1b1*
ZDB-GENE-050522-501	*cyp1c1*
ZDB-GENE-050705-1	*cyp1c2*
ZDB-GENE-050604-1	*cyp3a65*
ZDB-GENE-030131-5128	*eef2b*
ZDB-GENE-020806-5	*esr1*
ZDB-GENE-070424-74	*foxq1a*
ZDB-GENE-030131-9854	*grhl3*
ZDB-GENE-020806-4	*gstp1*
ZDB-GENE-061207-54	*hipk3a*
ZDB-GENE-030131-3102	*hmox1a*
ZDB-GENE-990415-91	*hsp70.1*
ZDB-GENE-050309-169	*im:7150988*
ZDB-GENE-030131-556	*keap1a*
ZDB-GENE-080508-1	*keap1b*
ZDB-GENE-060316-2	*krt1-11b*
ZDB-GENE-040711-2	*nceh1a*
ZDB-GENE-061110-43	*nceh1b.1*
ZDB-GENE-030723-2	*nfe2l2a*
ZDB-GENE-030131-1226	*nqo1*

ZDB-GENE-031006-8	*nt5c2l1*
ZDB-GENE-030131-12	*si:ch211-117m20.5*
ZDB-GENE-051014-1	*smpd2a*
ZDB-GENE-990415-258	*sod1*
ZDB-GENE-030131-7447	*sort1b*
ZDB-GENE-030131-2144	*sult1st1*
ZDB-GENE-030804-27	*sult1st2*
ZDB-GENE-030804-28	*sult1st3*
ZDB-GENE-050809-2	*sult1st5*
ZDB-GENE-050417-228	*sult6b1*
ZDB-GENE-030131-73	*tgfbi*
ZDB-GENE-031002-47	*tiparp*
ZDB-GENE-040718-150	*ufd1l*
ZDB-GENE-100113-1	*unm_it275*
ZDB-GENE-001201-1	*vtg1*
ZDB-GENE-031010-24	*zgc:77439*
ZDB-GENE-030131-1107	*zgc:77849*

References and Notes:

55. M. W. Pfaffl, A new mathematical model for relative quantification in real-time RT-PCR. *Nucleic Acids Res* **29**, e45 (2001).
56. L. Lozza *et al.*, Crosstalk between human DC subsets promotes antibacterial activity and CD8+ T-cell stimulation in response to bacille Calmette-Guerin. *Eur J Immunol* **44**, 80-92 (2014).
57. A. Mohammadi-Bardbori, Assay for quantitative determination of CYP1A1 enzyme activity using 7-Ethoxyresorufin as standard substrate (EROD assay). (2014).
58. M. E. Ritchie *et al.*, limma powers differential expression analyses for RNA-sequencing and microarray studies. *Nucleic Acids Res* **43**, e47 (2015).
59. J. Weiner 3rd, Domaszewska, T., tmod: an R package for general and multivariate enrichment analysis. *PeerJ Preprints* **4:e2420v1**, (2016).
60. J. Zyla, M. Marczyk, J. Weiner, J. Polanska, Ranking metrics in gene set enrichment analysis: do they matter? *BMC Bioinformatics* **18**, 256 (2017).
61. N. Eswar *et al.*, Comparative protein structure modeling using Modeller. *Curr Protoc Bioinformatics* **Chapter 5**, Unit-5 6 (2006).
62. M. Y. Shen, A. Sali, Statistical potential for assessment and prediction of protein structures. *Protein Sci* **15**, 2507-2524 (2006).
63. T. A. Halgren *et al.*, Glide: a new approach for rapid, accurate docking and scoring. 2. Enrichment factors in database screening. *J Med Chem* **47**, 1750-1759 (2004).
64. N. Huang *et al.*, Crystal structure of the heterodimeric CLOCK:BMAL1 transcriptional activator complex. *Science* **337**, 189-194 (2012).
65. C. Nüsslein-Volhard, Dahm, R., *Zebrafish*. C. Nüsslein-Volhard, Dahm, R., Ed., (Oxford University Press, 2002), pp. 303.
66. D. C. Nacci, L; Kuhn,A; Champlin, D; Munns, W; Specker, J; Cooper, K, Nondestructive indicator of ethoxyresorufin-O-deethylase activity in embryonic fish. *ENVIRONMENTAL TOXICOLOGY AND CHEMISTRY* **17**, 2481-2486 (1998).
67. V. Link, A. Shevchenko, C. P. Heisenberg, Proteomics of early zebrafish embryos. *BMC Dev Biol* **6**, 1 (2006).
68. S. Subramoni, V. Venturi, LuxR-family 'solos': bachelor sensors/regulators of signalling molecules. *Microbiology* **155**, 1377-1385 (2009).
69. A. Neumann, D. Patzelt, I. Wagner-Dobler, S. Schulz, Identification of new N-acylhomoserine lactone signalling compounds of Dinoroseobacter shibae DFL-12(T) by overexpression of luxI genes. *Chembiochem* **14**, 2355-2361 (2013).
70. M. Elasri *et al.*, Acyl-homoserine lactone production is more common among plant-associated Pseudomonas spp. than among soilborne Pseudomonas spp. *Appl Environ Microbiol* **67**, 1198-1209 (2001).
71. R. L. Ulrich *et al.*, Role of quorum sensing in the pathogenicity of Burkholderia pseudomallei. *J Med Microbiol* **53**, 1053-1064 (2004).
72. R. L. Ulrich, D. Deshazer, H. B. Hines, J. A. Jeddeloh, Quorum sensing: a transcriptional regulatory system involved in the pathogenicity of Burkholderia mallei. *Infect Immun* **72**, 6589-6596 (2004).

73. G. Brader, S. Sjoblom, H. Hyytiainen, K. Sims-Huopaniemi, E. T. Palva, Altering substrate chain length specificity of an acylhomoserine lactone synthase in bacterial communication. *J Biol Chem* **280**, 10403-10409 (2005).
74. A. M. Pomini, G. P. Manfio, W. L. Araujo, A. J. Marsaioli, Acyl-homoserine lactones from Erwinia psidii R. IBSBF 435T, a guava phytopathogen (Psidium guajava L.). *J Agric Food Chem* **53**, 6262-6265 (2005).
75. O. Geisenberger *et al.*, Production of N-acyl-L-homoserine lactones by P. aeruginosa isolates from chronic lung infections associated with cystic fibrosis. *FEMS Microbiol Lett* **184**, 273-278 (2000).
76. G. D. Geske, J. C. O'Neill, D. M. Miller, M. E. Mattmann, H. E. Blackwell, Modulation of bacterial quorum sensing with synthetic ligands: systematic evaluation of N-acylated homoserine lactones in multiple species and new insights into their mechanisms of action. *J Am Chem Soc* **129**, 13613-13625 (2007).
77. G. D. Geske, R. J. Wezeman, A. P. Siegel, H. E. Blackwell, Small molecule inhibitors of bacterial quorum sensing and biofilm formation. *J Am Chem Soc* **127**, 12762-12763 (2005).
78. V. Nagar, V. Sinha, J. R. Bandekar, Diverse Profiles of N-acyl Homoserine L-Lactones, Biofilm, Virulence Genes and Integrons in Food-Borne Aeromonas Isolates. *J Food Sci* **80**, M1861-1870 (2015).
79. A. L. Schaefer *et al.*, A new class of homoserine lactone quorum-sensing signals. *Nature* **454**, 595-599 (2008).
80. K. Riedel *et al.*, N-acylhomoserine-lactone-mediated communication between Pseudomonas aeruginosa and Burkholderia cepacia in mixed biofilms. *Microbiology* **147**, 3249-3262 (2001).
81. P. Williams, Quorum sensing, communication and cross-kingdom signalling in the bacterial world. *Microbiology* **153**, 3923-3938 (2007).
82. J. P. Kirwan *et al.*, Quorum-sensing signal synthesis by the Yersinia pestis acyl-homoserine lactone synthase YspI. *J Bacteriol* **188**, 784-788 (2006).
83. C. A. Ortori *et al.*, Comprehensive profiling of N-acylhomoserine lactones produced by Yersinia pseudotuberculosis using liquid chromatography coupled to hybrid quadrupole-linear ion trap mass spectrometry. *Anal Bioanal Chem* **387**, 497-511 (2007).
84. A. Rajput, K. Kaur, M. Kumar, SigMol: repertoire of quorum sensing signaling molecules in prokaryotes. *Nucleic Acids Res* **44**, D634-639 (2016).
85. M. W. Tan, S. Mahajan-Miklos, F. M. Ausubel, Killing of Caenorhabditis elegans by Pseudomonas aeruginosa used to model mammalian bacterial pathogenesis. *Proc Natl Acad Sci U S A* **96**, 715-720 (1999).
86. E. K. Shiner *et al.*, Pseudomonas aeruginosa autoinducer modulates host cell responses through calcium signalling. *Cell Microbiol* **8**, 1601-1610 (2006).